

## Proton-Transfer-Reaction Mass Spectrometry: Applications in Atmospheric Sciences

Bin Yuan,<sup>\*,†,‡,§,||</sup> Abigail R. Koss,<sup>‡,§,⊥</sup> Carsten Warneke,<sup>\*,‡,§</sup> Matthew Coggan,<sup>‡,§</sup> Kanako Sekimoto,<sup>‡,§</sup> and Joost A. de Gouw<sup>\*,§,⊥,||</sup>

<sup>†</sup>Institute for Environment and Climate Research, Jinan University, Guangzhou 510632, China

<sup>‡</sup>Chemical Sciences Division, NOAA Earth System Research Laboratory (ESRL), Boulder, Colorado 80305, United States

<sup>§</sup>Cooperative Institute for Research in Environmental Sciences, University of Colorado at Boulder, Boulder, Colorado 80309, United States

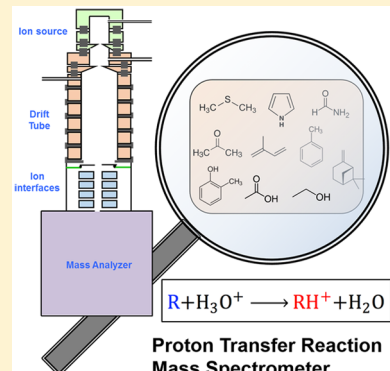
<sup>||</sup>Laboratory of Atmospheric Chemistry, Paul Scherrer Institute, Villigen 5232, Switzerland

<sup>⊥</sup>Department of Chemistry and Biochemistry, University of Colorado, Boulder, Colorado 80309, United States

<sup>#</sup>Graduate School of Nanobioscience, Yokohama City University, Yokohama 236-0027, Japan

### S Supporting Information

**ABSTRACT:** Proton-transfer-reaction mass spectrometry (PTR-MS) has been widely used to study the emissions, distributions, and chemical evolution of volatile organic compounds (VOCs) in the atmosphere. The applications of PTR-MS have greatly promoted understanding of VOC sources and their roles in air-quality issues. In the past two decades, many new mass spectrometric techniques have been applied in PTR-MS instruments, and the performance of PTR-MS has improved significantly. This Review summarizes these developments and recent applications of PTR-MS in the atmospheric sciences. We discuss the latest instrument development and characterization work on PTR-MS instruments, including the use of time-of-flight mass analyzers and new types of ion guiding interfaces. Here we review what has been learned about the specificity of different product ion signals for important atmospheric VOCs. We present some of the recent highlights of VOC research using PTR-MS including new observations in urban air, biomass-burning plumes, forested regions, oil and natural gas production regions, agricultural facilities, the marine environment, laboratory studies, and indoor air. Finally, we will summarize some further instrument developments that are aimed at improving the sensitivity and specificity of PTR-MS and extending its use to other applications in atmospheric sciences, e.g., aerosol measurements and OH reactivity measurements.



### CONTENTS

1. Introduction	13188	3.1. Methods to Attribute Masses to VOC Species	13200
2. Proton-Transfer-Reaction Mass Spectrometry	13190	3.1.1. GC-PTR-MS Studies	13200
2.1. Instrument Configurations	13190	3.1.2. Intercomparison Studies	13201
2.1.1. Drift Tube	13190	3.1.3. Chemical Formulas from PTR-TOF in Aid of VOC Identification	13201
2.1.2. Mass Analyzers	13190	3.2. Detection of Specific VOCs by PTR-MS	13202
2.1.3. Ion Interfaces between Drift Tube and Mass Analyzer	13192	<i>m/z</i> 18	13202
2.2. Ion Chemistry	13193	<i>m/z</i> 28	13202
2.3. Analysis of PTR-TOF Data	13194	<i>m/z</i> 31	13202
2.3.1. ToF Data-Processing Procedures	13194	<i>m/z</i> 33	13203
2.3.2. Availability of Software Tools	13195	<i>m/z</i> 35	13203
2.3.3. Errors from High-Resolution Peak Fitting	13195	<i>m/z</i> 42	13203
2.4. Operations and Performance	13196	<i>m/z</i> 44	13204
2.4.1. Determination of Background	13196	<i>m/z</i> 45	13204
2.4.2. Calibrations	13196	<i>m/z</i> 47	13204
2.4.3. Sensitivity of PTR-MS	13197	<i>m/z</i> 59	13204
2.4.4. Detection Limits	13199	<i>m/z</i> 61	13204
2.4.5. Response Time	13199	<i>m/z</i> 63	13204
3. Interpretation of Mass Spectra	13200		

Received: June 7, 2017

Published: October 4, 2017

<i>m/z</i> 69	13204
<i>m/z</i> 71	13205
<i>m/z</i> 73	13205
<i>m/z</i> 75	13205
<i>m/z</i> 77	13205
<i>m/z</i> 79	13205
<i>m/z</i> 93	13205
<i>m/z</i> 95	13205
<i>m/z</i> 97	13206
<i>m/z</i> 107	13206
<i>m/z</i> 121	13206
<i>m/z</i> 129	13206
<i>m/z</i> 137	13206
<i>m/z</i> 205	13206
<i>m/z</i> 371	13206
3.3. Analysis of Mass Spectra for Bulk Chemical Information	13207
4. Research Highlights	13207
4.1. Urban Emissions	13207
4.2. Biomass-Burning Emissions	13208
4.3. Biogenic Emissions	13208
4.4. Oil and Gas Emissions	13210
4.5. Agricultural Emissions	13210
4.6. Marine Environments	13211
4.7. Laboratory Studies of Atmospheric Chemistry	13212
4.8. Indoor Air	13212
5. Other Instrument Developments	13212
5.1. Switchable Reagent Ions	13212
5.2. Improvement of the Sensitivity	13214
5.3. Improved Separation of Isobars and Isomers	13214
5.4. Aerosol Measurements	13215
5.5. OH Reactivity Measurements and Other Indirect Measurements	13216
6. Conclusion and Future Outlook	13216
Associated Content	13217
Supporting Information	13217
Author Information	13217
Corresponding Authors	13217
ORCID	13217
Notes	13217
Biographies	13217
Acknowledgments	13217
References	13217

## 1. INTRODUCTION

Volatile organic compounds (VOCs) are released to the Earth's atmosphere from many different natural and manmade sources.<sup>1</sup> In polluted air containing nitrogen oxides, the photochemical transformation of VOCs leads to the formation of ozone. Chemical transformations of VOCs can also lead to formation of less-volatile and more-soluble compounds that can partition into existing fine particles or contribute to new particle formation.<sup>2</sup> Both ozone and fine particles are pollutants that affect human and ecosystem health and have been targeted by air-quality regulations in many countries.<sup>3</sup> Ozone and fine particles also affect the Earth's radiation balance and are important in the climate system.<sup>4</sup>

Thousands of different VOCs have been observed in the atmosphere.<sup>5</sup> VOCs are removed from the atmosphere on time scales ranging from minutes to years, and oxygenated compounds like aldehydes, ketones, peroxides, and acids are

formed as a result.<sup>6</sup> The shorter-lived VOCs cannot be transported very far from their sources, and the atmosphere shows strong gradients in their concentrations both horizontally and vertically. The short lifetime of reactive VOCs prevents the buildup of their concentrations, even when total emissions are high,<sup>7</sup> and volume mixing ratios for many compounds of interest are in the parts-per-trillion by volume (pptv) range or less. The longer-lived VOCs become more homogeneously distributed across the global atmosphere.<sup>8</sup> The chemical complexity and low concentrations of VOCs in the atmosphere challenge even the most sophisticated analytical methods for VOC measurements. Strong temporal and spatial gradients for reactive compounds mean that many measurements in time and space are needed to gain meaningful information about the distribution of a compound.<sup>9</sup> Less-reactive VOCs that become more homogeneously distributed put more severe constraints on the accuracy of VOC measurements.

The most comprehensive VOC measurements often involve gas-chromatographic separation and detection using mass spectrometry (GC-MS) or flame-ionization detection (GC-FID).<sup>10</sup> Comprehensive or 2-dimensional chromatography has been used to improve the separation of different compounds,<sup>11</sup> allowing separate measurements of hundreds of compounds.<sup>12</sup> The nonresolved signal can also be used to quantify higher-molecular-weight compounds that are particularly important as organic aerosol precursors.<sup>13</sup> The sensitivity and chemical detail that have been achieved with GC methods are impressive. Drawbacks of GC techniques include the fact that they are time- and labor-intensive, which limits the number of samples that can be analyzed in practice. Also, preconcentration of VOCs is needed to achieve the lowest detection limits, and the pretreatment of sample air to remove water, ozone, and/or carbon dioxide can lead to sampling issues that require extensive characterization. Real-time measurements of VOCs by mass spectrometry and optical methods have been developed to overcome these limitations of GC measurements. For example, proton-transfer-reaction mass spectrometry (PTR-MS) allows measurements of VOCs with a high time response and sensitivity and without the need for sample treatment.<sup>14</sup> The main drawback to PTR-MS is that the molecular mass of VOCs is a useful but by no means unique indicator of VOC identity. Optical methods like absorption spectroscopy,<sup>15,16</sup> laser-induced fluorescence,<sup>17</sup> or photoacoustic spectroscopy<sup>18</sup> make use of the unique optical properties of VOCs but are only suitable for a limited number of compounds.

PTR-MS was developed in the late 1990s by Lindner and co-workers at the University of Innsbruck in Austria.<sup>14,19</sup> The technique uses proton-transfer reactions with H<sub>3</sub>O<sup>+</sup> (hydronium) ions to ionize atmospheric VOCs and mass-spectrometric detection of the product ions. The proton-transfer chemistry takes place in a drift-tube reactor, which enhances the ion kinetic energy and effectively limits cluster ion formation with the abundant water molecules in ambient air. This simplifies both the proton-transfer chemistry and the interpretation of the mass spectra. The exothermicity of the proton-transfer reactions is low enough that the extent of product ion fragmentation is limited and product ion masses can be used as unique identifiers for many important atmospheric VOCs.<sup>20,21</sup> In the original PTR-MS instrument, a quadrupole mass spectrometer was used to select and detect product ions. Since then, several other types of mass

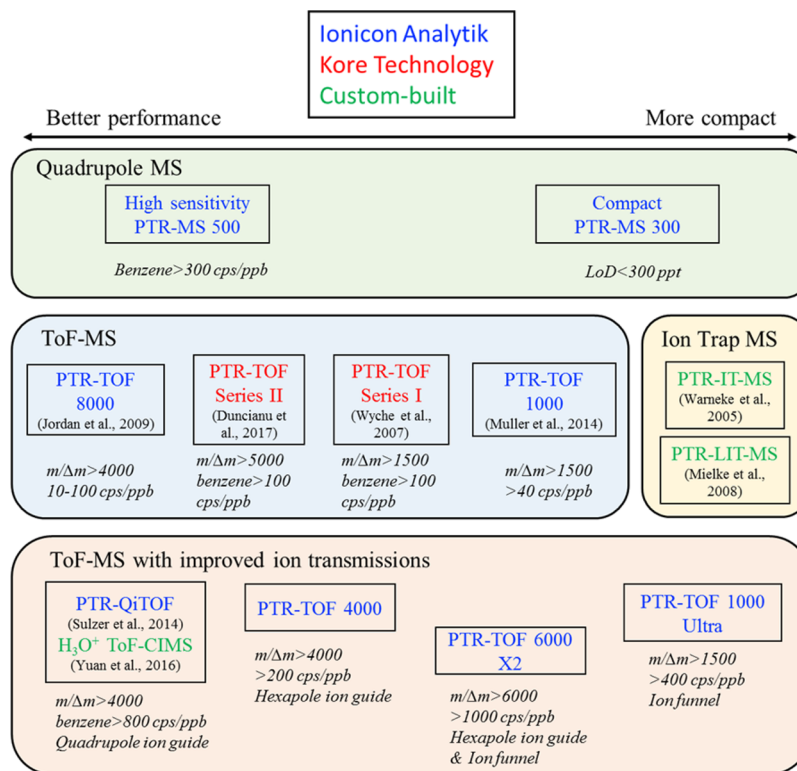


**Figure 1.** Product family of PTR-MS in the literature. Note that we only include selected custom-built PTR-MS instruments for the sake of clarity. The reader is referred to the text for other custom-built instruments.

spectrometers, such as ion traps and time-of-flight analyzers, have been incorporated into PTR-MS instrumentation. In the late 2000s, progress in time-of-flight mass spectrometry (ToF-MS) allowed the development of PTR-MS instruments with a much higher mass resolution ( $R = m/\Delta m$ , where  $\Delta m$  is the full width at half-maximum of the isolated ion peak) than the quadrupole mass filters used in earlier instruments.<sup>22,23</sup> This had the important advantage that isobaric ions with different elemental compositions could be separately measured. Further improvements in the transmission of ions from the drift tube to the time-of-flight region significantly improved the detection limits of such instruments.<sup>24</sup> Ion-trap mass spectrometry was also used in PTR-MS instruments,<sup>25,26</sup> which allowed tandem mass spectrometry: product ions could be selected by mass and dissociated and the fragment ion spectra could be determined. These types of instruments provided additional means to separate isobaric ions, but they have not found widespread use so far. Other instrument developments focused on the use of reagent ions other than  $H_3O^+$  for chemical ionization.<sup>27</sup> We remind readers to note the difference between isomers and isobars: isomers have the same molecular formula and functionality, and they often produce the same ions in PTR-MS (e.g., ethylbenzene vs *m*-xylene), whereas isobars have the same nominal molecular weight but have different molecular formulas (e.g., formic acid vs ethanol).

In this Review, we will review the use of proton-transfer-reaction mass spectrometry for measurements of VOCs in the atmosphere. Section 2 will describe the growing number of PTR-MS-type instruments that have been developed including quadrupole, time-of-flight, and ion-trap mass spectrometers. The characterization of these instruments and the various steps needed in the analysis of data are described. Section 3 summarizes what has been learned about the specificity of

different product ion signals for important atmospheric VOCs. While the nominal mass and elemental composition of product ions hold important information about VOC identity, there are many cases where different compounds are detected at the same exact product ion masses. Research using gas-chromatographic interfaces and data intercomparisons with other VOC measurements have resulted in a large body of information on how to interpret PTR-MS measurements in different regions of the atmosphere, and they will be reviewed in this section. Section 4 summarizes some of the recent highlights of VOC research using PTR-MS including new observations in urban air, biomass-burning plumes, forested regions, oil and natural gas production regions, agricultural facilities, the marine environment, laboratory studies, and indoor air. Finally, section 5 discusses some other instrument developments that have been aimed at improving the sensitivity and specificity of PTR-MS and extending its use to other applications in atmospheric sciences. The use of reagent ions other than  $H_3O^+$  facilitates measurements of compounds that do not react with  $H_3O^+$  or allow better separation of isomeric VOCs. PTR-MS has also been used for the chemical analysis of fine particles and for determining bulk chemical properties of an air mass, such as the lifetime of hydroxyl (OH) radicals.

Several reviews of PTR-MS have been published previously. The Lindner group published several summaries of the design and operation of the quadrupole PTR-MS instruments and results from applications in the environmental, food, and medical fields.<sup>14,28,29</sup> Hewitt and co-workers published a tutorial review specific to the use of PTR-MS for measurements of atmospheric VOCs.<sup>30</sup> A later review from our own group summarized what had been learned about the sensitivity and selectivity of atmospheric VOC measurements by PTR-MS.<sup>21</sup> Blake and co-workers published a detailed and more general

review of PTR-MS and applications to atmospheric chemistry, plant studies, food science, and medical applications.<sup>31</sup> Biasioli and co-workers reviewed PTR-MS in the context of other real-time mass spectrometry methods such as atmospheric-pressure ionization (APCI) mass spectrometry and selected-ion flow-tube mass spectrometry (SIFT-MS).<sup>32</sup> Since then only a brief summary of PTR-MS was published by Hartungen and co-workers, which included some of the newest instrument developments.<sup>33</sup> Ellis and Mayhew published a book to introduce the principles of PTR-MS and its applications in environmental sciences, food sciences, medical science, and the field of safety and security.<sup>34</sup> It is the purpose of this Review to provide a synthesis of the information needed to interpret atmospheric VOC measurements by PTR-MS, summarize some recent research highlights, and introduce some other applications and instrument developments. Much of this research is based on PTR-MS instruments with high-resolution time-of-flight mass spectrometers, which were only in their infancy at the time of most of the above review articles.

## 2. PROTON-TRANSFER-REACTION MASS SPECTROMETRY

### 2.1. Instrument Configurations

A PTR-MS instrument usually consists of four different parts, namely, ion source, drift tube, ion interfaces, and mass analyzer. The ion source produces high-purity hydronium ions ( $\text{H}_3\text{O}^+$ ), which are introduced to the drift tube for proton-transfer reactions. In the drift tube, a VOC species (R) with higher proton affinity than  $\text{H}_2\text{O}$  (691 kJ mol<sup>-1</sup>) can be ionized via proton transfer with  $\text{H}_3\text{O}^+$  to produce the product ions ( $\text{RH}^+$ ) (eq 1).



Along with  $\text{H}_3\text{O}^+$ , the product ions are then transmitted through the ion interfaces to a mass analyzer for detection.

As discussed in section 1, many versions of PTR-MS instruments have been developed in the past decade. The different versions of PTR-MS introduced by commercial companies (Ionicon Analytik and Kore Technology) or custom-built by various research groups are illustrated in Figure 1. In this section, we summarize the evolution of instrument configurations for PTR-MS and describe the improvement from recent instrument developments.

**2.1.1. Drift Tube.** The drift tube of PTR-MS commonly consists of stainless steel rings at different voltages to establish a homogeneous electric field that prevents the formation of hydronium water clusters. The stainless steel rings are usually separated by Teflon rings to seal the vacuum and electrically isolate the charged stainless steel rings.<sup>21</sup> The reagent ion distribution and ion chemistry in the drift tube are well-understood. The reagent ion distribution in the drift tube highly depends on the reduced electric field parameter  $E/N$ ,<sup>21</sup> where  $E$  is the electric field and  $N$  is the number density of the gas in the drift tube. The  $\text{H}_3\text{O}^+$  ions dominate the reagent ions when  $E/N$  is  $>100$  Td (Townsend, 1 Td =  $10^{-17}$  V cm<sup>2</sup>), whereas  $\text{H}_3\text{O}^+(\text{H}_2\text{O})$  ions are most abundant at lower  $E/N$  (60–100 Td).<sup>21</sup> Higher hydronium water clusters (e.g.,  $\text{H}_3\text{O}^+(\text{H}_2\text{O})_2$ ) are not important under the operating conditions of PTR-MS.<sup>21</sup> The drift tube is typically ~10 cm long, and it is commonly held at a pressure of ~2.0–4.0 mbar (pressures in higher range have been used for the PTR-QiTof<sup>24</sup>). By applying a voltage of 600–700 V to the two ends

of the drift tube along with a resistor network to divide the overall voltage, the drift tube can be operated at the desired electric field. The temperature of the drift tube is commonly maintained at an elevated temperature (40–60 °C) to minimize memory effects but below 100 °C to avoid melting of the Teflon rings.

The drift-tube configurations have changed little in the last two decades, although many new versions of PTR-MS have been introduced (e.g., with ToF-MS and other ion guides) (Figure 1). The exceptions include (1) the ion funnel introduced by Kore Technology, in which the first part acting as the drift tube is operated at lower  $E/N$  (this will be discussed later in this section);<sup>35,36</sup> (2) the novel PTR3 instrument, in which a triple is used as the reaction chamber (see detailed description in section 5.2).<sup>37</sup> For these two instruments, the reagent ion distribution and ion chemistry in the drift tube (or reaction chamber) are different from those in the conventional PTR-MS.

Other materials have been considered for the construction of the drift tube for PTR-MS. Resistive glass has been used with the aim of minimizing the internal surfaces and operating the drift tube at elevated temperature (up to 250 °C), which facilitates detection of low-volatility species for aerosol-measurement applications<sup>38</sup> and reduces response time for sticky compounds (e.g., ammonia).<sup>39</sup> Recently, a PTR-MS with a drift tube made of conductive polyether ether ketone (PEEK) demonstrated better quantification of organic peroxides resulting from isoprene oxidation (isoprene hydroxy hydroperoxides, ISOPOOH), as these labile compounds easily undergo decompositions on contact with metal surfaces.<sup>40</sup>

**2.1.2. Mass Analyzers.** The initial development of PTR-MS<sup>19</sup> and the commercial version later introduced by Ionicon Analytik<sup>14,28</sup> used a quadrupole mass spectrometer (QMS) for the ion detection. With the exception of a few field studies that scanned all of the nominal masses in the selected mass range (e.g.,  $m/z$  21–160),<sup>41,42</sup> PTR-QMS instruments in most studies only recorded 10–20 masses consecutively, each with a dwell time between 0.1 s and several seconds (often referred to as selected ion mode or SIM).<sup>43</sup> The time resolution of PTR-QMS is usually sufficient for ground measurements but not ideal for measurements from research aircraft and for eddy covariance flux measurements. Research aircraft can travel at a speed of ~100 m/s, which results in a spatial resolution of 1–2 km for typical aircraft-measurement settings (scanning 10–15 masses each at 1 s). The spatial resolution of 1–2 km may impose some limitations on characterizing narrow pollution plumes, e.g., small fires<sup>44</sup> or industrial sources. For flux measurements, the direct eddy covariance method is usually not used with PTR-QMS because measuring multiple VOC species at 10 Hz is not possible.<sup>45</sup> An alternative method, referred to as virtual disjunct-eddy covariance (vDEC), has been adopted for numerous flux measurements using PTR-QMS. In vDEC, air is continuously introduced into the instrument and each mass is recorded at ~0.1 s to achieve a disjunct time interval of 1–2 s.<sup>45</sup> Another drawback of quadrupole mass analyzers is their low ion transmission of heavier masses, leading to low sensitivities of high-mass compounds and difficulty to detect them in PTR-QMS.<sup>46,47</sup> In addition to ordinary PTR-QMS, a PTR-MS equipped with a triple quadrupole tandem mass spectrometer (QqQ-MS) demonstrated the applications of MS/MS studies through collision-induced dissociation (CID) to explore the separation of isomers<sup>48</sup> (see details in section 5.3).

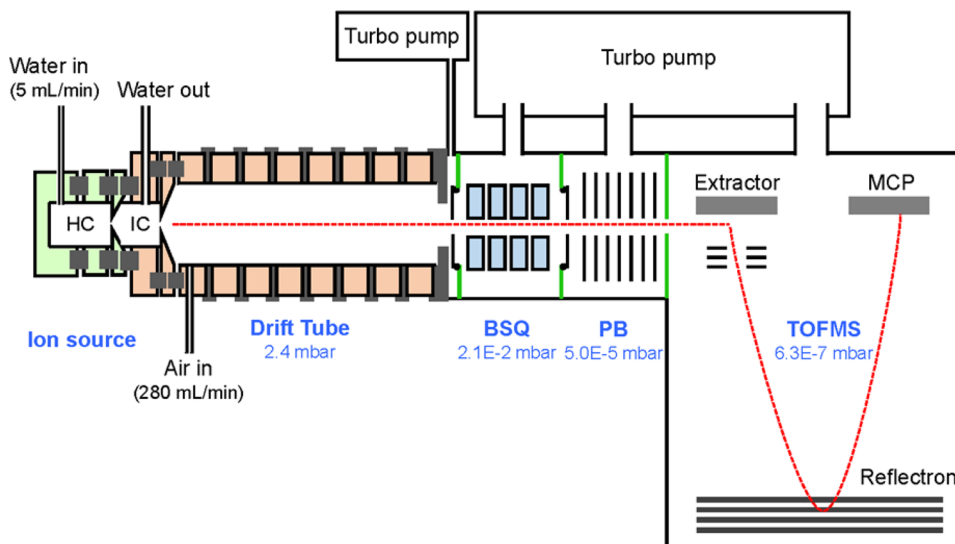


**Figure 2.** Schematic drawing of the NOAA  $\text{H}_3\text{O}^+$  ToF-CIMS. The instrument is modified from the one reported by Yuan et al.<sup>51</sup> by removing the small segmented quadrupole (SSQ). We note that this instrument is conceptually similar to the PTR-QiTof<sup>24</sup> introduced by Ionicon Analytik. HC, hollow-cathode discharge; IC, intermediate chamber; BSQ, big segmented quadrupole; PB, primary beam; MCP, microchannel plate detector.

To overcome the limitations of quadrupole mass analyzers, PTR-MS instruments using other mass analyzers have been developed. A PTR-MS with an ion-trap analyzer (PTR-IT-MS, also referred to as PIT-MS) was demonstrated first by Prazeller and co-workers.<sup>49</sup> This prototype instrument had a poor sensitivity with detection limits at ~100 parts per billion by volume (ppbv), limiting its use in ambient measurements. Later, several PTR-IT-MS instruments were constructed by other groups using quadrupole ion traps or linear ion traps as mass analyzers.<sup>25,26,50</sup> The main advantages of PTR-IT-MS over PTR-QMS have been experimentally demonstrated:<sup>25,26</sup> (1) The IT-MS can analyze a whole mass spectrum almost simultaneously (~20 ms). (2) CID analysis can be performed in the ion trap, which can be useful in distinguishing different ions with the same nominal mass (this will be discussed in detail in section 5.3). In addition, buffer gas containing certain VOCs can be introduced into the ion trap to induce further reactions, which can afford additional selectivity.<sup>51</sup> However, the application of PTR-IT-MS to atmospheric measurements has been limited, as the result of (1) high detection limits for some instruments and (2) the lack of a commercially available PTR-IT-MS. Measurements of VOCs in the atmosphere using PTR-IT-MS were mainly performed by the NOAA group in urban plumes<sup>52,53</sup> and biomass-burning emissions.<sup>54</sup>

The third mass analysis technique used for PTR-MS is time-of-flight mass spectrometry (ToF-MS). Several abbreviations have been used for PTR-MS with time-of-flight mass spectrometer. In this Review, the most common acronym, PTR-TOF, will be used. The first application of ToF-MS in PTR-MS was demonstrated by the group at the University of Leicester.<sup>55,56</sup> This PTR-TOF instrument contained an orthogonal reflectron ToF (mass resolution  $\approx 1000$ ) and a radioactive ion source. The sensitivity of the PTR-TOF was low (up to 0.17 counts per second per ppbv, i.e., cps/ppbv),<sup>56</sup> resulting in relatively high detection limits for various VOCs (~10 ppbv for 1 min integration time).<sup>55</sup> Later, two other PTR-TOF instruments were built by British<sup>57</sup> and Japanese groups<sup>58,59</sup> using reflectron ToF-MS and linear ToF-MS, respectively. Similar to the instrument developed by Blake et al.,<sup>56</sup> these early PTR-TOF instruments had low sensitivities

(<5 cps/ppbv) and relatively high detection limits (>1 ppbv for 1 min integration time). A PTR-TOF instrument with substantially higher sensitivities (10–50 cps/ppbv) and lower detection limits (pptv level for 1 min integration time) was demonstrated by a prototype built at University of Innsbruck<sup>22</sup> and was later commercialized by Ionicon Analytik (PTR-TOF 8000).<sup>23</sup> Originally, the Ionicon PTR-TOF instruments used orthogonal reflectron ToF-MS (both HTOF and C-TOF) from Tofwerk AG with mass resolution of >4000 and >1500, respectively. Later, a TOF-MS designed by Ionicon with a mass resolution of ~1000 was used for compact PTR-TOF instruments (PTR-TOF 1000).<sup>60</sup> A prototype PTR-TOF 1000 was deployed on the NASA P3-B aircraft to provide high-spatial-resolution measurements of many VOC species in the Central Valley region of California.<sup>60</sup>

Several advantages of PTR-TOF over PTR-QMS led to a quick expansion of PTR-TOF applications in the atmospheric sciences. First, PTR-TOF can acquire the whole mass spectrum simultaneously (on the order of 30–50  $\mu\text{s}$ ).<sup>22</sup> This multiplexing advantage helped to increase the sensitivity of the measurements. An example is shown in an intercomparison study between a PTR-TOF and a PTR-QMS: an earlier commercial version of PTR-TOF (i.e., PTR-TOF 8000) detected more ions at the same concentration (i.e., counts/ppbv) than PTR-QMS, provided the PTR-QMS scanned more consecutive masses than 10–35 compounds, even though the sensitivity of this PTR-TOF was ~10–35 times lower than PTR-QMS when only one VOC is measured.<sup>43</sup> For measurements on aircraft or other mobile platforms, a much higher time (e.g., 1 s) and spatial resolution can be achieved with PTR-TOF, compared to 10–20 s for deployments of PTR-QMS.<sup>60,61</sup> Second, the high mass resolution of PTR-TOF enables separation of isobaric masses. It has greatly enhanced the analytical capabilities of the technique, by increasing the number of compounds that can be quantified and reducing the possibility of chemical interferences for the targeted compounds. For example, the separation of isoprene ( $\text{C}_5\text{H}_8\text{H}^+$ ) and furan ( $\text{C}_4\text{H}_4\text{OH}^+$ ) at  $m/z$  69 in biomass-burning emissions makes measurements of both compounds possible. In addition, some impurity ions from the ion source may contribute to the background signals of

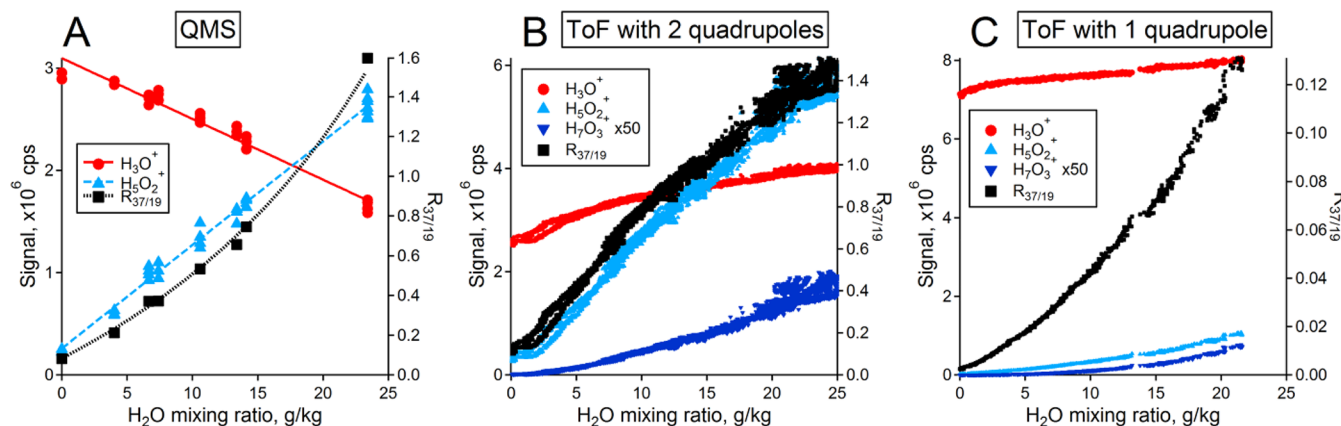


**Figure 3.** Reagent ion signals as a function of water vapor mixing ratios for (A) PTR-QMS,<sup>21</sup> (B)  $\text{H}_3\text{O}^+$  ToF-CIMS with two RF-only quadrupoles,<sup>61</sup> and (C)  $\text{H}_3\text{O}^+$  ToF-CIMS with one RF-only quadrupole ion guide that is very similar to the design of PTR-QiTof with only one quadrupole as ion guide. The ratio of  $\text{H}_5\text{O}_2^+$  to  $\text{H}_3\text{O}^+$  ( $R_{37/19}$ ) is also shown in the right axis.

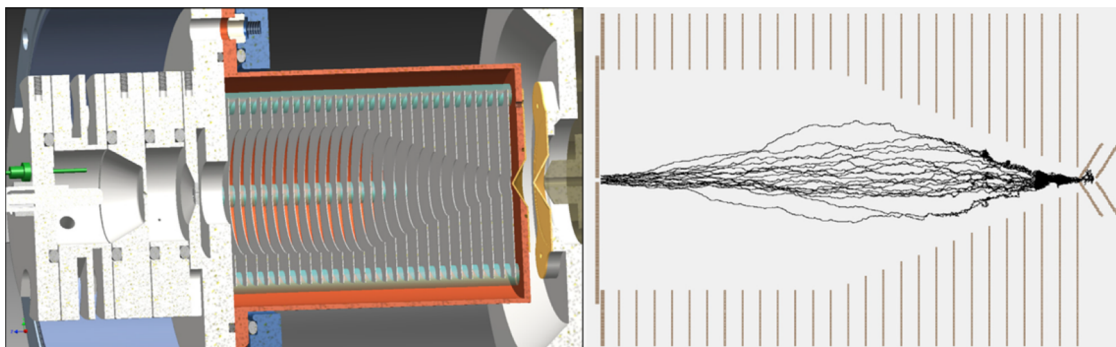


**Figure 4.** (Left) 3-D design image of an ion funnel in a PTR-MS instrument. The ion funnel consists of a series of 27 plates, mounted on PEEK rods and housed in a vacuum chamber (red). Ion source and skimmers are also shown. (Right) Ion trajectories calculated using SIMION 8.0.4 for  $m/z$  107 with RF = 240 V,  $f$  = 820 kHz, dc = 60 V, and buffer gas pressure 1.80 mbar. Reprinted with permission from ref 36. Copyright 2017 Elsevier.

several compounds in PTR-TOF, e.g.,  $\text{O}_2\text{H}^{+60}$  at  $m/z$  33 where methanol is detected and  $\text{CO}_2\text{H}^+$  at  $m/z$  45 where acetaldehyde is detected. Separation of these impurity ions from VOC ions can reduce the background signals of these VOCs.

Other types of mass spectrometers may be used as mass analyzers for PTR-MS as well. In particular, ultrahigh-resolution mass spectrometers, such as Fourier transform ion cyclotron resonance (FTICR) and orbitrap,<sup>62</sup> would allow better separation of isobaric peaks and accurate assignments of elemental compositions. Proton-transfer chemistry was induced by introducing water and VOC in sequence to the ion cyclotron resonance cell of a FTICR mass spectrometer for VOCs measurements from both gasoline evaporation<sup>63</sup> and polypropylene thermal oxidation.<sup>64</sup> However, coupling the conventional ion source and drift tube of PTR-MS to FTICR or orbitrap mass spectrometers has not been attempted yet. These mass analyzers are more expensive and are not as portable as the other above-mentioned mass analyzers.

**2.1.3. Ion Interfaces between Drift Tube and Mass Analyzer.** In PTR-QMS, ions from the drift tube pass through a differential pumping stage containing electrostatic ion lenses before entering the quadrupole mass analyzer. An additional differential pumping stage pulled by a third turbo pump was added in the ion lenses region of QMS in the mid-2000s, so that the sampling orifice for the QMS could be increased to improve ion-transmission efficiency.<sup>21</sup> This improved PTR-QMS was referred to as high-sensitivity PTR-QMS by Ionicon Analytik.

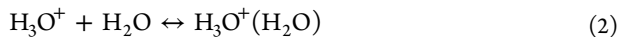
The first version of PTR-TOF from Ionicon followed a similar design as PTR-QMS for ion transmission: a differential pumping stage and an Einzel-lens system for ion transmission and focusing.<sup>22</sup> A PTR-TOF instrument equipped with a radio frequency (RF)-only quadrupole ion guide that transmits ions more efficiently was introduced by Ionicon in 2014 (PTR-QiTof).<sup>24</sup> The PTR-QiTof enabled an average increase of sensitivity by a factor of 25, compared to PTR-TOF using the conventional lens system.<sup>24</sup> A similar PTR-TOF instrument modified from the Aerodyne time-of-flight chemical ionization mass spectrometer (ToF-CIMS) using RF-only quadrupole ion guides was constructed by the NOAA group (referred to as  $\text{H}_3\text{O}^+$  ToF-CIMS). The current version is shown in Figure 2. The  $\text{H}_3\text{O}^+$  ToF-CIMS has VOC sensitivities in the range of 100–1000 cps/ppbv. These were also significantly higher than those for the Ionicon PTR-TOF using the conventional lens system.<sup>61</sup> Although PTR-TOF instruments that use quadrupole ion guide(s) have significantly better sensitivity resulting from more efficient ion transmission, there are some surprising consequences from the use of quadrupole ion guides.<sup>61</sup> The low-mass cutoff of RF-only quadrupoles<sup>65</sup> leads to a lower transmission efficiency of  $\text{H}_3\text{O}^+$  relative to other ions.<sup>61</sup> It can result in the increase of both  $\text{H}_3\text{O}^+$  and water cluster signals with increasing humidity (Figure 3), and their relationship is usually not possible to describe using linear functions. This makes it difficult to understand the distribution of  $\text{H}_3\text{O}^+(\text{H}_2\text{O})_n$  water cluster ions in the drift tube. This issue also complicates the normalization to the reagent ions, because defining a signal

that describes the intensity of the ion source but is humidity-independent is challenging.<sup>61</sup> The difference between the initial version of H<sub>3</sub>O<sup>+</sup> ToF-CIMS shown by Yuan et al.<sup>61</sup> and the PTR-QiTof is the number of quadrupole ion guides: H<sub>3</sub>O<sup>+</sup> ToF-CIMS has two in series (SSQ and BSQ), whereas PTR-QiTof only uses one. Yuan et al.<sup>61</sup> showed that there might be some secondary chemistry in the first quadrupole (SSQ) operated at a relatively high pressure (1.3 mbar), which induces stronger humidity dependence of the reagent ions and normalized product ion signals. A further modification by removing the first quadrupole in the H<sub>3</sub>O<sup>+</sup> ToF-CIMS (Figure 2) resulted in a significantly weaker humidity dependence, but the low-mass cutoff still remains (although less severe than before) (Figure 3C). The PTR-QiTof instrument has not been described in similar detail but may be expected to behave similarly to the modified H<sub>3</sub>O<sup>+</sup> ToF-CIMS. In addition to RF-only quadrupole, Ionicon Analytik recently introduced a new version of PTR-TOF using hexapoles as ion guides (PTR-TOF 4000) ([www.ionicon.com/product/ptr-ms/ptr-tofms-series/ptr-tof-4000](http://www.ionicon.com/product/ptr-ms/ptr-tofms-series/ptr-tof-4000)).

Some efforts have been made to enhance the extraction of ions from the drift tube. Radio frequency (RF) ion funnels are a type of novel ion guide that can be used to enhance the sampling of ions through an orifice.<sup>66</sup> In ion funnels, an RF electric field is applied to a series of electrodes with diminishing aperture sizes. The electrodes provide strongly repulsive effective potentials at the edge of the electrode, radially focusing the ions. The first demonstration of an ion funnel in PTR-MS was shown by Barber et al.<sup>35</sup> The first part of the ion funnel was used as a standard drift-tube reactor but was run at a lower E/N (60 Td) than standard PTR-MS (see Figure 4). The RF electric field was only applied to the second section with diminishing orifice sizes. The sensitivity of this PTR-MS instrument with an ion funnel was 1–2 orders of magnitude higher than standard PTR-MS but varied greatly by compound.<sup>35,36</sup> A subsequent characterization of the ion-funnel device indicated that heavier masses are favorably transmitted in the ion funnel.<sup>36</sup> It is also concluded that the increase in sensitivity was due to the combined effect of better focusing and longer reaction time.<sup>36</sup> Some unusual fragmentation patterns for several VOCs were also observed with the ion-funnel device.<sup>36</sup> The different electric fields in the two parts of the ion funnel created contrasting water-cluster distributions,<sup>36</sup> which might explain the distinctive response for various VOC species. The use of an ion funnel in PTR-TOF was also recently reported by Ionicon Analytik in the PTR-TOF 1000 Ultra instrument.<sup>67</sup> In contrast to the instrument described by Barber et al.,<sup>35</sup> the ion funnel in Ionicon instruments is used only to focus ions after they exit the drift tube.<sup>67</sup> A detailed introduction and characterization of the instruments with ion funnel from Ionicon Analytik is not available yet.

## 2.2. Ion Chemistry

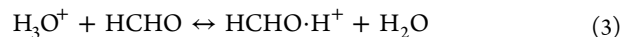
The reagent ion distribution and cluster formation in the drift tube of PTR-MS are well-understood. H<sub>3</sub>O<sup>+</sup> ions are the most abundant ions in the drift tube at typical operating conditions. Water-cluster ions, e.g., H<sub>3</sub>O<sup>+(H<sub>2</sub>O)</sup> and H<sub>3</sub>O<sup>+(H<sub>2</sub>O)<sub>2</sub></sup>, are present in the drift tube, and the abundance of water-cluster ions increases with humidity in the analyzed air.<sup>21</sup>



Trace water from the ion source can humidify the sample air, and this effect varies significantly among different PTR-MS

instruments. The drift tube in PTR-MS has been commonly run with an E/N of 100–120 Td. At this electric field range, the signals of water-cluster ions are small, and fragmentation of most product ions is not significant. The humidity dependence of the VOC sensitivity is usually stronger at lower E/N, whereas the VOC sensitivity may be compromised at higher E/N as the result of fragmentation and shorter reaction times. As discussed in section 2.1, most PTR-MS instruments still use the drift-tube design employed by the PTR-QMS reviewed by de Gouw and Warneke.<sup>21</sup> Thus, we do not expect large differences in the reagent ion distribution and ion chemistry in the drift tube for new versions of PTR-MS instruments (see exceptions in discussions of Drift Tube). However, the implementation of new ion interfaces in PTR-MS instruments may lead to an observed reagent ion distribution that differs from that in the standard drift tube (see examples in Figure 3). The discrepancies can come from secondary ion chemistry, declustering effects with stronger electric fields in the ion interfaces, and low-mass cutoff for RF-only multipoles.

In addition to the formation of water-cluster ions, water molecules can participate or alter the equilibrium of secondary reactions, which may affect VOC measurements. A well-known example is the PTR-MS measurement of formaldehyde. Due to the slightly higher proton affinity of formaldehyde (713 kJ mol<sup>-1</sup>) than that of water (691 kJ mol<sup>-1</sup>), the back-reaction of water molecules with protonated formaldehyde is competitive with the protonation reaction of formaldehyde, leading to a low and strongly humidity-dependent sensitivity of formaldehyde in PTR-MS.<sup>68–70</sup>



Similar strong humidity dependence is observed for several other species that have proton affinities only slightly higher than that of water, e.g., hydrogen cyanide (HCN),<sup>91,72</sup> hydrogen sulfide (H<sub>2</sub>S),<sup>73,74</sup> and isocyanic acid (HNCO).<sup>61</sup>

It is recognized that the protonated ions of alcohols fragment significantly by losing a water molecule during proton transfer.<sup>31,75</sup> The branching ratio of the protonated molecular ions and dehydrated ions exhibits a humidity dependence, associated with more dehydrated ions under dry conditions, which results in a higher sensitivity to alcohols at more humidified conditions.<sup>61,76</sup> Moreover, protonated ions for some VOCs can undergo reactions with water molecules to form hydrated product ions in PTR-MS. These hydrated product ions may complicate the interpretation of mass spectra and act as interferences for the detection of other VOCs at the same nominal mass, especially for PTR-QMS instruments without the ability to separate isobaric ions. Examples are the hydrated ion of acetaldehyde (C<sub>2</sub>H<sub>4</sub>OH(H<sub>2</sub>O)<sup>+</sup>) and DMS (C<sub>2</sub>H<sub>6</sub>SH<sup>+</sup>), which are both detected at *m/z* 63.<sup>20</sup> The humidity dependence shown in the above-mentioned examples reflects the fact that the abundance of water molecules in the drift tube can affect the equilibrium ratios of respective ion pairs for these dehydration and hydration reactions.<sup>61</sup> Moreover, the degrees of fragmentation for monoterpenes,<sup>77,78</sup> sesquiterpenes,<sup>79</sup> and C<sub>10</sub> aromatics<sup>77</sup> decrease with higher humidity, although the fragmentation involves no dehydration process. This humidity dependence of fragmentation is smaller than those involving dehydration but may be non-negligible for these species. The lower fragmentation with the presence of more water for these compounds may be due to different internal excitation from collisions with the H<sub>3</sub>O<sup>+</sup> and H<sub>3</sub>O<sup>+(H<sub>2</sub>O)</sup> reagent ions.<sup>78</sup>

### 2.3. Analysis of PTR-TOF Data

The data-reduction procedures of PTR-MS, i.e., converting ion signals to VOC concentrations, usually involves signal normalization to the reagent ions, background correction, and calculation of concentrations based on the determined sensitivities. The procedures of data analysis of PTR-MS were discussed in several previous publications<sup>20,80</sup> and were summarized in a previous review.<sup>21</sup> For PTR-TOF instruments, additional analysis steps are needed to acquire the signals of individual ions from the collected raw mass spectra. This section will provide a general guideline to this additional ToF-MS data processing. Some of the data-reduction procedures related to converting raw signals to VOC concentrations are provided in section 2.4.

**2.3.1. ToF Data-Processing Procedures.** As shown earlier in section 2.1, PTR-TOF can have much higher mass resolution ( $m/\Delta m$ ) than PTR-QMS. Many studies have shown that PTR-TOF instrument with an  $m/\Delta m$  of 4000–6000 (a typical mass resolution for HTOF products from Tofwerk AG, e.g., PTR-QiTof and PTR-TOF 8000) is sufficient to distinguish many isobaric masses below  $m/z$  200.<sup>22</sup> Distinction of isobaric masses is also possible for a limited number of lighter masses (below  $m/z$  100) using a PTR-TOF with a lower  $m/\Delta m$  of 1000–2000 (a typical mass resolution for CTOF products from Tofwerk, such as PTR-TOF 2000, and the TOF built by Ionicon Analytik, such as PTR-TOF 1000) using an advanced data-processing algorithm.<sup>60,81</sup> However, even with high-resolution PTR-TOF, many isobaric ions are not fully resolved, i.e., the peaks overlap. The intensities of these masses can be retrieved using high-resolution “peak-fitting” algorithms. Other algorithms are needed to account for detector response, converting from time-of-flight to mass-to-charge ratio, and other ToF-specific corrections. Some of the routines are also applicable to lower-resolution PTR-TOF instruments ( $m/\Delta m = 1000–2000$ ), such as conversion from ToF time scale to mass scale and limited high-resolution peak fitting. The details of this analysis are similar to those used in other instrumentation employing TOF technology (e.g., Aerodyne Aerosol Mass Spectrometer and Aerodyne TOF-CIMS).<sup>82,83</sup>

The data-processing procedures from raw PTR-TOF mass spectra to individual ion signals usually involve the following analysis steps: (I) combined Poisson counting statistics and dead time correction; (II) baseline correction; (III) determination of peak shape; (IV) mass calibration; (V) generation of peak list; (VI) high-resolution peak fitting; and (VII) correction of ToF mass discrimination.

(I) Combined Poisson counting statistics and dead time correction: For PTR-TOF instruments equipped with time-to-digital converters (TDCs) that can only detect either 0 or 1 ions per time bin, the raw mass spectra need to be corrected for Poissonian counting statistics and instrumental dead times before other data analysis.<sup>84,85</sup> The two effects result in underestimation of ion signals with high intensities and limit the dynamic range of ion measurements.<sup>86</sup> Titzmann et al.<sup>84</sup> developed a simple formula to correct for both effects. We note that some TOF-MS equipped with an analogue-to-digital converter (ADC) (e.g., NOAA  $\text{H}_3\text{O}^+$  ToF-CIMS) do not need this correction, as the ADC can convert raw signals to counts using a premeasured single-ion signal (SIS), and hence a larger dynamic range can be achieved.<sup>87</sup>

(II) Baseline correction: The baseline is the signal underneath a peak that is from background ions and electronic noise in the ToF mass spectra. Note that the baseline should not be

confused with instrument backgrounds discussed later, which are instrument signals when VOCs are absent from the air sample. Baseline correction is commonly performed by finding the signals at the middle points of two adjacent nominal masses and interpolating these signals over the range of measured masses using various methods, such as polynomial fits.<sup>83,87</sup> A smoothing method that uses a low-pass filter is also proposed as an effective way for baseline correction.<sup>88</sup>

(III) Determination of peak shape: It has been shown that mass-spectral peaks do not usually exhibit an ideal Gaussian shape. The peak shape can be influenced by the exact settings of the instrument. The peak shape is one of the required constraints for high-resolution peak fittings. Thus, it is important to determine the unique peak shape in the mass spectra. Ion peaks are first normalized using their centered locations and peak widths, which is expected to show a linear relationship with  $m/z$ .<sup>87,88</sup> Peak shape is subsequently obtained by averaging the normalized peak shapes of isolated ion peaks, i.e., nominal masses that are predominately contributed by one ion.

(IV) Mass calibration: The mass calibration (or  $m/z$  calibration) is used to convert the ion time-of-flight to mass-to-charge ratio ( $m/z$ ). Ion time-of-flight in TOF-MS is theoretically proportional to the square root of  $m/z$  of the ion.<sup>65</sup> Fitting the equation ( $\text{ToF} = a + b\sqrt{m/z}$ ) to isolated peaks is the common practice for mass calibration. Sometimes, a modified equation may be used ( $\text{ToF} = a + b(m/z)^c$ ) to account for potential nonideal extraction processes that can cause the term  $c$  to be slightly different from 0.5.<sup>83</sup> Several reagent ions, impurity ions, and ions from ubiquitous VOCs can be used for the mass calibration of PTR-TOF, e.g.,  $\text{H}_3\text{O}^+$ ,  $\text{H}_3\text{O}^+(\text{H}_2\text{O})$ ,  $\text{O}_2^+$ ,  $\text{NO}^+$ , and  $\text{C}_3\text{H}_6\text{OH}^+$  mainly from acetone.<sup>89</sup> Ions originating from transition metals released from the ion source may also serve as the purpose, e.g.,  $\text{FeH}_5\text{O}_4\text{H}^+$  ( $m/z$  125.961).<sup>61</sup> However, ions above  $m/z$  130 that are suitable for mass calibration are usually absent. Internal standards for mass calibration can be continuously added to the PTR-TOF inlet using simple diffusion sources. Compounds used for the internal standard include 1,4-dichlorobenzene,<sup>22,85</sup> 1,2,4-trichlorobenzene,<sup>22,85</sup> 1,3,5-trichlorobenzene,<sup>61</sup> and 1,3-diiodobenzene.<sup>90</sup> These compounds do not fragment significantly in PTR-TOF, or their fragmentation ions do not overlap with VOC ions of interest. An overall mass-calibration accuracy of 5–10 parts-per-million (ppm) is typically achieved for high-resolution PTR-TOF.

(V) Generation of peak lists: The peak list is important in the peak fitting of mass spectra. Two methods can be used to supply the peak list: (a) a user-defined peak list or (b) a computer-generated peak list. For a user-defined peak lists, users need to load or create a list of ions with defined  $m/z$  and chemical formulas before peak fitting. If the chemical formula is unknown or difficult to determine, ions with only their  $m/z$  (unknown peaks) can be used. To create the user-defined peak list, the users need to explore the mass spectra and compare observed peaks with possible chemical formulas that are relevant for the type of measurement, e.g., biomass burning or urban atmospheres. For computer-generated peak lists, the peak-fitting software uses various algorithms to detect peaks and their locations, commonly based on user-provided criteria (e.g., residual threshold).<sup>85,87</sup> Compared to user-defined peak lists, computer-generated peak lists significantly reduce the time burden on the users. However, peak fitting using user-defined peak lists may produce more accurate results, assuming the

assignments of chemical formulas to the ions are correct. First, chemical formulas in the user-defined peak list can provide the isotopic distribution of each ion. The isotopic signals from lower masses can be subtracted from measured signals at higher masses before peak fitting for the higher mass. This can be especially important for even masses associated with large proportions of signals from isotopes. Second, the ions in the computer-generated peak lists usually deviate from the respective “true” locations calculated from chemical formulas, which can induce errors in the peak-fitting process.

(VI) High-resolution peak fitting: Using the determined peak lists and peak shape, high-resolution peak fitting determines the amplitude of each overlapping ion, by minimizing the least-squares difference between measured and calculated signals at each nominal mass.<sup>83</sup> The fits are commonly performed in the time-of-flight space, and the results are converted to  $m/z$  space,<sup>83</sup> owing to the nonlinear transformation between them. Several algorithms fit directly to the measured signals. A slightly different method, which fits the cumulative distributions of signals for each nominal mass, has also been developed.<sup>81,84,85</sup>

(VII) Correction for mass discrimination: Smaller ions pass more quickly through the orthogonal extraction region of the ToF-MS, which introduces a mass-dependent discrimination between different ions. A correction for this duty-cycle bias is commonly applied.<sup>85</sup> As the duty cycle of the masses is proportional to  $\sqrt{m/z}$ , the mass signals at  $m/z$  are usually multiplied by the term  $\sqrt{(m/z)_0/(m/z)}$ , where  $(m/z)_0$  is the reference  $m/z$ . The choice of the reference  $m/z$  is arbitrary and is commonly chosen as either the maximum  $m/z$  for the recorded mass spectra<sup>85,91</sup> or another important mass.<sup>61</sup> We stress that whether duty-cycle correction is performed (and the reference  $m/z$  used for the correction) should be mentioned for PTR-TOF data in scientific papers. This is necessary to compare ion signals between different instruments. It is important to note that the raw signals without duty-cycle correction should be used to calculate the counting statistics errors for ions (e.g., calculation of detection limits or error matrix for positive matrix factorization (PMF) analysis). Another mass discrimination induced by operating the microchannel plate (MCP) detectors at low gain is not easy to correct and should be avoided during operation.<sup>92</sup>

**2.3.2. Availability of Software Tools.** There are several software tools available for analyzing PTR-ToF data, including the Tofwerk/Aerodyne Tofware program,<sup>83,88</sup> the PTR-TOF Data Analyzer from the University of Innsbruck,<sup>85</sup> and the PTRwid from Utrecht University.<sup>93</sup> A comparison between the three software tools is shown in Table 1. A tool provided by Ionicon (PTR-MS Viewer) is also available to analyze Ionicon PTR-TOF data, e.g., mass calibration and high-resolution peak fitting. There are significant differences among these tools, ranging from available software environments to the detailed methods used for each data-processing procedure. Because of these differences, an intercomparison using the same sample data set would be extremely useful for the user community. It is worth noting that another Matlab-based software tool for analyzing ToF data was developed at the University of Helsinki,<sup>94</sup> but its use in analyzing PTR-TOF data has yet to be demonstrated.

**2.3.3. Errors from High-Resolution Peak Fitting.** The high-resolution peak fitting can introduce errors in the retrieved signals of the high-resolution peaks. Several recent studies have identified the sources of errors, including errors in mass

Table 1. Comparison between the Software Tools for Analysis of ToF Data

software	Tofwerk Tofware <sup>83,88</sup>	PTR-TOF data analyzer <sup>85</sup>	PTRwid <sup>93</sup>
webpage	<a href="https://goo.gl/g7m0KI">https://goo.gl/g7m0KI</a>	<a href="https://goo.gl/NK5Zmk">https://goo.gl/NK5Zmk</a>	<a href="https://goo.gl/9rV7pg">https://goo.gl/9rV7pg</a>
software availability	Igor Pro, available for both PC and Mac license from Tofwerk	Matlab or Matlab virtual machine, available for both PC and Mac free for research purpose	IDL or IDL virtual machine free
instrumentation	all instruments using Tofwerk ToF products (e.g., PTR-QTOF and PTR-TOF 8000)	all Ionicon PTR-TOF	tested for PTR-TOF 8000, PTR-QTOF, and PTR-TOF 1000
updates	periodical updates	updates, but less frequently	some updates (two versions now)
tutorial	group/individual tutorial	tutorial video	quick start instructions and brief manual in the PTRwid paper
mass calibration	user-defined list; user can provide different lists for different periods; time series of mass-calibration accuracy can be checked	user-defined list; the list needs to be the same as the list to determine peak shape	fully automated mass-scale calibration
peak shape peak list	automatic and manual calculation of peak shape user-provided list; peak list can be generated from mass spectra (rarely used)	use the same list for mass calibration can only be generated from the mass spectra; newer versions (v4.2) provide an option to change or generate a peak list and assign ions to chemical formula	automatic determination of peak shape individual peak lists are generated from each file and can be combined to a unified peak list
peak fitting	least-squares fit directly to the signals	fiting to the cumulative distributions of the signals	integrating signals for each peak within 2 standard deviations around the peak maximum; limited ability to separate overlapping peaks

calibration,<sup>95</sup> errors in peak shape,<sup>95</sup> and errors due to separation of overlapping peaks.<sup>81,96</sup> For simple well-separated peaks, the errors are mainly caused by the bias and imprecision of the mass calibration and the errors can be scaled linearly with the signals (usually a few percent of the signals, ~4%).<sup>95</sup> As a result, the peak-fitting imprecision may dwarf the imprecision from Poisson counting statistics for high-intensity signals (which scales as the square root of the signals).<sup>95</sup>

The errors from peak separation are important for overlapping peaks. For a peak separation of ~2–3 times of the half-width at half-maximum (HWHM), the imprecision of signals is similar to that of well-resolved peaks.<sup>96</sup> For smaller peak separations and higher ion counts (>1000), the imprecision of signals is primarily contributed by mass-calibration errors, whereas peak overlap dominates the errors for ions with smaller peak separation and lower ion counts.<sup>96</sup> The precision deterioration due to overlapping peaks is significantly larger for the weaker ions (i.e., with low signal intensity) relative to the stronger ions.<sup>81,95,96</sup> This is important in interpreting smaller peaks that reside at the shoulder of nearby larger peaks in the measurements: in addition to a decrease in precision, these smaller peaks can experience a significant bias (sometimes the signals can be overestimated by >100%; see examples in paper by Müller et al.<sup>81</sup>).

We stress that all of the above-mentioned results on errors of peak fitting are based on theoretical analysis using synthetic data sets. These results may deviate from the “real” measurements in the atmosphere. We have conducted a series of laboratory experiments to address this issue using the H<sub>3</sub>O<sup>+</sup> ToF-CIMS by introducing two VOCs that have product ions at the same nominal mass, with concentrations of one held constant and the other one varied (peak ratio from 0.01 to >10) (see [Supporting Information](#)). Our laboratory results indicate that the increased noise due to the large neighboring peak can be significantly higher than the prediction from the parametrization proposed by Cubison and Jimenez<sup>96</sup> (eq 3 in the reference). Further analysis on the data also confirms substantial effects on peak-fitting precision (and accuracy) from mass calibration, peak shape, and peak width. The reader is referred to [Supporting Information](#) for details.

Different advanced methods (e.g., Monte Carlo simulations) were applied to synthetic data sets in previous studies to investigate errors of high-resolution peak fitting, but these methods are difficult to implement in ambient data sets. A sensitivity-analysis method by perturbing mass calibration was proposed to roughly evaluate the effect of mass-calibration errors to the fitted peak signals.<sup>88</sup> The mass-calibration scales are typically perturbed between ±20 ppm and the same high-resolution peak fittings are conducted at each perturbation to explore potential changes of fitted signals. This method has been incorporated in the Tofware tool and was used in several recent studies.<sup>88,97</sup>

The results for peak-fitting procedures and associated errors from high-resolution peak fittings are also relevant to applications of TOF-MS in other areas of atmospheric sciences, namely, aerosol mass spectrometers (AMSs) and ToF-CIMS introduced by Aerodyne Inc. that use the same TOF-MS supplied by Tofwerk.

#### 2.4. Operations and Performance

**2.4.1. Determination of Background.** The PTR-MS background at each mass, i.e., the product ion signal in the absence of VOCs in the sampled air, is usually determined

using a catalytic conversion method. Air samples pass through a catalytic converter, consisting of platinum wool (the product used in our group is from Shimadzu, high-sensitivity catalyst for TOC analyzer, Part no. 630-00996) heated at 350 °C to efficiently remove VOCs from the air.<sup>21</sup> The catalytic converter provides VOC-free air but maintains ambient humidity. PTR-MS backgrounds are known to depend on humidity for many species. Thus, the platinum catalytic converter technique has been widely accepted by the PTR-MS community as the best approach to determine instrument backgrounds.<sup>21</sup> It should be noted that some absorbents (e.g., activated charcoal) have been used to determine PTR-MS background, but this method can remove water vapor from the sample. We strongly recommend the catalytic converter method over those using absorbents.

Ideally, the instrument background of PTR-MS should be determined on similar time scales as changes in the air mass, i.e., minutes for aircraft measurements and tens of minutes for measurements on the ground. Instrument backgrounds have been commonly obtained every 0.5–1 h for field campaigns by switching a valve to direct air through the catalytic converter. Long-term measurements lasting months or years may use less-frequent background measurements, e.g., every several hours. As it is not possible to determine backgrounds continuously while measuring ambient air, instrument backgrounds for the periods of ambient measurements are determined by interpolating adjacent background measurements. The most widely used interpolation method is linear interpolation. It is worth mentioning that linear interpolation may not be accurate enough under certain circumstances.<sup>61</sup> First, if the background of a certain mass is strongly dependent on humidity, finding an empirical relationship between background signals and humidity or humidity indicators (e.g., H<sub>3</sub>O<sup>+(H<sub>2</sub>O)/H<sub>3</sub>O<sup>+</sup>, H<sub>3</sub>O<sup>+(H<sub>2</sub>O)<sub>2</sub>/H<sub>3</sub>O<sup>+</sup>) is more appropriate. Second, the instrument backgrounds may not be stable after a recent instrument start-up or immediately after switching from samples with high concentrations to low concentrations. The decrease in instrument backgrounds during this period is typically exponential, and an exponential interpolation is justified. In our group, we have developed an automatic procedure to consider the three types of background-correction methods and use the method that best describes the background data.<sup>61</sup></sup></sup>

**2.4.2. Calibrations.** Calibration of PTR-MS using authentic standards is an essential practice to ensure data quality. Calibrations are most often conducted by dynamically diluting a high-concentration gas standard by clean air downstream of the catalytic converter.

Authentic gas standards for PTR-MS calibrations are frequently stored in gravimetrically prepared gas cylinders with known concentrations of targeted species (usually 1–10 ppm by volume, i.e., ppbv). However, many VOC species are unstable or unavailable in gas cylinders. As the number of measurable VOC species has expanded through PTR-TOF, other techniques for calibration have grown in popularity. These techniques include permeation tubes, diffusion cells, liquid-solution-based methods, and other online-generation methods for certain specific compounds. Permeation tubes<sup>98</sup> and diffusion cells<sup>99</sup> have been used to calibrate gas-phase instruments for many years. Both techniques are able to provide stable and reliable concentrations of targeted species. Permeation tubes can be purchased from commercial companies or prepared in the laboratory. The permeation rate of a permeation tube was traditionally determined by measuring the weight loss of the permeation tube over a long

period (e.g., several weeks). An alternative method for compounds containing carbon is quantitative conversion of VOCs from permeation tubes (or diffusion cells) to CO<sub>2</sub>, followed by a CO<sub>2</sub> measurement.<sup>100</sup> The liquid solution-based methods usually involve an injection of a liquid solution with targeted VOCs through a liquid flow controller or syringe pump into an air stream to generate a gas standard with known concentrations.<sup>101</sup> Heating the injection port and/or nebulizing the liquid flow can assist evaporation of VOCs from the solution. A liquid calibration unit (LCU) based on this principle was recently commercialized by Ionicon Analytic and has been deployed in several field campaigns for calibrations of some novel species (e.g., organic acids).<sup>60,97,102</sup>

The sensitivity of PTR-MS with respect to different VOCs can vary with the humidity of the sampled air,<sup>21</sup> so calibrations must be made at different humidities. The humidity dependence of the PTR-MS sensitivity is taken into account by either applying VOC-specific scaling factors for H<sub>3</sub>O<sup>+</sup> and H<sub>3</sub>O<sup>+(H<sub>2</sub>O)</sup> reagent ions<sup>20,21</sup> or deriving an empirical function to describe the humidity dependence, for example, the humidity correction for formaldehyde.<sup>69,70</sup> As shown in section 2.1, PTR-TOF has enabled the detection of numerous novel species in the atmosphere. Often, the PTR-MS response to these species is unknown and proper calibration of these species is necessary. Detailed characterization of the ion chemistry in an instrument through calibrations at varying humidity levels is also highly desirable for new PTR-MS instruments, especially instruments that use novel multipole ion guides and ion-funnel devices. In these instruments, the proton-transfer reactions take place in a nonhomogeneous and time-varying electric field. The cluster-ion distributions vary with time, which complicates the detection of species such as benzene and other hydrocarbons that react much more efficiently with H<sub>3</sub>O<sup>+</sup> than with H<sub>3</sub>O<sup>+(H<sub>2</sub>O)</sup> clusters.

**2.4.3. Sensitivity of PTR-MS.** According to the proton-transfer reaction between the H<sub>3</sub>O<sup>+</sup> reagent ions and a VOC producing protonated molecule RH<sup>+</sup>, the signals of RH<sup>+</sup> ions ([RH<sup>+</sup>]) at the end of the drift tube can be described as follows,<sup>21,80</sup>

$$[\text{RH}^+] = [\text{H}_3\text{O}^+]_0 (1 - \exp(-k[R]\Delta t)) \quad (4)$$

where  $k$  is the reaction rate constant,  $[\text{H}_3\text{O}^+]_0$  is the signal of H<sub>3</sub>O<sup>+</sup> ions before reaction,  $[R]$  is the number concentration of the VOC in the drift tube, and  $\Delta t$  is the reaction time for H<sub>3</sub>O<sup>+</sup> traversing the drift tube.

If the proton-transfer reactions only convert a small fraction of H<sub>3</sub>O<sup>+</sup> into protonated molecule RH<sup>+</sup>, [RH<sup>+</sup>] can be approximately expressed as

$$[\text{RH}^+] \approx [\text{H}_3\text{O}^+]k[R]\Delta t \quad (5)$$

where [H<sub>3</sub>O<sup>+</sup>] is the signal of H<sub>3</sub>O<sup>+</sup> ions after the end of the drift tube. The rationality of the approximation in eq 5 determines the linearity range of VOC measurements by PTR-MS. On the basis of the reported VOC sensitivity in the range of 10–40 cps/ppbv at 10<sup>6</sup> reagent ions for common PTR-MS instruments,<sup>80</sup> a decrease of the reagent ions by 10% (i.e., difference in eqs 4 and 5 at 5.2%) due to proton-transfer reactions corresponds to the total VOC concentration at 2.5–10 ppmv, which is significantly higher than ambient concentrations and can be comparable to those encountered in emission studies (e.g., biomass burning<sup>103</sup>).

If we include the possibility of fragmentation for the protonated ions in the drift tube or in the ion-transmission regions, a term  $F_{\text{RH}^+}$  can be introduced to represent the fraction of product ions detected as RH<sup>+</sup> ions ( $0 \leq F_{\text{RH}^+} \leq 1$ ).<sup>80</sup> For nonfragmenting compounds,  $F_{\text{RH}^+} = 1$ . Then, eq 5 becomes

$$[\text{RH}^+] \approx [\text{H}_3\text{O}^+]k[R]\Delta t F_{\text{RH}^+} \quad (6)$$

The signals of H<sub>3</sub>O<sup>+</sup> ( $I_{\text{H}_3\text{O}^+}$ ) and RH<sup>+</sup> ions ( $I_{\text{RH}^+}$ ) measured by the mass analyzer (in cps) can be related to the signals of H<sub>3</sub>O<sup>+</sup> ([H<sub>3</sub>O<sup>+</sup>]) and RH<sup>+</sup> ([RH<sup>+</sup>]) ions at the end of the drift tube, using their respective transmission efficiencies ( $T_{\text{H}_3\text{O}^+}$  and  $T_{\text{RH}^+}$ ) from the drift tube to the detector:<sup>21,80</sup>

$$I_{\text{H}_3\text{O}^+} = [\text{H}_3\text{O}^+]T_{\text{H}_3\text{O}^+} \quad (7)$$

$$I_{\text{RH}^+} = [\text{RH}^+]T_{\text{RH}^+} \quad (8)$$

The sensitivity of PTR-MS with respect to a certain VOC is commonly defined as the ion signal of RH<sup>+</sup> normalized to the H<sub>3</sub>O<sup>+</sup> ion signal of 10<sup>6</sup> cps at a volume-mixing ratio of 1 ppbv. Thus, PTR-MS sensitivity has a unit of normalized cps per ppbv, i.e., ncps/ppbv.

$$\text{Sensitivity} = \frac{\frac{I_{\text{RH}^+}}{I_{\text{H}_3\text{O}^+}} \times 10^6}{\frac{[R]}{N} \times 10^9} \quad (9)$$

In eq 9,  $N$  is the number density of the gas in the drift tube. On the basis of the definition of the sensitivity in eq 9, the concentrations of VOCs measured by PTR-MS are usually reported as mixing ratio by volume (e.g., ppbv). Inserting eqs 6–8 into eq 9, we obtain

$$\text{Sensitivity} = N \times 10^{-3} \times \Delta t \frac{T_{\text{RH}^+}}{T_{\text{H}_3\text{O}^+}} F_{\text{RH}^+} \times k \quad (10)$$

On the right side of eq 10, the first three terms ( $N \times 10^{-3} \times \Delta t$ ) are the same for different VOCs. Therefore, the sensitivity of a certain VOC depends on the ion-transmission efficiency of the protonated ion ( $T_{\text{RH}^+}$ ), the degree of fragmentation for the protonated ion ( $F_{\text{RH}^+}$ ), and the reaction rate constant of the VOC with H<sub>3</sub>O<sup>+</sup> ( $k$ ). The PTR-MS sensitivity in eqs 9 and 10 is expressed as ncps/ppbv, such that the PTR-MS sensitivity is not affected by temporal variations of the reagent ions. However, PTR-MS sensitivity expressed as cps/ppbv should be used for comparison of the performance between instruments (see discussions on **Detection Limits**). For similar reasons, groups reporting sensitivity as ncps/ppbv should also report the primary ion signal.

The transmission efficiency of an ion in a PTR-TOF instrument can be affected by mass discrimination in the ion interfaces, the duty cycle of the orthogonal extraction region in the ToF,<sup>65</sup> and mass discrimination induced by MCP aging.<sup>92</sup> The duty-cycle mass discrimination can be corrected easily (see discussions in section 2.3),<sup>65</sup> whereas MCP-aging-induced mass discrimination should be avoided by setting an appropriate MCP voltage.<sup>92</sup> The mass discrimination in ion interfaces is difficult to predict and depends on the types of ion interfaces and their settings. Mass discrimination may also be present in the drift tube as the result of different ion mobilities of ions.<sup>104</sup> Relative transmission curves ( $T_{\text{RH}^+}/T_{\text{H}_3\text{O}^+}$  vs  $m/z$ ) can be obtained by introducing large amounts of various VOCs into the PTR-MS and measuring the ratio between the decrease of

reagent ions and the increase of product ions (including isotopic ions).<sup>47,61,79,105</sup>

The degree of product-ion fragmentation in PTR-MS is highly dependent on the types of VOCs. Figure 5 shows the

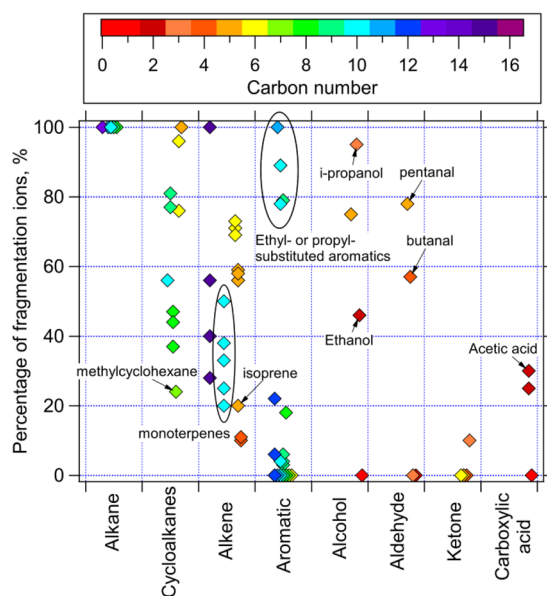


**Figure 5.** Percentages of fragmentation ions to total product ions for different types of VOCs in PTR-MS at  $E/N \approx 120$  Td. The fragmentation percentages for cycloalkanes are the fractions for the ions other than M–H ions, as these M–H ions are usually used for quantification of cycloalkanes in PTR-MS.<sup>115</sup> Data points are color-coded using carbon numbers in VOC molecules. Data sources: alkanes, cycloalkanes, alkenes, and aromatics from Gueneron et al.,<sup>106</sup> isoprene from Kalogridis et al.,<sup>107</sup> monoterpenes from Tani et al.,<sup>78</sup> 2-methyl-3-butene-2-ol (MBO) and sesquiterpenes from Kim et al.,<sup>79</sup> ethanol from Inomata and Tanimoto,<sup>108</sup> i-propanol and carboxylic acids from Baasandorj et al.,<sup>76</sup> and aldehydes and ketones from Warneke et al.<sup>109</sup>

importance of fragmentation of different VOC species in PTR-MS, based on literature results.<sup>76,78,79,106–109</sup> Alkanes, cycloalkanes, many alkenes, and ethyl- and propyl-substituted aromatics<sup>106</sup> can fragment substantially in PTR-MS, while oxygenated VOCs usually fragment less. It is clear that heavier molecules usually fragment more for each VOC class. The fragmentation pattern can be acquired by introducing single compounds into the instrument to observe the signals of various product ions in the mass spectra (see examples by Gueneron et al.<sup>106</sup>). PTR-MS coupling with GC (GC-PTR-MS, see discussions in section 3.1) has also been used as a convenient way to study fragmentation of a large number of VOCs in PTR-MS by analyzing complex mixtures.<sup>110</sup> In addition to dehydration for alcohols and carboxylic acids<sup>76,111</sup> during fragmentation as shown in section 2.2, there are a number of other fragmentation mechanisms in PTR-MS: loss of alkyl group for alkanes and alkenes, H<sub>2</sub> elimination for cycloalkanes, and HNO<sub>3</sub> loss for organic nitrates.<sup>112,113</sup> Tandem mass spectrometry (MS/MS) studies (or CID) may provide information on fragmentation of various ions in PTR-MS mass spectra, which may be worth further investigation.<sup>114</sup>

After ion-transmission efficiency and the degree of fragmentation are taken into account (eq 10), the sensitivities of VOCs in PTR-MS are expected to be linearly correlated with the reaction rate constants between H<sub>3</sub>O<sup>+</sup> and VOCs in the

drift tube. Room-temperature rate constants between H<sub>3</sub>O<sup>+</sup> and various VOCs were measured in many studies, including selected-ion flow-tube (SIFT) mass spectrometry.<sup>75,116–118</sup> There are also a number of parametrizations to calculate the reaction rate constants of H<sub>3</sub>O<sup>+</sup> with VOCs, including the average-dipole-orientation (ADO) theory<sup>119,120</sup> and the parametrized trajectory calculations.<sup>121</sup> Zhao and Zhang<sup>122</sup> applied the ADO theory to calculate the reaction rate constants of H<sub>3</sub>O<sup>+</sup> with a large number of VOCs. However, the room-temperature rate constants measured by SIFT studies and calculated by the ADO theory are not fully representative for the reactions in the drift tube of PTR-MS, because the ion–molecule collisions in the PTR-MS drift tube are substantially more energetic than room-temperature collisions. This is illustrated by the much higher effective ion translational temperature ( $T_{\text{eff}}$ ) ( $\sim 1000$  K).<sup>21,31</sup> The ADO theory has not been extended to enhanced collision energies, i.e., the coefficients for the calculations at the effective ion temperature in a drift tube are not available.<sup>91</sup> Proton-transfer-reaction rate constants in PTR-MS were calculated by Cappellin and co-workers using the trajectory-parametrization method, by taking the effective ion temperature into account.<sup>91,123</sup> They found that the calculated rate constants from the trajectory parametrizations can be significantly lower (0–39%) than the values at room temperature from the ADO theory for compounds with high dipole-moment values.<sup>91,123</sup> The polarizability and permanent dipole moment of the VOCs are used as the input parameters for the calculation of rate constants in both the ADO theory and the trajectory-parametrization method. A recent study showed that the polarizability and permanent dipole moment can be estimated for various VOCs using the information from PTR-TOF measurements, i.e., molecular mass, elemental composition, and functionality of the VOCs.<sup>124</sup>

The linear relationship between VOC sensitivity and reaction rate constants is demonstrated by Cappellin et al.<sup>91</sup> by inversely calculating reaction rate constants from an equation similar to eq 10 and comparing the calculated rate constants with theoretical predictions. They found that the rate constants usually agreed within a few percent for most of the investigated compounds (<8%).<sup>91</sup> On the basis of this evidence, a simple method to predict sensitivity of certain VOCs in PTR-MS was proposed:<sup>124</sup> (1) plotting the VOC sensitivities obtained from calibrations using authentic standards versus their respective rate constants ( $k$ ) and finding an empirical relationship from the scatterplots using linear regression (Sensitivity =  $a \times k$ ), and (2) using the obtained empirical relationship of sensitivity versus rate constant to predict the sensitivity of an uncalibrated VOC based on its reaction rate constant. The results for 29 VOC species from the NOAA H<sub>3</sub>O<sup>+</sup> ToF-CIMS are shown in Figure 6. A strong correlation between VOC sensitivities and rate constants is observed for 19 different VOC compounds (blue data points), which are used for the calculation of VOC sensitivities for other uncalibrated compounds by Sekimoto et al.<sup>124</sup> However, calibration results indicate that many other VOCs (red data points, 10 of 29) have significantly lower slopes than these 19 VOCs (as large as a factor of 2). The observed lower slopes of these additional compounds are not fully understood, and this issue needs further investigation for better evaluating the accuracy in calculation of PTR-MS sensitivity. As a result, we recommend that the calculated sensitivities using the method by Sekimoto et al.<sup>124</sup> should be viewed as upper limits for uncalibrated VOCs.

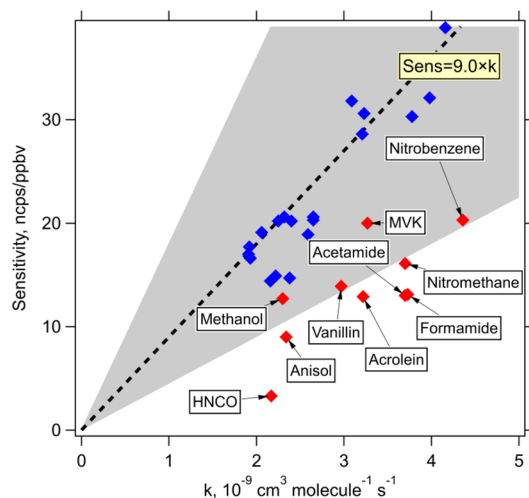


**Figure 6.** Sensitivities of the NOAA  $\text{H}_3\text{O}^+$  ToF-CIMS as a function of the calculated rate constants for proton-transfer reactions using the trajectory-parametrization method for 29 different VOCs. The blue and red diamond markers indicate the species used and not used, respectively, in the sensitivity calculation by Sekimoto et al.<sup>124</sup> The black dashed line is the linear fit to the blue data points. The shaded area indicates deviations from the black dashed line by a factor of 2.

**2.4.4. Detection Limits.** The precision and detection limits of PTR-MS measurements are limited by the counting statistics of product ions. The counting statistics for detecting ions follows a Poisson distribution: the  $1-\sigma$  error of counting  $N$  ions is  $\sqrt{N}$ . If we define a species  $X$  with a sensitivity of  $C_f$  (cps/ppbv) in PTR-MS and the background signal is  $B$  (cps), the signal  $S$  (counts) from a measurement period of  $t$  (s) at a concentration of  $[X]$  (ppbv) is

$$S = C_f[X]t \quad (11)$$

Considering that the signal ( $S$ ) is determined from the difference between total ambient signal ( $C_f[X]t + Bt$ ) and total background signal ( $Bt$ ) for the period of  $t$  (s), the error of the signal can be determined by

$$\begin{aligned} \text{Noise} &= \sqrt{(\sqrt{C_f[X]t + Bt})^2 + (\sqrt{Bt})^2} \\ &= \sqrt{C_f[X]t + 2Bt} \end{aligned} \quad (12)$$

As a result, signal-to-noise ratio ( $S/N$ ) of the measurement is obtained by<sup>125</sup>

$$\frac{S}{N} = \frac{C_f[X]t}{\sqrt{C_f[X]t + 2Bt}} \quad (13)$$

In addition to the counting error, additional noise of ion signals can be introduced from high-resolution peak fitting to PTR-TOF mass spectra.<sup>95,96</sup> Yuan et al.<sup>61</sup> showed that the standard deviations of background signals for various high-resolution ions can be as high as two times the predicted errors from Poisson distribution, which indicates significant additional uncertainty resulting from high-resolution peak fitting. Thus, a scaling factor ( $\alpha$ ), estimated from scatterplots of the standard deviation of the background signals versus the background signals, is proposed to take the additional error into account.<sup>61</sup> As a result, eq 13 becomes

$$\frac{S}{N} = \frac{C_f[X]t}{\alpha \times \sqrt{C_f[X]t + 2Bt}} = 3 \quad (14)$$

The detection limits are commonly defined as the concentrations where the  $S/N$  is 3, i.e., the detection limits are obtained by finding the root for  $[X]$  in eq 14. We note that eqs 13 and 14 are slightly different from the equations shown in the previous review,<sup>21</sup> in which the term  $C_f[X]t$  in the denominator ( $\sqrt{C_f[X]t + 2Bt}$ ) is omitted.

Figure 7 shows the detection limits along with sensitivities from different PTR-MS instruments. Figure 7 illustrates several issues: (1) The detection limits of PTR-MS are compound-dependent, because of different background signals and sensitivities for various VOCs. (2) Over the last two decades, the performance of PTR-QMS has greatly improved, in terms of higher sensitivity (cps/ppbv) and lower detection limits. This is a result of continuous developments by both Ionicon Analytik and the research community, including improvements to the ion source and an additional differential pumping region as documented by Warneke et al.<sup>70</sup> (3) The first version of PTR-TOF (i.e., PTR-TOF 8000) from Ionicon had significantly higher sensitivities than previous PTR-TOF instruments but lower than the contemporary PTR-QMS. However, this comparison is of the absolute sensitivity (cps/ppbv) of a single VOC measured over 1 s and does not take into account the duty cycle of QMS for measuring multiple compounds. Considering a typical QMS duty cycle, which scans individual selected masses for 1 s every 10–35 s, the total counts for a certain period (e.g., 15 s in the graph) and the 15 s detection limits are actually comparable between the two instruments.<sup>43</sup> (4) The PTR-TOF instruments coupled with the new ion interfaces (i.e., quadrupole ion guide and ion funnel) have markedly better sensitivity than PTR-TOF instruments with conventional ion-lens systems.<sup>24,61,67</sup> The sensitivities of PTR-TOF instruments with new ion interfaces (cps/ppbv) are comparable to or even larger than those of the well-running PTR-QMS. Taking into account the duty cycle of the PTR-QMS, the detection limits of these instruments dramatically outperform PTR-QMS. The 1 s detection limits of the state-of-the-art PTR-TOF instruments are around or lower than 100 pptv, which is generally sufficient for ambient measurements. Nevertheless, further performance advances of PTR-TOF instruments are needed to improve the quality of VOC data and the detection of rarely studied VOCs at low concentrations.

**2.4.5. Response Time.** The response time of PTR-MS is determined by the drift-tube design, inlet configurations, and the residence time of sampled gas in both the inlet and drift tube. As discussed by de Gouw and Warneke,<sup>21</sup> the inner diameter of the drift tube and the isolating drift-tube rings were optimized for better response time in PTR-MS over many years of PTR-QMS operations. A short and heated inlet is an effective method to reduce the response time of PTR-MS. The air flowing into the drift tube of PTR-MS is usually at ~20–30 mL/min. Significant increase of the flow into the drift tube to 800 mL/min was implemented in a PTR-MS for better response time.<sup>40</sup> The flow into the drift tube of NOAA  $\text{H}_3\text{O}^+$  ToF-CIMS was also increased to ~200 mL/min (35 mL/min in the original setup) (see Figure 2). PTR-MS inlets have been commonly constructed using Teflon (either polytetrafluoroethylene (PTFE) or perfluoroalkoxy (PFA)) and/or polyether ether ketone (PEEK) tubing. The effects of inlet materials and

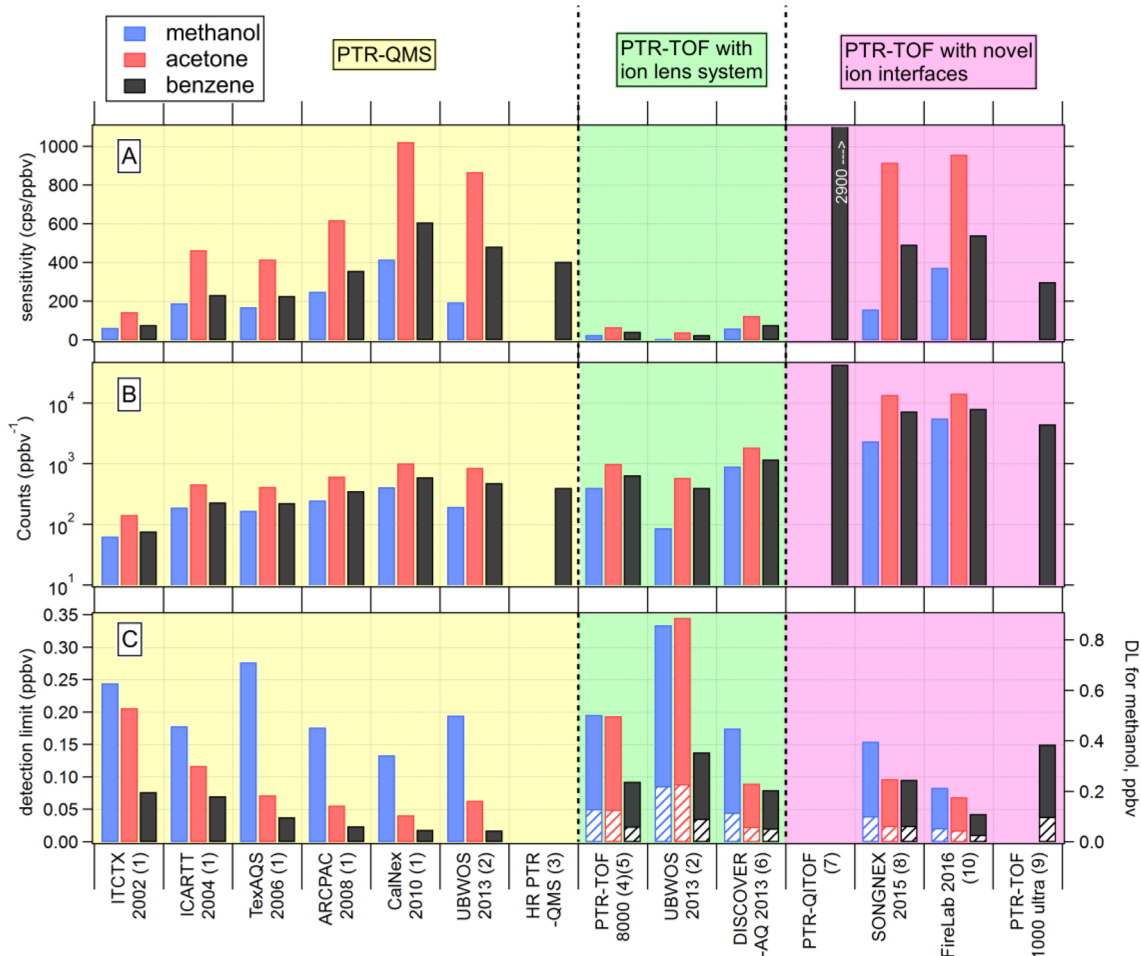


**Figure 7.** Comparison of the PTR-MS sensitivities (A), total ion counts from measurements in a period of 15 s (B), and 1 s detection limits (C) of methanol, acetone, and benzene for different versions of the PTR-MS instruments shown in Figure 1. In (B), we assume that the PTR-QMS instrument was operated at the typical cycle length of 15 s with a 1 s dwell time for each compound. This is typical for aircraft measurements. The 15 s detection limits of PTR-TOF instruments are also shown with the pattern-filled bars in C. Note that the detection limits (DLs) of methanol in (C) are plotted on the right axis. The data are from various publications indicated by numbers in parentheses of the label of x-axis: (1) NOAA PTR-QMS;<sup>70</sup> (2) NOAA PTR-QMS and a PTR-TOF 8000 instrument during UBWOS 2013;<sup>43</sup> (3) high-sensitivity PTR-QMS introduced by Ionicon Analytik;<sup>27</sup> (4, 5) PTR-TOF 8000 introduced by Ionicon Analytik (and its prototype);<sup>22,23</sup> (6) compact PTR-TOF, i.e., the prototype of PTR-TOF 1000;<sup>60</sup> (7) PTR-QiTOf introduced by Ionicon Analytik;<sup>24</sup> (8) NOAA H<sub>3</sub>O<sup>+</sup> ToF-CIMS;<sup>61</sup> (9) PTR-TOF 1000 ultra with an ion funnel introduced by Ionicon Analytik;<sup>67</sup> (10) unpublished results from our group for the current version of the NOAA H<sub>3</sub>O<sup>+</sup> TOF-CIMS (Figure 2).

inlet lengths on the response time of PTR-MS have not been systematically investigated.

Another approach to improve the response time of PTR-MS is operating the drift tube at an elevated temperature. As demonstrated by Mikoviny et al.,<sup>39</sup> the response times for sticky compounds or compounds associated with low volatility were drastically reduced by operating the PEEK drift tube at 250 °C, which facilitates measurements of particle-bound organic compounds. A similar PTR-MS with a drift tube operated at 180 °C enabled eddy covariance flux measurements of ammonia in the atmosphere.<sup>126</sup> However, higher temperature in the drift tube may promote surface-assisted reactions (e.g., catalytical conversion of hydroperoxides to carbonyls by metals<sup>40,127</sup>), and the effects should be explored in such instruments.

### 3. INTERPRETATION OF MASS SPECTRA

#### 3.1. Methods to Attribute Masses to VOC Species

PTR-MS only obtains the mass-to-charge ratios ( $m/z$ ) of the ions and does not provide *a priori* information on the

compounds contributing to a particular  $m/z$ . The combination of PTR-TOF and high-resolution peak fitting can provide chemical formulas for many masses, which reduces potential candidates for the high-resolution peaks, but it is still difficult to attribute each mass channel to one specific VOC or the sum of several VOCs. This is especially true for larger masses, for which many isobars and structural isomers are possible. Several methods are commonly used in the PTR-MS community to aid the identification of masses.

**3.1.1. GC-PTR-MS Studies.** The gas chromatography (GC) method has been used to separate organic mixtures in the atmosphere. The coupling of GC with PTR-MS (GC-PTR-MS) was shown to be a useful approach to identify the VOCs contributing to various masses.<sup>109,128</sup> A GC interface slows the measurement speed to that of the GC. Because of the much-slower time resolution, GC-PTR-MS has been mainly deployed at ground sites<sup>53,129</sup> and in laboratory experiments.<sup>54,110,130,131</sup> In GC-PTR-MS measurements at ground sites, characteristic samples are obtained as “snapshots” in order to aid in species identification. Recently, Ionicon Analytik commercialized a fast-

GC module that can be coupled to new or existing Ionicon instruments.<sup>132</sup> The fast-GC module uses a short (3–6 m) metallic column that is heated quickly (>10 °C/s). The fast-GC module has been used to separate mixtures containing monoterpenes in the laboratory.<sup>133,134</sup> However, the fast-GC module has relatively high detection limits (1.2 ppbv for monoterpene experiments),<sup>133</sup> due to the lack of a cryogenic preconcentration unit. The application of the fast-GC module for ambient environments has not been reported. Previous GC-PTR-MS applications mainly chose nonpolar or midpolar GC columns that are suitable for measurements of hydrocarbons and some carbonyls,<sup>54</sup> leading to the inability to measure many polar compounds (e.g., organic acids). High-polarity GC columns should be tested in future studies with GC-PTR-MS.

**3.1.2. Intercomparison Studies.** In the two decades since the inception of PTR-MS, numerous intercomparison experiments have been conducted to compare PTR-MS to other PTR-MS instruments, other CIMS techniques, chromatography techniques, and optical techniques. Intercomparison between PTR-MS and other analytical methods can provide valuable information on the attribution of PTR-MS masses and possible chemical interferences to various VOCs. An example was recently shown for the detection of ethylene glycol at  $m/z$  45 as interferences for acetaldehyde measurements in PTR-MS under certain (rare) circumstances.<sup>135</sup> It was found that the  $m/z$  45 signals were significantly higher than acetaldehyde concentrations measured by GC-FID from measurements in a highway tunnel, indicating that other compounds contributed to  $m/z$  45.<sup>135</sup> These high  $m/z$  45 signals were attributed to ethylene glycol, which is used as engine coolant in gasoline vehicles.<sup>135</sup>

The results of PTR-MS intercomparisons are collected from the literature and compiled in Table S1. We include a total of 274 pairs of intercomparison results from 58 peer-reviewed papers, a population significantly larger than the 51 pairs of intercomparison results from 11 papers compiled in the review 10 years ago.<sup>21</sup> Slope statistics from the intercomparison indicate the typical accuracy of PTR-MS instrument, whereas the intercept statistics shed light on typical levels of background interferences. Figure 8 shows the histograms of the reported

Warneke<sup>21</sup> (0.20 pptv/pptv in 2007 paper), while comparable values are obtained for the intercept (12 pptv in 2007 paper). This shows that the accuracy of most published PTR-MS measurements is better than 20–27%. Detailed calibrations and significant efforts are needed to improve the accuracy for individual compounds, which is not always practical for a data set with many VOCs. The analysis also shows that positive measurement biases are common. These are attributed to interference from other VOCs and can be much harder to take into account.

We further determined the distribution of the slopes for two VOC subgroups, namely, more commonly measured species (including methanol, acetonitrile, acetaldehyde, acetone, isoprene, methyl ethyl ketone (MEK), benzene, toluene, C8 aromatics, C9 aromatics, and monoterpenes) and other species (including formaldehyde, organic acids, phenol, and others). The widths of slope distributions for the two groups are 0.26 and 0.38, respectively. The broader width obtained for the “other” species is not surprising, as these species are more challenging to measure for various reasons, including stronger humidity dependencies (e.g., formaldehyde and H<sub>2</sub>S), challenges in acquiring a reliable gas standard (e.g., organic acids and phenol), and interferences by isobaric compounds when using PTR-QMS (e.g., DMS and naphthalene).

As shown in section 2.1, PTR-TOF instruments can distinguish many isobaric masses, which should lead to more accurate VOC measurements by PTR-TOF. Intercomparison results between PTR-TOF and other methods (including PTR-QMS) yielded a smaller width (0.10 pptv/pptv) but a slope slightly higher than unity (1.07 pptv/pptv) for the distribution of slopes. Most of the intercomparison results using PTR-TOF (20 pairs out of 27) are actually from a single study (Table S1).<sup>136</sup> Additional intercomparison work using PTR-TOF is needed to draw stronger conclusions.

The intercomparison results indicate that an accuracy for PTR-MS measurement of ~20% can be achieved for compounds with reliable gas standards, careful quality-control procedures, and little chemical interference in the measurements. As the conclusions are drawn based on statistics in peer-reviewed papers, the intercomparison results and PTR-MS accuracy for many other unpublished or unreported measurements may be significantly higher (i.e., survival bias). A controlled large-scale intercomparison campaign involving three PTR-MS instruments also provided similar insights on the importance of instrument characterization: although PTR-MS has the potential to make high-quality VOC measurements, the potential cannot be realized unless there is full characterization of the PTR-MS instruments for different environments of the atmosphere.<sup>137</sup>

Intercomparison experiments have been mainly conducted in urban areas and biogenic-dominated regions. While there are several studies reporting intercomparison results for a large number of species from biomass-burning emissions in the laboratory,<sup>54,131,138,139</sup> only a single study reported intercomparison between PTR-MS with other methods in ambient biomass-burning plumes.<sup>140</sup>

**3.1.3. Chemical Formulas from PTR-TOF in Aid of VOC Identification.** Using high-mass-resolution data from PTR-TOF, chemical formulas for many masses can be determined without ambiguity. This is especially true for lighter masses that have fewer possible isobaric overlapping peaks. The chemical formula can be valuable to attribute a certain mass to either a specific compound or a group of compounds (i.e., intermediate

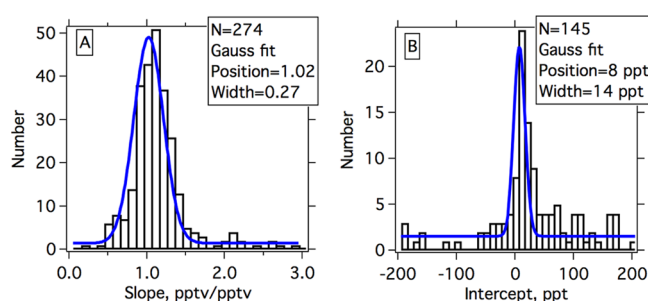


**Figure 8.** Histograms of the determined slopes and intercepts from the intercomparison results between PTR-MS and other analytical methods for various VOC species (see Table S1). The blue curves are the fitted results using a Gaussian distribution.

slopes and intercepts from these intercomparison experiments. The blue curves in Figure 8 show the results of fitting a Gaussian distribution to these data. The fitted distribution of reported slopes centered at 1.02 pptv/pptv with a width of 0.27, whereas the distribution of intercepts is centered at 8 pptv with a width of 14 pptv. The derived width of the slope distribution is slightly higher than the value reported by de Gouw and

levels of identification), which can be sufficient to answer many atmospheric problems.<sup>10</sup> For masses containing only C, H, and O, two parameters derived from chemical formulas can be used together for mass attribution: (1) the number of oxygen atoms (O); (2) the double bond equivalent (DBE), also known as degree of unsaturation (DU), which is calculated as  $1 + C - 0.5 \times H$  (C and H are the number of carbon and hydrogen atoms). For example, an ion with O = 1 and DBE = 0 comes from either an alcohol (C < 3) or an ether; an ion with O = 1 and DBE = 1 comes from an aldehyde or a ketone; an ion with O = 2 and DBE = 1 could be an acid or a hydroxy carbonyl species, etc. The Kendrick mass-defect plot can be used as a convenient visual tool for this analysis.<sup>141</sup> For masses containing nitrogen or sulfur, it is more complicated to perform the analysis. Other derived parameters may also be useful under certain circumstances, such as the aromaticity equivalent ( $X_C = (2C - H)/DBE + 1$ ) as an effective criteria for the presence of aromatics ( $X_C \geq 2.5000$ ).<sup>142</sup> These above-mentioned analyses assume that the targeted masses are mainly contributed by protonated molecular ions. The identification of a fragment mass from other ions is impeded without knowing the fragmentation mechanism.

The distribution of signals for a series of masses can aid chemical attribution of PTR-MS masses. Figure 9 shows the

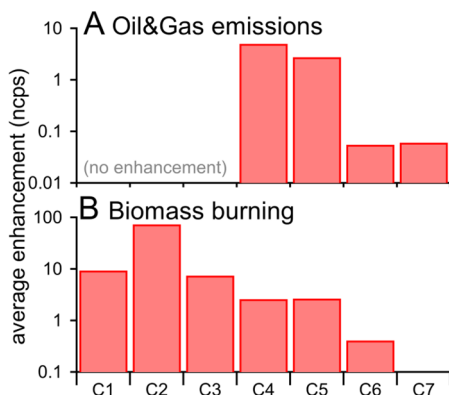


**Figure 9.** Comparison of the distribution of unsaturated nitrogen species  $C_nH_{2n-1}NH^+$  between (a) oil- and gas-related VOCs and (b) a biomass-burning plume from an aircraft measurements. The series is  $m/z$  28  $HCN^+$ ,  $m/z$  42  $C_2H_3NH^+$ ,  $m/z$  56  $C_3H_5NH^+$ ,  $m/z$  70  $C_4H_7NH^+$ , etc. The values shown are the average signal enhancement (ncps enhancement) in the boundary layer for oil and gas measurement and the average signal enhancement (ncps enhancement) in the biomass-burning plume over signals measured immediately before the plume. Reprinted with permission from ref 115. Copyright 2017 Koss and co-workers; CC Attribution 3.0 License.

distribution of signals for a series of ions ( $C_nH_{2n-1}NH^+$ ) from a biomass-burning plume and emissions from an oil/gas extraction region measured by a PTR-TOF onboard a research aircraft.<sup>115</sup> The signals of these ions from the biomass-burning plume generally decrease as carbon number increases. However, the signals in oil/gas emissions show the largest enhancements for the ions with 4–5 carbons but no enhancement for masses with smaller carbon numbers (1–3). This suggests that the masses should be from cyclic molecules, e.g., pyrrolines, rather than linear nitriles as in the biomass-burning plume.<sup>115</sup> This method can be potentially used for other mass series,<sup>115</sup> providing an effective approach to determine the presence of ring structure in the molecules.

### 3.2. Detection of Specific VOCs by PTR-MS

On the basis of the findings from GC-PTR-MS and intercomparison studies, the attribution of individual masses in PTR-MS to specific commonly detected VOC species in the literature is summarized in Table 2. In this section, we discuss important PTR-MS masses for VOC detection in detail. We also show important implications (if any) for VOC measurements at these masses using data from high-resolution PTR-TOF ( $m/\Delta m > 4000$ ). Several inorganic species measurable by PTR-MS are also covered, including ammonia, hydrogen sulfide, and isocyanic acid.

**m/z 18.** Ammonia is detected at  $m/z$  18.034 ( $NH_3H^+$ ). Measurements of ammonia at  $m/z$  18 suffer from high background signals, leading to poor detection limits.<sup>60</sup> Measurements of ammonia by PTR-MS have only been reported in emissions of biomass burning<sup>131</sup> and near agricultural sources.<sup>60,143</sup> Comparison of ammonia measurements between PTR-TOF and a cavity ringdown spectroscopy (CRDS) instrument showed reasonably good agreement during airborne measurements over a region with strong emissions from dairy farms.<sup>60</sup> Ammonia measurements using  $O_2^+$  as reagent ions in PTR-MS have been proposed, as much lower detection limits can be achieved.<sup>170,171</sup>

**m/z 28.** HCN is measured at  $m/z$  28.018 ( $HCN^+$ ) in PTR-MS. The proton affinity of HCN ( $PA = 712.9\text{ kJ mol}^{-1}$ ) is only slightly higher than that of water ( $PA = 691\text{ kJ mol}^{-1}$ ), and as a result the sensitivity of HCN decreases quickly with increasing humidity.<sup>71,72</sup> Other ions detected at  $m/z$  28 are  $N_2^+$  ( $m/z$  28.006) and  $C_2H_4^+$  ( $m/z$  28.031) ions, the latter of which is from the charge-transfer reaction of ethene ( $C_2H_4$ ) with  $O_2^+$  ions. PTR-TOF is able to separate  $HCN^+$  ions from  $N_2^+$  and  $C_2H_4^+$  ions.<sup>72</sup>

**m/z 31.** Formaldehyde is detected at  $m/z$  31.018 ( $CH_2OH^+$ ). Similar to HCN, the proton affinity of formaldehyde ( $715.7\text{ kJ mol}^{-1}$ ) is just slightly higher than that of water ( $PA = 691\text{ kJ mol}^{-1}$ ). In the last few decades, the humidity dependence of formaldehyde sensitivity in PTR-MS has been investigated intensively in a number of papers, and measurements of formaldehyde by PTR-MS were conducted at several ground sites<sup>68,69,172</sup> and on an aircraft.<sup>70</sup> Intercomparison between PTR-MS and other methods (DOAS and Hantzsch) resulted in reasonably good agreements with slopes between 0.99 and 1.17, provided that calibrations at different humidity levels are performed carefully.<sup>68–70</sup> Sample drying using a cold trap in the inlet was proposed to eliminate the strong humidity dependence of the formaldehyde sensitivity,<sup>173</sup> but some lower-volatile species may be lost in the cold trap. A blind intercomparison between PTR-MS with four other techniques in a smog chamber confirmed PTR-MS as a promising tool for formaldehyde, but the study also revealed some chemical interferences in formaldehyde measurements by PTR-MS, e.g., positive interferences at high ozone levels.<sup>174</sup> The possible interferences in formaldehyde measurements at  $m/z$  31 can come from reactions of  $O_2^+$  with methanol or ethanol,<sup>68,175</sup> dehydration of protonated methyl peroxide ( $CH_4O_2H^+$ ),<sup>68</sup> and fragmentation of protonated glyoxal.<sup>176</sup> However, the only GC-PTR-MS study for formaldehyde showed little interference at  $m/z$  31 from other compounds.<sup>70</sup> Because the same ions are generated from the interfering reactions mentioned earlier, PTR-TOF is not helpful in separating these possible interferences.

**m/z 33.** Methanol is monitored at  $m/z$  33.033 ( $CH_4OH^+$ ) in PTR-MS. Most (14 of 16) of the intercomparison results for

Table 2. Identified Compounds from Mass List of PTR-MS

nominal masses	formula	<i>m/z</i>	species	nominal masses	formula	<i>m/z</i>	species
18	NH <sub>3</sub> H <sup>+</sup>	18.034	ammonia <sup>60,143</sup>	79	C <sub>6</sub> H <sub>6</sub> H <sup>+</sup>	79.054	benzene <sup>21</sup>
28	HCN <sup>+</sup>	28.018	hydrogen cyanide <sup>71,72</sup>	81	C <sub>6</sub> H <sub>9</sub> <sup>+</sup>	81.070	monoterpenes fragment; <sup>21</sup> PAH fragment <sup>106</sup>
31	CH <sub>2</sub> OH <sup>+</sup>	31.018	formaldehyde <sup>68–70</sup>	83	C <sub>5</sub> H <sub>6</sub> OH <sup>+</sup>	83.049	methyl furan <sup>90,158</sup>
33	CH <sub>4</sub> OH <sup>+</sup>	33.033	methanol <sup>21,60,144</sup>	C <sub>6</sub> H <sub>11</sub> <sup>+</sup>	83.085	methylcyclopentane <sup>106,130,159</sup>	
35	H <sub>2</sub> SH <sup>+</sup>	34.995	H <sub>2</sub> S <sup>73,74</sup>	85	C <sub>4</sub> H <sub>4</sub> O <sub>2</sub> H <sup>+</sup>	85.028	furanone <sup>44</sup>
41	C <sub>3</sub> H <sub>5</sub> <sup>+</sup>	41.039	fragmentation from isoprene <sup>80</sup>	C <sub>5</sub> H <sub>8</sub> OH <sup>+</sup>	85.065	cyclopentanone <sup>115</sup>	
42	C <sub>2</sub> H <sub>3</sub> NH <sup>+</sup>	42.034	acetonitrile <sup>21</sup>	87	C <sub>4</sub> H <sub>6</sub> O <sub>2</sub> H <sup>+</sup>	87.044	butanedione; <sup>44,74</sup> methacrylic acid
43	C <sub>2</sub> H <sub>3</sub> O <sup>+</sup>	43.018	fragmentation from acetic acid <sup>76</sup>	C <sub>5</sub> H <sub>10</sub> OH <sup>+</sup>	87.080	2-methyl-3-butene-2-ol (MBO); <sup>46</sup> pentanones + pentanal <sup>131</sup>	
	C <sub>3</sub> H <sub>7</sub> <sup>+</sup>	43.054	fragmentation from hydrocarbons <sup>106,130</sup> and propanols <sup>61</sup>	89	C <sub>3</sub> H <sub>4</sub> O <sub>3</sub> H <sup>+</sup>	89.023	pyruvic acid
44	CHNOH <sup>+</sup>	44.013	isocyanic acid <sup>61,145–149</sup>	C <sub>4</sub> H <sub>8</sub> O <sub>2</sub> H <sup>+</sup>	89.060	butyric acid <sup>143</sup>	
45	C <sub>3</sub> H <sub>4</sub> OH <sup>+</sup>	45.033	acetaldehyde <sup>21</sup>	93	C <sub>7</sub> H <sub>8</sub> H <sup>+</sup>	93.070	toluene <sup>21</sup>
46	NO <sub>2</sub> <sup>+</sup>	45.992	PAN fragmentation; <sup>44</sup> methyl nitrate; <sup>41</sup> other nitrogen-containing compounds	95	C <sub>6</sub> H <sub>6</sub> OH <sup>+</sup>	95.049	phenol <sup>97,131,158,160</sup>
	CH <sub>3</sub> NOH <sup>+</sup>	46.029	formamide <sup>143,145</sup>	97	C <sub>5</sub> H <sub>4</sub> O <sub>2</sub> H <sup>+</sup>	97.028	furfural <sup>44,90,161</sup>
	C <sub>2</sub> H <sub>7</sub> NH <sup>+</sup>	46.065	dimethylamine <sup>143</sup>	C <sub>7</sub> H <sub>13</sub> H <sup>+</sup>	97.101	methylcyclohexane <sup>106,130,159</sup>	
47	CH <sub>2</sub> O <sub>2</sub> H <sup>+</sup>	47.013	formic acid <sup>76</sup>	99	C <sub>4</sub> H <sub>2</sub> O <sub>3</sub> H <sup>+</sup>	99.008	maleic anhydride <sup>44,158</sup>
	C <sub>2</sub> H <sub>6</sub> OH <sup>+</sup>	47.049	ethanol <sup>61</sup>	C <sub>5</sub> H <sub>6</sub> O <sub>2</sub> H <sup>+</sup>	99.044	furfuryl alcohol <sup>90</sup>	
54	C <sub>3</sub> H <sub>3</sub> NH <sup>+</sup>	54.034	acrylonitrile <sup>54,131</sup>	C <sub>6</sub> H <sub>10</sub> OH <sup>+</sup>	99.080	hexenals; <sup>162–164</sup> cyclohexanone <sup>115</sup>	
57	C <sub>3</sub> H <sub>4</sub> OH <sup>+</sup>	57.033	acrolein; <sup>150</sup> MTBE <sup>53</sup>	101	C <sub>6</sub> H <sub>12</sub> OH <sup>+</sup>	101.096	hexanal <sup>147</sup>
	C <sub>4</sub> H <sub>9</sub> <sup>+</sup>	57.070	butenes; fragmentation from hydrocarbons <sup>106,130</sup>	103	C <sub>5</sub> H <sub>10</sub> O <sub>2</sub> H <sup>+</sup>	103.075	pentanoic acid <sup>143</sup>
58	C <sub>2</sub> H <sub>3</sub> NOH <sup>+</sup>	58.029	methyl isocyanate; <sup>148</sup> glycolonitrile	104	C <sub>7</sub> H <sub>5</sub> NH <sup>+</sup>	104.049	benzonitrile <sup>54</sup>
59	C <sub>3</sub> H <sub>6</sub> OH <sup>+</sup>	59.049	acetone + propanal <sup>21</sup>	105	C <sub>8</sub> H <sub>8</sub> H <sup>+</sup>	105.070	styrene <sup>21</sup>
60	C <sub>2</sub> H <sub>5</sub> NOH <sup>+</sup>	60.044	acetamide <sup>143,145</sup>	107	C <sub>7</sub> H <sub>6</sub> OH <sup>+</sup>	107.049	benzaldehyde <sup>61</sup>
	C <sub>3</sub> H <sub>9</sub> NH <sup>+</sup>	60.081	trimethylamine <sup>143,151</sup>	C <sub>8</sub> H <sub>10</sub> H <sup>+</sup>	107.086	C8 aromatics <sup>21,61</sup>	
61	C <sub>2</sub> H <sub>4</sub> O <sub>2</sub> H <sup>+</sup>	61.028	acetic acid; <sup>76,152</sup> glycolaldehyde; <sup>76</sup> fragmentation of ethyl acetate <sup>53,153</sup>	109	C <sub>7</sub> H <sub>8</sub> OH <sup>+</sup>	109.065	cresols <sup>90,143,158</sup>
63	C <sub>2</sub> H <sub>6</sub> SH <sup>+</sup>	63.026	dimethyl sulfide <sup>21,154</sup>	111	C <sub>6</sub> H <sub>6</sub> O <sub>2</sub> H <sup>+</sup>	111.044	benzenediols; <sup>44,90</sup> methylfurfural <sup>90,158</sup>
68	C <sub>4</sub> H <sub>5</sub> NH <sup>+</sup>	68.049	pyrrole <sup>155</sup>	C <sub>8</sub> H <sub>14</sub> H <sup>+</sup>	111.117	C2 cyclohexanes <sup>106,130,159</sup>	
69	C <sub>4</sub> H <sub>4</sub> OH <sup>+</sup>	69.033	furan <sup>44,60,90</sup>	118	C <sub>8</sub> H <sub>7</sub> NH <sup>+</sup>	118.065	benzyl cyanide; <sup>54</sup> indole <sup>74</sup>
	C <sub>5</sub> H <sub>8</sub> H <sup>+</sup>	69.070	isoprene and fragmentation of 2-methyl-3-butene-2-ol (MBO); <sup>136</sup> fragmentation of cyclohexanes <sup>106,130</sup>	121	C <sub>9</sub> H <sub>12</sub> H <sup>+</sup>	121.101	C9 aromatics <sup>21</sup>
70	C <sub>4</sub> H <sub>7</sub> NH <sup>+</sup>	70.065	butane nitrile; <sup>147</sup> pyrroline <sup>115</sup>	123	C <sub>8</sub> H <sub>10</sub> OH <sup>+</sup>	123.080	C2 phenols <sup>90,158</sup>
71	C <sub>4</sub> H <sub>6</sub> OH <sup>+</sup>	71.049	methyl vinyl ketone + methacrolein; <sup>21</sup> crotonaldehyde; <sup>131</sup> ISOPOOH <sup>127</sup>	125	C <sub>7</sub> H <sub>8</sub> O <sub>2</sub> H <sup>+</sup>	125.060	guaiacol; <sup>90,158</sup> methyl benzenediols
	C <sub>5</sub> H <sub>11</sub> <sup>+</sup>	71.086	fragmentation from hydrocarbons <sup>106,130</sup>	129	C <sub>10</sub> H <sub>8</sub> H <sup>+</sup>	129.070	naphthalene <sup>54,160</sup>
73	C <sub>3</sub> H <sub>4</sub> O <sub>2</sub> H <sup>+</sup>	73.028	methylglyoxal; <sup>43</sup> acrylic acid	135	C <sub>10</sub> H <sub>14</sub> H <sup>+</sup>	135.117	C10 aromatics <sup>53</sup>
	C <sub>4</sub> H <sub>8</sub> OH <sup>+</sup>	73.065	methyl ethyl ketone + butanals <sup>21</sup>	137	C <sub>10</sub> H <sub>16</sub> H <sup>+</sup>	137.132	monoterpenes <sup>136</sup>
75	C <sub>3</sub> H <sub>6</sub> O <sub>2</sub> H <sup>+</sup>	75.044	hydroxyacetone; <sup>131,156</sup> propanoic acid <sup>44</sup>	139	C <sub>9</sub> H <sub>14</sub> OH <sup>+</sup>	139.112	nopinone <sup>46</sup>
				140	C <sub>6</sub> H <sub>5</sub> NO <sub>3</sub> H <sup>+</sup>	140.034	nitrophenol <sup>165,166</sup>
77	C <sub>2</sub> H <sub>4</sub> O <sub>3</sub> H <sup>+</sup>	77.023	PAN; <sup>20,136,157</sup> peracetic acid <sup>76</sup>	149	C <sub>8</sub> H <sub>4</sub> O <sub>3</sub> H <sup>+</sup>	149.023	phthalic anhydride <sup>158</sup>
				C <sub>10</sub> H <sub>12</sub> OH <sup>+</sup>	149.096	methyl chavicol <sup>101</sup>	
				169	C <sub>10</sub> H <sub>16</sub> O <sub>2</sub> H <sup>+</sup>	169.122	pinonaldehyde <sup>46</sup>
				205	C <sub>15</sub> H <sub>24</sub> H <sup>+</sup>	205.195	sesquiterpenes <sup>79,167,168</sup>
				371	C <sub>10</sub> H <sub>30</sub> O <sub>5</sub> Si <sub>3</sub> H <sup>+</sup>	371.101	decamethylcyclopentasiloxane (DS) <sup>169</sup>

methanol obtained agreements within 25%. No significant chemical interference for methanol measurements has been observed. Compared to PTR-QMS, PTR-TOF is able to distinguish CH<sub>4</sub>OH<sup>+</sup> ions from the background O<sub>2</sub>H<sup>+</sup> (*m/z* 32.997) ions produced in the ion source, which decreases both the magnitude and humidity dependence of the instrument background for methanol measurements.<sup>60,144</sup>

**m/z 35.** Hydrogen sulfide (H<sub>2</sub>S) is detectable at *m/z* 34.995 (H<sub>2</sub>SH<sup>+</sup>) in PTR-MS. Similar to HCN and formaldehyde, the sensitivity of H<sub>2</sub>S in PTR-MS depends strongly on ambient humidity levels, due to the small difference in proton affinities of H<sub>2</sub>S (705 kJ mol<sup>-1</sup>) and water (691 kJ mol<sup>-1</sup>).<sup>73,74</sup> The intercomparison of H<sub>2</sub>S concentrations measured by PTR-MS and CRDS yielded fair agreement ( $R^2 = 0.3$ , slope = 1.24), but it was limited as well by the precision of the CRDS measurements.<sup>73,115</sup> Other ions contributing *m/z* 35 signals include O<sup>18</sup>OH<sup>+</sup> (*m/z* 35.002) and CH<sub>4</sub><sup>18</sup>OH<sup>+</sup> (*m/z* 35.038),

which are both distinguishable from H<sub>2</sub>SH<sup>+</sup> using a PTR-TOF.<sup>73</sup>

**m/z 42.** Acetonitrile is detected at *m/z* 42.034 (C<sub>2</sub>H<sub>3</sub>NH<sup>+</sup>) in PTR-MS. Previous GC-PTR-MS studies confirmed acetonitrile as the dominant species at *m/z* 42 in urban environments<sup>53,109,177</sup> and in biomass-burning plumes,<sup>54,131</sup> although interferences from alkanes (C<sub>3</sub>–C<sub>5</sub>) through reactions with O<sub>2</sub><sup>+</sup> are known.<sup>178</sup> The interference ions include C<sub>3</sub>H<sub>6</sub><sup>+</sup> ions (*m/z* 42.046) from reactions of NO<sup>+</sup> and O<sub>2</sub><sup>+</sup> with C<sub>3</sub>–C<sub>5</sub> alkanes, cyclopropane, and propene, <sup>13</sup>C-isotopes of C<sub>3</sub>H<sub>5</sub><sup>+</sup> produced from various reactions,<sup>179</sup> and C<sub>2</sub>H<sub>2</sub>O<sup>+</sup> ions (*m/z* 42.010) from fragmentation of higher-molecular-weight species.<sup>158</sup> The interfering ions contributed 5–41% of the total ion signals at *m/z* 42 in a PTR-QMS, and it is difficult to correct for this interference.<sup>179</sup> These interfering ions are easily separated by PTR-TOF from the acetonitrile ions, leading to more-accurate measurement of acetonitrile.

**m/z 44.** Isocyanic acid ( $\text{HNCO}$ ) can produce ions at  $m/z$  44.013 ( $\text{HNCOH}^+$ ) in PTR-MS.<sup>148,149</sup> The feasibility of measuring  $\text{HNCO}$  using PTR-MS is important, as  $\text{HNCO}$  has been associated with potential health effects.<sup>180</sup> The proton affinity of  $\text{HNCO}$ <sup>181</sup> was estimated to be 720 kJ mol<sup>-1</sup>, which is relatively close to that of water (691 kJ mol<sup>-1</sup>). Note that this is different from the value for  $\text{HNCO}$  in the latest review of proton affinity<sup>182</sup> (see discussions in paper by Bunkan et al.<sup>181</sup>). A significantly lower sensitivity for  $\text{HNCO}$  in PTR-MS than for other compounds was reported,<sup>146</sup> and a strong humidity dependence of the  $\text{HNCO}$  sensitivity was found.<sup>61</sup> High signals of  $m/z$  44 were detected by a PTR-ToF instrument at a site in Kathmandu with strong biomass-burning influence; however, the PTR-TOF instrument was not calibrated for  $\text{HNCO}$ .<sup>145</sup> On the basis of mass spectra obtained by PTR-TOF, other ions at  $m/z$  44 include  $\text{CO}_2^+$  ( $m/z$  43.989),  $\text{N}_2\text{O}^+$  ( $m/z$  44.000),  $\text{C}_2\text{H}_4\text{O}^+$  ( $m/z$  44.026) ( $\text{O}_2^+$  or  $\text{NO}^+$  reactions with acetaldehyde),  $\text{C}_2\text{H}_5\text{NH}^+$  ( $m/z$  44.049), and isotopes from  $m/z$  43 (<sup>13</sup> $\text{CCH}_3\text{O}^+$  and <sup>13</sup> $\text{CC}_2\text{H}_7^+$ ). Thus, a PTR-TOF is preferred for  $\text{HNCO}$  measurements.

**m/z 45.** Acetaldehyde is detected at  $m/z$  45.033 ( $\text{C}_2\text{H}_4\text{OH}^+$ ) in PTR-MS. Although both earlier and recent GC-PTR-MS studies indicated little interference at  $m/z$  45 for acetaldehyde, potential measurement artifacts of acetaldehyde by PTR-MS were inferred from other observations in several studies (see detailed discussions in paper by de Gouw and Warneke<sup>21</sup>). When the de Gouw and Warneke<sup>21</sup> review was published, there was only one intercomparison between PTR-MS and another method available.<sup>20</sup> In the past decade, intercomparisons of acetaldehyde measurements between PTR-MS and various methods (including online GC-MS, DNPH-HPLC, and PTR-MS itself) were published in seven studies (Table S1).<sup>53,54,136,140,172,183,184</sup> The average obtained slope from the seven studies is  $0.93 \pm 0.29$  ( $1.00 \pm 0.26$  if excluding the results by Kajos et al.<sup>183</sup>), suggesting reasonably good agreements in various polluted environments. However, a systematically blind intercomparison of acetaldehyde in a smog chamber suggested that acetaldehyde measurements by PTR-MS (and other techniques) may be problematic in clean background air.<sup>137</sup> A recent study demonstrated that ethylene glycol, a major component in the engine coolant of vehicles, may exist as a significant interference for acetaldehyde near sources of vehicular emissions, but the interference should be minor in most urban environments.<sup>135</sup>  $\text{CO}_2\text{H}^+$  ions ( $m/z$  44.997), contributing to the  $m/z$  45 signal as well, are distinguishable from  $\text{C}_2\text{H}_4\text{OH}^+$  ions using PTR-TOF.

**m/z 47.** Two important VOCs produce ions at  $m/z$  47 in PTR-MS, namely, formic acid ( $\text{CH}_2\text{O}_2\text{H}^+$ ,  $m/z$  47.013) and ethanol ( $\text{C}_2\text{H}_6\text{OH}^+$ ,  $m/z$  47.049). In addition to  $m/z$  47, ethanol fragments significantly to form ions at  $m/z$  29 ( $\text{C}_2\text{H}_5^+$ ) and  $m/z$  19 ( $\text{H}_3\text{O}^+$ ),<sup>108</sup> resulting in much lower sensitivity than formic acid.<sup>76</sup> As a result, signals of  $m/z$  47 in PTR-MS have been commonly attributed to formic acid. Intercomparisons of formic acid measurements using  $m/z$  47 signals of PTR-MS with other methods (Fourier transform infrared (FTIR) and acetate CIMS) were reported in biomass-burning emissions, achieving slopes at 0.80–0.90.<sup>131,185</sup> It should be noted that the ethanol sensitivity increases with higher humidity,<sup>61,76</sup> which reflects the fact that the equilibrium between the parent and hydrated ions is affected by the abundance of water molecules.<sup>61</sup> High-resolution PTR-TOF can separate the two ions at  $m/z$  47. However, the measurements of the two VOCs by PTR-TOF have not yet been compared to other techniques.

A recent study showed that  $\text{NO}^+$  chemistry can achieve a much better detection limit for ethanol than for  $\text{H}_3\text{O}^+$ .<sup>110</sup>

**m/z 59.** Signals of  $m/z$  59 in PTR-MS are mainly attributed to acetone ( $\text{C}_3\text{H}_6\text{OH}^+$ ,  $m/z$  59.049) in the atmosphere, with minor contributions from propanal (0–10%).<sup>21</sup> The intercomparisons (see Table S1) and GC-PTR-MS results<sup>53</sup> from the past decade confirmed the conclusions by de Gouw and Warneke.<sup>21</sup> Although it was demonstrated that PTR-TOF is able to distinguish the ions from acetone/propanal ( $\text{C}_3\text{H}_6\text{OH}^+$ ) and glyoxal ( $\text{C}_2\text{H}_2\text{O}_2\text{H}^+$ ,  $m/z$  59.013) using synthetic air in the laboratory,<sup>22</sup> recent results indicated that glyoxal has an extremely low sensitivity in PTR-MS, resulting in a high detection limit (250 pptv) that prevents ambient glyoxal measurements using PTR-TOF.<sup>176</sup> This is also consistent with observations from ambient measurements in our group that the glyoxal peak at  $m/z$  59 is not observed.

**m/z 61.** Acetic acid is usually detected at  $m/z$  61 ( $\text{C}_2\text{H}_4\text{O}_2\text{H}^+$ ,  $m/z$  61.028) in PTR-MS. Glycolaldehyde also contributes to this ion at  $m/z$  61. Intercomparison studies in biomass-burning plumes showed that acetic acid concentrations based on  $m/z$  61 signals agreed well (slopes between 0.79 and 1.13) with FTIR results,<sup>54,131</sup> as glycolaldehyde is four times lower than acetic acid in biomass-burning emissions.<sup>131</sup> Good agreement (slope = 1.14) of acetic acid concentrations between PTR-MS based on  $m/z$  61 signals and mist chamber coupled with ion chromatography (MC/IC) at a rural site indicated that acetic acid dominated the signals at this mass channel.<sup>152</sup> As the two VOCs produce the same ion, PTR-TOF does not allow for their separation. An alternate method using an acid trap in the inlet was proposed recently.<sup>76</sup> Other potential interferences for the measurements of acetic acid/glycolaldehyde include methyl formate and fragmentation of ethyl acetate, which were both observed during a GC-PTR-MS study in an urban environment.<sup>53</sup> Small signals of propanols (*n*-propanol and 2-propanol) can be present at  $m/z$  61 ( $\text{C}_3\text{H}_8\text{OH}^+$ ,  $m/z$  61.065) and are distinguishable from  $\text{C}_2\text{H}_4\text{O}_2\text{H}^+$  ions by PTR-TOF.

**m/z 63.** Dimethyl sulfide (DMS) is detected at  $m/z$  63.026 ( $\text{C}_2\text{H}_6\text{SH}^+$ ) in PTR-MS. The acetaldehyde–water cluster ( $\text{C}_2\text{H}_6\text{O}_2\text{H}^+$ ,  $m/z$  63.044) is known to be interference for DMS measurements at  $m/z$  63. Two intercomparison studies included in the paper by de Gouw and Warneke<sup>21</sup> obtained reasonable agreements with slopes between 0.64 and 1.11, after correcting for the interferences from the acetaldehyde–water cluster. Only one additional intercomparison study for DMS has been reported.<sup>186</sup> This comparison, between PTR-TOF and GC-FID for source samples of municipal wastes, obtained fair agreement (slope = 1.27).<sup>186</sup> The DMS ions and acetaldehyde–water clusters are separable using PTR-TOF.

**m/z 69.** Isoprene is detected at  $m/z$  69.070 ( $\text{C}_5\text{H}_8\text{H}^+$ ), but many other compounds can be present as substantial interferences in various environments,<sup>21</sup> including furan in biomass-burning plumes,<sup>54,140</sup> cycloalkanes in urban environments or oil/gas regions,<sup>106,130</sup> 2-methyl-3-buten-2-ol (MBO) emitted from certain pine trees,<sup>45,46</sup> and some leaf-wound compounds (e.g., methylbutanals and 1-peten-3-nol).<sup>129</sup> Despite the presence of these interferences, many intercomparisons of isoprene obtained good agreement in environments with large biogenic emissions. Several studies compared concentrations calculated from  $m/z$  69 with the summed concentrations of several compounds measured by other methods (e.g., isoprene + furan in biomass-burning plumes and isoprene + MBO in ponderosa pine forest), achieving good agreement (slopes between 0.87 and 1.08) as well.<sup>136,140</sup> PTR-

TOF can distinguish furan ( $C_4H_4OH^+$ ,  $m/z$  69.033) from  $C_5H_8H^+$ , allowing more accurate measurements of both compounds in biomass-burning plumes. However, other compounds listed above are not distinguishable from isoprene using PTR-TOF, as the same ions are produced. A study in a ponderosa pine forest demonstrated that  $NO^+$  chemistry allows selective measurements of isoprene and MBO.<sup>187</sup> In addition to  $C_5H_8H^+$  and  $C_4H_4OH^+$ , a small peak ( $C_3O_2H^+$ ,  $m/z$  68.997) attributed to carbon suboxide is observed at  $m/z$  69 in PTR-TOF mass spectra.<sup>188</sup>

**$m/z$  71.** The signals of  $m/z$  71 are commonly attributed to the sum of methyl vinyl ketone (MVK) and methacrolein (MACR) ( $C_4H_6OH^+$ ,  $m/z$  71.049), which are both oxidation products of isoprene under high- $NO_x$  conditions. PTR-MS measurements of MVK and MACR compared well with alternative techniques in biogenic, urban, and biomass-burning plumes in both earlier studies compiled by de Gouw and Warneke<sup>21</sup> and more recent work (Table S1). More recent GC-PTR-MS studies identified some potential interferences for MVK and MACR measurements, including crotonaldehyde in biomass-burning emissions,<sup>54,131</sup> C5 alkenes,<sup>53</sup> and C5 or higher alkanes<sup>106,130</sup> in urban regions or oil/gas regions. Moreover, it has been shown that isoprene hydroxy hydroperoxides (ISOPOOH), the oxidation products of isoprene under low- $NO_x$  conditions, can be converted to MVK or MACR through catalytic reactions on metal surfaces, and they are detected as MVK or MACR in PTR-MS as well as other analytical techniques (e.g., GC-FID or GC-MS).<sup>127</sup> Thus, the agreement found for MVK and MACR measurements from earlier intercomparison studies cannot entirely rule out common artifacts from ISOPOOH.<sup>127</sup> PTR-TOF can distinguish ions of MVK and MACR ( $C_4H_6OH^+$ ) from the ions produced by alkenes and alkanes ( $C_5H_{11}^+$ ,  $m/z$  71.086), but the interferences from crotonaldehyde and ISOPOOH still exist. Selective measurements of MVK + MACR and ISOPOOH may be achieved by ancillary techniques, such as a cold trap in the inlet<sup>189,190</sup> or  $NO^+$  chemistry with a novel drift tube.<sup>40</sup>

**$m/z$  73.** Methyl ethyl ketone (MEK) is detected at  $m/z$  73.065 ( $C_4H_8OH^+$ ). Recent GC-PTR-MS studies in urban<sup>53</sup> and biomass-burning emissions<sup>54,131</sup> identified methyl *tert*-butyl ether (MTBE) and butanals (*n*-butanal and methyl propanal) as potential interferences at this mass channel. Other ions that contribute to  $m/z$  73 include  $C_3H_4O_2H^+$  ( $m/z$  73.028) from methylglyoxal or acrylic acid and the  $H_3O^+(H_2O)_3$  water cluster ( $m/z$  73.050),<sup>191</sup> both of which can be separated by PTR-TOF from MEK. Intercomparison studies generally obtained reasonable agreements with slopes at  $1.19 \pm 0.52$  for MEK in various environments, implying that MEK usually dominates the ion channel.

**$m/z$  75.** The signal at  $m/z$  75 is mainly attributed to two compounds, namely, hydroxyacetone and propanoic acid ( $C_3H_6O_2H^+$ ,  $m/z$  75.044).<sup>192</sup> Hydroxyacetone was believed to be the primary contributor to  $m/z$  75 signals at a tropical rainforest site with high isoprene emissions.<sup>186</sup> Intercomparison of hydroxyacetone concentrations derived from  $m/z$  75 signals obtained slopes at 0.74 and 0.81 with FTIR in two biomass-burning studies.<sup>131,138</sup> Recently,  $m/z$  75 signals were attributed to propanoic acid at a site in boreal forest dominated by monoterpene emissions.<sup>193</sup> Intercomparison of propanoic acid concentrations with a recently developed GC-MS system obtained good correlation ( $R = 0.72$ ) but poor agreement (slope = 0.43), possibly due to calibration issues.<sup>193</sup> Other potential interferences at  $m/z$  75 include methyl acetate

( $C_3H_6O_2H^+$ ), glyoxylic acid ( $C_2H_2O_3H^+$ ,  $m/z$  75.008), and diethyl ether ( $C_4H_{10}OH^+$ ,  $m/z$  75.080). There is no reported GC-PTR-MS study for  $m/z$  75, as both hydroxyacetone and propanoic acid were not recovered from the GC columns used in previous GC-PTR-MS studies. PTR-TOF does not allow for the separation of hydroxyacetone and propanoic acid (or methyl acetate).

**$m/z$  77.** It has been shown that peroxyacetyl nitrate (PAN) can be detected at  $m/z$  77 in PTR-MS ( $C_2H_4O_3H^+$ ,  $m/z$  77.023), which is formed from the reaction of protonated PAN with water.<sup>157</sup> Two intercomparisons of PAN measurements between PTR-MS and specific PAN instruments obtained promising agreement with slopes at 0.72 and 1.37, respectively.<sup>20,136</sup> The two studies speculated about possible interferences: water cluster of protonated acetone ( $C_3H_8O_2H^+$ ,  $m/z$  77.060) and protonated peracetic acid ( $C_2H_4O_3H^+$ ).<sup>20,136</sup> Contributions from glycolic acid ( $C_2H_4O_3H^+$ ) need to be considered as well. It is worth noting that less-promising results from an intercomparison of PAN measurements by PTR-MS have been observed in our laboratory for reasons that were not understood.<sup>115</sup> In PTR-TOF, the water clusters of protonated acetone would not be an interfering issue, but peracetic acid and glycolic acid remain as interferences for PAN measurements.

**$m/z$  79.** Benzene is detected at  $m/z$  79.054 ( $C_6H_6H^+$ ) in PTR-MS. Numerous intercomparison and GC-PTR-MS studies indicate benzene is the dominant species in many different environments. Minor interferences can come from fragmentation of higher aromatics (e.g., ethylbenzene, *n*-propylbenzene, and isopropylbenzene) and water cluster of protonated acetic acid,<sup>21</sup> the latter of which is distinguishable from benzene in PTR-TOF (see Figure 4 in paper by Kaser et al.<sup>136</sup>). In source samples of agricultural or municipal wastes emissions, dimethyl sulfoxide (DMSO,  $C_2H_6SOH^+$ ,  $m/z$  79.021) and the fragmentation of dimethyl disulfide (DMDS) ( $CH_3S_2^+$ ,  $m/z$  78.967) can contribute to  $m/z$  79,<sup>154</sup> but they should only account for minor fractions of  $m/z$  79 in most ambient environments.

**$m/z$  93.** Toluene is detected at  $m/z$  93.070 ( $C_7H_8H^+$ ). Similar to benzene, the measurements of toluene at  $m/z$  93 have been validated through many intercomparisons and GC-PTR-MS studies. GC-PTR-MS studies suggested a possible contribution to  $m/z$  93 from fragmentation of higher aromatics (e.g., *p*-cymene),<sup>53,130</sup> but the concentrations of these larger aromatics are typically much lower than those of toluene. Some monoterpenes can fragment to  $m/z$  93, but the interferences from monoterpenes were reported to be negligible even at a site with higher monoterpene concentrations than toluene (factor 2–30).<sup>194</sup>

**$m/z$  95.**  $m/z$  95 in PTR-MS is commonly attributed to phenol ( $C_6H_5OH^+$ ,  $m/z$  95.049). Measured phenol concentrations from  $m/z$  95 in two biomass-burning studies agreed well with FTIR measurements (slope = 0.84 and 1.02).<sup>131,138</sup> Another intercomparison study of phenol from PTR-MS in an urban environment obtained good agreement for a gas standard (slope = 0.96) but only fair agreement with DOAS for ambient measurements ( $R = 0.53$  and slope = 0.68).<sup>160</sup> Two interferences were identified from the only GC-PTR-MS study of  $m/z$  95 conducted in biomass-burning emissions, with one attributed to vinylfuran and the other one unidentified.<sup>131</sup> PTR-TOF mass spectra at  $m/z$  95 further demonstrated the contribution of  $C_7H_{11}^+$  ( $m/z$  95.086) ions to  $m/z$  95 signals, which might be fragments of higher alkanes.<sup>97</sup>

PTR-TOF can distinguish  $C_6H_6OH^+$  ions from  $C_7H_{11}^+$ , but it cannot differentiate phenol from vinylfuran.

**m/z 97.** The signals of  $m/z$  97 in PTR-MS were attributed to several different VOC species. A GC-PTR-MS analysis of the  $m/z$  97 signal was conducted for biomass-burning emissions.<sup>131</sup> On the basis of this study, C2-substituted furans ( $C_6H_8OH^+$ ,  $m/z$  97.065) and 2- or 3-furaldehydes ( $C_5H_4O_2H^+$ ,  $m/z$  97.028) accounted for 79% and 21% of  $m/z$  97 signals, respectively.<sup>131</sup> Recently, it has also been reported that  $m/z$  97 signals ( $C_7H_{13}^+$ ,  $m/z$  97.101) are mainly contributed by methylcyclohexane in oil and gas extraction regions and in the evaporation of gasoline.<sup>106,130,159</sup> The protonated ions from the reactions of  $H_3O^+$  with methylcyclohexane (and several other cycloalkanes) usually fragment by  $H_2$  elimination to yield M-H ions.<sup>195</sup> Intercomparison of methylcyclohexane concentrations from  $m/z$  97 in an oil- and gas-extraction region showed strong correlation and reasonably good agreements with GC measurements.<sup>159</sup> However, a later comparison of methylcyclohexane between PTR-MS and GC only obtained poor agreement, with some evidence indicating that secondary VOCs fragment to  $C_7H_{13}^+$  ions.<sup>115</sup> A PTR-TOF study in an urban environment with some influence of residential wood burning confirmed the presence of the three ions ( $C_7H_{13}^+$ ,  $C_6H_8OH^+$ , and  $C_5H_4O_2H^+$ ) in the mass spectra.<sup>161</sup>

**m/z 107.** The signals at  $m/z$  107 are commonly attributed to the sum of C8 aromatics ( $C_8H_{10}H^+$ ,  $m/z$  107.086), including ethylbenzene, *m*-xylene, *p*-xylene, and *o*-xylene. The measured total concentrations of C8 aromatics generally compared well with alternative techniques (Table S1). Benzaldehyde ( $C_7H_6OH^+$ ,  $m/z$  107.049) was observed to account for small fractions of  $m/z$  107 signals in several GC-PTR-MS studies.<sup>54,109</sup> It was suggested that benzaldehyde may become more important in aged air masses.<sup>109</sup> A recent study showed that benzaldehyde contributed significant fractions to  $m/z$  107 signals in a PTR-TOF mass spectra over an oil- and gas-extraction region (Permian Basin)<sup>61</sup> but not for another oil and gas region (Uintah Basin).<sup>196</sup> Deployments of PTR-TOF in other environments would help to understand the importance of benzaldehyde at  $m/z$  107.

**m/z 121.** The sum of C9 aromatics is detected at  $m/z$  121 ( $C_9H_{12}H^+$ ,  $m/z$  121.101). Eight isomers are possible: two propyl benzenes (*n*-propyl and isopropyl), three ethyl toluenes, and three trimethylbenzenes. As shown by de Gouw and Warneke,<sup>21</sup> intercomparison studies between PTR-MS and other methods for C9 aromatics are limited compared to other lighter aromatics, because all of the isomers need to be quantified for the comparison. Several GC-PTR-MS studies in both urban and biomass-burning plumes showed no significant interference at this mass channel.<sup>53,54</sup> Recent results from PTR-TOF in our group indicate that substantial fractions from tolualdehyde signals ( $C_8H_8OH^+$ ,  $m/z$  121.065) at  $m/z$  121 are observed for both fresh and aged biomass-burning plumes and minor but non-negligible fractions in an urban area. Similar to  $m/z$  107, more PTR-TOF studies are needed to better constrain this issue. It is worth mentioning that the proposed  $C(^{37}Cl)_2^{35}Cl^+$  ions from  $CCl_4$  are not detectable at  $m/z$  121 in mass spectra of PTR-TOF, which is contrary to the suggestion by de Gouw and Warneke.<sup>21</sup>

**m/z 129.** The signals of  $m/z$  129 are frequently attributed to naphthalene ( $C_{10}H_8H^+$ ,  $m/z$  129.070). There is only one study comparing measured naphthalene from PTR-MS with another technique (DOAS) at an urban site, obtaining fair agreement with significant scatter ( $R = 0.54$  and slope = 0.60).<sup>160</sup> The only

GC-PTR-MS study for  $m/z$  129 was conducted for biomass-burning emissions, obtaining a single peak from naphthalene.<sup>54</sup> However, oxygenated ions can also contribute to  $m/z$  129, including  $C_8H_{16}OH^+$  ( $m/z$  129.127) (e.g., octanals),  $C_7H_{12}O_2H^+$  ( $m/z$  129.091), and  $C_6H_8O_3H^+$  ( $m/z$  129.055). PTR-TOF would be able to separate these ions and provide more accurate measurements of naphthalene.

**m/z 137.** The sum of monoterpenes is detected at  $m/z$  137.132 ( $C_{10}H_{16}H^+$ ). In addition to protonated ions at  $m/z$  137, monoterpenes fragment to  $m/z$  81 ( $C_6H_9^+$ ) and other minor ions (e.g.,  $m/z$  67,  $m/z$  93, and  $m/z$  95).<sup>77,78</sup> Intercomparisons between PTR-MS and alternative methods (mainly GC techniques) obtained mixed results (slopes between 0.64 and 2.16, average =  $1.28 \pm 0.45$ ), partially due to the need to quantify multiple isomers for the comparison, which are rarely all quantified by GC-MS.<sup>21</sup> Using GC-PTR-MS, no other contribution to  $m/z$  137 was seen in either urban areas or biomass-burning plumes.<sup>53,54</sup> Recent PTR-TOF studies observed several ions at  $m/z$  137, including  $C_9H_{12}OH^+$  ( $m/z$  137.096),  $C_8H_8O_2H^+$  ( $m/z$  137.060), and  $C_7H_4O_3H^+$  ( $m/z$  137.023) in both biomass-burning plumes<sup>90</sup> and in an orange grove,<sup>197</sup> which remain unidentified for specific oxygenated species.

**m/z 205.** The signals at  $m/z$  205 have been attributed to sesquiterpenes ( $C_{15}H_{24}H^+$ ,  $m/z$  205.195). In addition to the protonated ions at  $m/z$  205, sesquiterpenes fragment significantly to  $m/z$  149 ( $C_{11}H_{16}^+$ ) and other minor ions ( $m/z$  81,  $m/z$  95,  $m/z$  109, and  $m/z$  137), and the fragmentation patterns depend on electric field (i.e.,  $E/N$ ) in the drift tube and are different for different species.<sup>79,167,168</sup> The strong fragmentation results in lower sensitivities of sesquiterpenes at  $m/z$  205 in PTR-MS.<sup>79</sup> The low mass transmission of higher masses in the quadrupole also contributes to low sensitivities of sesquiterpenes by PTR-QMS.<sup>79</sup> Measurements of sesquiterpenes have been reported in a ponderosa pine forest by a PTR-QMS<sup>46,79</sup> and also by a PTR-TOF using the exact  $C_{15}H_{24}H^+$  ions.<sup>102</sup> The contributions of other high-resolution ions to  $m/z$  205 were not shown. Intercomparisons of sesquiterpenes concentrations between PTR-MS and other techniques have not been reported.

**m/z 371.** Recently, the signal at  $m/z$  371.101 has been attributed to decamethylpentasiloxane (D5 siloxane,  $C_{10}H_{30}Si_5O_5H^+$ ) from PTR-TOF measurements.<sup>169</sup> High-resolution peak fitting indicates D5 siloxane dominates the signal at  $m/z$  371 in urban environments. D5 siloxane is a silicon-containing compounds commonly found in personal care products such as lotions, shampoos, and deodorants as well as industrial products such as sealants and lubricants.<sup>198–200</sup> In urban environments, the variability of D5 siloxane has been primarily attributed to emissions from personal care products.<sup>200–202</sup> D5 siloxane fragments in PTR-MS by loss of a methyl group to yield  $C_9H_{27}Si_5O_5H^+$  at  $m/z$  355.069. Approximately 50% of the signal associated with D5 siloxane can be found at the  $m/z$  355.069 fragment. These masses appear to be ubiquitous in urban environments and may be useful to extend the range in mass or peak-width calibrations. The discovery of the possibility to measure these siloxanes by PTR-MS is an excellent example in illustrating the advantages in scanning whole mass spectra by PTR-TOF, rather than recording a few preselected masses for PTR-QMS.

### 3.3. Analysis of Mass Spectra for Bulk Chemical Information

Attribution of each mass in PTR-MS mass spectra to specific VOC species is important for PTR-MS studies. However, even without explicit identification of each individual mass, the ion signals or derived concentrations from PTR-MS mass spectra can be useful in understanding VOC sources and atmospheric processes (e.g., oxidation of VOCs). Here, we will summarize two analytical methods on PTR-MS mass spectra for bulk chemical information on VOCs mixtures: factor analysis and the analysis based on chemical formulas of PTR-TOF masses.

Receptor models have been widely used to investigate the sources of VOCs for a long time.<sup>203</sup> VOC species measured by PTR-MS are usually combined with VOC measurements from other analytical techniques (commonly GC methods). Various receptor models have been used, including principal component analysis (PCA)<sup>87,192,204</sup> and positive matrix factorization (PMF).<sup>53,205,206</sup> Factor analysis using the PMF technique has been more popular for VOC studies, as PMF utilizes positively constrained algorithms that are more realistic for atmospheric sciences. As PMF does not need a priori knowledge of source profiles, ion signals or VOC concentrations from PTR-MS (either unit mass-resolution data or high-resolution data from PTR-TOF) can be used as the input data for PMF analysis.

A PMF study using unit mass-resolution mass spectra from a PTR-QMS between  $m/z$  20 and  $m/z$  150 was conducted at a rural site in Canada.<sup>42</sup> Recently, PTR-MS mass spectra were merged with mass spectra from AMS for combined PMF analysis,<sup>207,208</sup> which provides additional information on emission sources and atmospheric processing beyond what can be obtained from an individual instrument. There is no study reporting PMF results based on high-resolution PTR-TOF mass spectra yet. Moreover, source apportionment using the multilinear engine (ME-2), a more-advanced factor-analysis tool that allows the user to supply some or all of the initial factor profiles,<sup>209</sup> was applied to an early data set of PTR-MS.<sup>210</sup> It should be noted that photochemistry (and other atmospheric processes, e.g., gas-particle partitioning) in the atmosphere may distort the results of PMF analysis (and other factor-analysis methods), and this effect should be considered in interpretation of resolved PMF factors.<sup>53,205</sup>

The large number of masses and chemical formulas provided by PTR-TOF now allow the applications of many well-established mass spectrometry analysis tools, such as Van Krevelen diagrams and carbon oxidation state ( $OS_C$ ) analysis, which are useful in studying atmospheric oxidation of VOCs. The hydrogen-to-carbon ratios (H/C) and oxygen-to-carbon ratios (O/C) for the total measured VOCs can be determined by averaging individual masses in the mass spectra weighted by their signals (or determined concentrations if available). The Van Krevelen diagram, i.e., the scatterplot of H/C versus O/C, is a useful diagnostic tool for atmospheric oxidation.<sup>211</sup> In the van Krevelen diagram, the addition of the functional groups is characterized by different slopes.<sup>211</sup> For example, the addition of a carboxylic acid group is associated with a slope of  $-1$ .<sup>211</sup> Carbon oxidation state, approximately calculated as  $2 \times O/C - H/C$ , along with carbon number can deliver a two-dimensional (2D) visual analysis tool to describe chemical evolution of organic carbon in the atmosphere.<sup>212</sup> Recently, an alternative method based on mass-defect information from the raw mass spectra without the need for peak fitting was also proposed to

determine  $OS_C$ .<sup>83</sup> For detailed discussions on these mass-spectral analysis, we refer to a recent review paper.<sup>10</sup>

Despite the widespread use of the two analysis tools in the aerosol community (especially AMS applications) for studying the evolution of organic aerosol, they have not been widely applied to PTR-MS data. In a chamber study of 1,3,5-trimethylbenzene photooxidation, O/C ratios increased with the oxidation processes, whereas H/C ratios remained relatively constant.<sup>213</sup> According to the  $OS_C$ -carbon number space, photooxidation of 1,3,5-trimethylbenzene was dominated by fragmentation reactions in the beginning and acquisition of functional groups in the later period.<sup>213</sup> It should be noted that ion fragmentation upon protonation in PTR-MS (e.g., loss of  $H_2O$  for compounds with hydroxyl and hydroperoxy groups and loss of  $HNO_3$  for compounds with nitrate group) may affect the determination of the bulk parameters shown earlier.<sup>213</sup> In addition, the bulk average of other parameters shown in section 3.1, e.g., DBE and aromaticity equivalent,<sup>142</sup> can be calculated from PTR-MS mass spectra to explore VOC oxidation.

## 4. RESEARCH HIGHLIGHTS

### 4.1. Urban Emissions

PTR-MS has been used extensively to measure VOC emissions from vehicles. Several early studies deployed PTR-MS on mobile laboratories to measure individual or fleet-average emissions of many VOC species, including benzene, toluene, C8 aromatics, C9 aromatics, methanol, and acetaldehyde.<sup>214–216</sup> Recently, PTR-MS was used to characterize vehicular emissions of some novel species. From a series of chassis dynamometer experiments and ambient measurements at an intersection,<sup>165,217,218</sup> nitromethane was frequently observed from vehicular emissions, with good correlations with other hydrocarbons and CO. Further results indicated that emissions of nitromethane from gasoline vehicles were significantly lower than those from diesel vehicles.<sup>218</sup> Emissions of other nitro-compounds (e.g., nitrophenols) were also detected, associated with large variations among vehicle types.<sup>165</sup> In a recent study, PTR-MS was configured to measure long-chain alkanes in exhausts of diesel vehicles.<sup>219</sup> The results indicated that emissions of these long-chain alkanes are high, with emission intensities at similar levels as C6–C10 aromatics.<sup>219</sup> Emissions of HCN from vehicles measured by PTR-TOF were also reported.<sup>72</sup> The highly time-resolved VOC measurements of vehicular emissions by PTR-MS suggested that cold-start emissions occur almost entirely in the first 30–60 s, whereas hot-stabilized emissions with much lower intensities than cold-start emissions may only exceed the amount of cold-start emissions after a long driving distance (e.g., 200 miles) for new vehicles.<sup>220</sup> These results imply that cold start may dominate the vehicular emissions in the near future in the United States.<sup>220</sup> Recently, VOC emissions from aircrafts, which affect air quality near airports, were measured by a PTR-TOF.<sup>221</sup>

PTR-MS measurements have provided valuable insights into VOC emissions and chemistry in urban air.<sup>7,222</sup> The highly time-resolved VOC data were reported to be important in accurately constraining OH reactivity of VOC.<sup>223</sup> Additional species measured by PTR-TOF may help to explain “missing” organic carbon, inferred from both carbon-balance studies<sup>7</sup> and OH reactivity work.<sup>224</sup> However, deployments of PTR-TOF in urban environments are surprisingly limited. The studies in the

literature are mainly from Indian researchers, who have deployed PTR-TOF in two south Asian cities in winter time.<sup>145,225,226</sup> In particular, high concentrations of acetaldehyde, acetonitrile, and benzene were observed from a study in Kathmandu, Nepal. In addition, the authors also detected strong signals of formamide, acetamide, nitromethane, and isocyanic acid, which may pose significant human health concerns.<sup>145</sup>

Eddy covariance flux measurements of VOCs in urban areas are more challenging than areas covered by vegetation (e.g., forests) due to the requirements to measure on tall tower for obtaining fully representative fluxes from the underlying urban surface.<sup>227</sup> VOC flux measurements using PTR-MS were successfully performed in several cities, namely, Mexico City,<sup>227,228</sup> Manchester,<sup>229</sup> London,<sup>230,231</sup> and Helsinki.<sup>232</sup> For all of these studies, vehicular emissions were reported to be the major contributors to fluxes of aromatics. Nontraffic sources, including evaporative emissions and biogenic sources, might be important for some species, e.g., toluene and methanol in Mexico City<sup>228</sup> and methanol and isoprene in London.<sup>230,231</sup> In general, measured fluxes of aromatics agreed well with estimates in emission inventories, whereas emissions of oxygenated VOCs (OVOCs) were substantially higher than the estimates in emission inventories.<sup>229,230</sup> In addition to flux measurements at ground sites, airborne flux measurements of aromatics using PTR-MS have also been demonstrated.<sup>233,234</sup> As VOC concentrations from PTR-MS are reported as volumetric mixing ratios, flux measurements by PTR-MS can be influenced by the air-density fluctuations related to water concentrations in the air (the so-called WPL correction).<sup>235</sup> On the basis of previous estimates, this effect is usually minor,<sup>235</sup> because humidity dependence of the PTR-MS sensitivity is usually taken into account.

#### 4.2. Biomass-Burning Emissions

Biomass burning constitutes a major source of primary carbon in Earth's atmosphere. Communities downwind of wildfires are subject to elevated health risks associated with the inhalation of particulate matter and toxic VOCs.<sup>180,236</sup> In many cities, wood burning is a dominant source of wintertime pollution.<sup>237,238</sup> The increased importance of biomass burning has prompted a renewed interest of the VOCs emitted from these sources and their transformation in the atmosphere.

Many studies have utilized PTR-MS to study biomass-burning emissions in both laboratory<sup>54,90,131,138,158,239</sup> and field campaigns.<sup>44,240–242</sup> Earlier work identified and quantified biomass-burning constituents measured by PTR-MS via instrument intercomparison and/or coupling to GC.<sup>54,131,138</sup> These studies provided insights into the emission factors of important ozone and secondary organic aerosol (SOA) precursors, such as small oxygenates (e.g., formaldehyde and acetaldehyde), isoprenoid compounds (e.g., myrcene,  $\alpha$ -pinene, and isoprene), aromatics (e.g., benzene, toluene, and styrene), and alkenes (e.g., 1,3-butadiene and butenes). Particularly, the high-time-resolution acetonitrile measurements by PTR-MS have been widely used as a tracer of biomass burning,<sup>178</sup> although recent studies suggested that acetonitrile may not be suitable as a tracer for emissions from residential wood burning.<sup>158,161</sup>

Advances in PTR-TOF have afforded researchers the capability to separate common isobaric species (e.g., isoprene and furan,  $m/z$  69) and determine the chemical formula for previously unidentified constituents in biomass-burning emis-

sions.<sup>90,147,158</sup> Recently, substituted aromatic species (e.g., phenol, methoxy phenols, and benzenediols) and furan-like compounds (e.g., furanone, 2-furfuraldehyde, and methyl furan) have been identified as major reactive components in biomass-burning smoke from PTR-MS measurements.<sup>90,103,158</sup> Due to their high reactivity and functionality, substituted aromatics have the potential to significantly contribute to SOA and ozone formation.<sup>103,243</sup> For a summary of biomass-burning species identified using PTR-MS, we refer to these publications: refs 54, 90, 147, and 158.

A benefit of using PTR-MS in the measurements of biomass-burning emissions is its fast time resolution and high sensitivity toward a significant fraction of VOCs in smoke.<sup>90</sup> This advantage of PTR-MS allows the evaluation of differences in VOC emissions as a function of burn stage (i.e., modified combustion efficiency (MCE), which assesses the extent of flaming versus smoldering combustion). For example, furan is emitted under both flaming and smoldering conditions, whereas substituted aromatics, such as benzenediols, are generally observed more under smoldering conditions.<sup>103</sup> Measurements by PTR-TOF allow for the resolution of MCE-VOC relationships for species that may play a significant role in important atmospheric processes, such as SOA formation.

The measurement of biomass-burning emissions by PTR-MS has also enabled advances in the understanding of biomass-burning plume evolution. Müller et al.<sup>44</sup> modeled the evolution of an understory biomass-burning plume using a chemical box model that incorporated the top 16 VOCs measured by a PTR-TOF. The model successfully reproduced the evolution of O<sub>3</sub>, PAN, NO<sub>x</sub>, furan, and 2-furfural but could not recreate the evolution of other observed products, such as maleic anhydride. Bruns et al.<sup>158</sup> also observed production of maleic anhydride, as well as other oxygenates, such as formic acid, acetic acid, and signal attributed to phthalic anhydride. While the chemistry of a number of biomass-burning precursors has been studied in detail, the mechanism of highly reactive species, such as 2-furfuraldehyde, has yet to be evaluated.

#### 4.3. Biogenic Emissions

PTR-MS has been deployed in many field campaigns to measure concentrations of the most common biogenic compounds,<sup>107,156,244–246</sup> including isoprene, the sum of monoterpenes, methanol, acetaldehyde, and acetone. Measurements of several exotic biogenic species, e.g., MBO,<sup>187,247</sup> methylsalicylate,<sup>248</sup> sesquiterpenes,<sup>79</sup> and methyl chavicol (i.e., estragole),<sup>249</sup> have been developed for PTR-MS. The identification of other ions in the mass spectra of PTR-MS has been shown in several recent publications.<sup>46,197,250</sup>

PTR-MS has been used intensively to measure emissions and deposition fluxes of VOCs in various ecosystems.<sup>251</sup> Various techniques were used for flux measurements of biogenic emissions using PTR-MS, including eddy covariance,<sup>252</sup> disjunct-eddy covariance,<sup>45</sup> surface-layer gradient,<sup>253</sup> relaxed-eddy accumulation (REA),<sup>254</sup> mixed-layer gradient,<sup>255</sup> mixed-layer variance,<sup>255</sup> and mixed-layer mass balance.<sup>256</sup> A recent study suggested that the removal of oxygenated VOCs via dry deposition is substantially larger than is currently assumed for deciduous ecosystems.<sup>257</sup> Similar to deposition, emissions of isoprene and monoterpenes in emission inventories have significant uncertainties that need further investigation.<sup>256</sup> For example, isoprene emissions were reported to be under circadian control in a Malaysian rainforest, resulting in an

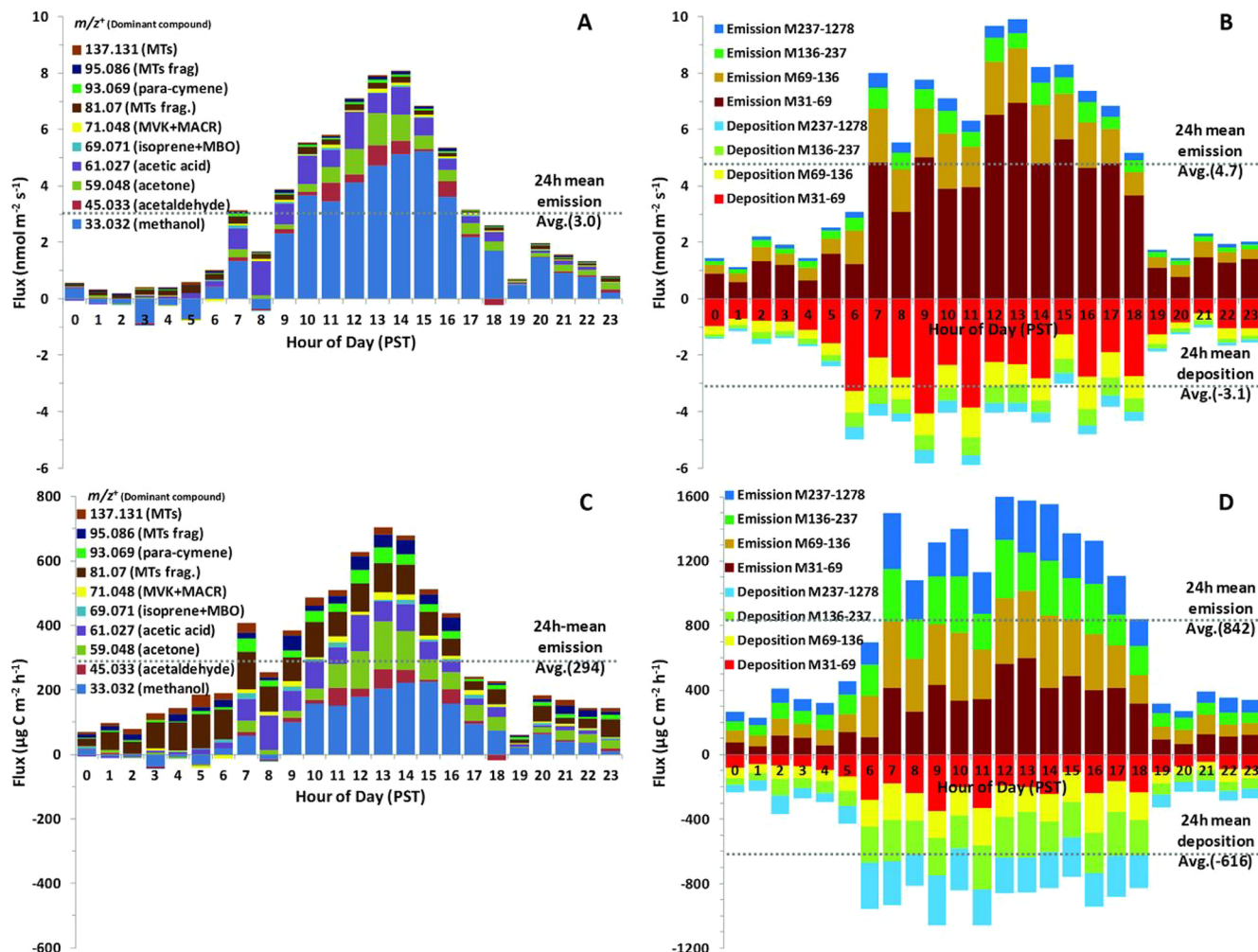


**Figure 10.** BVOC diurnal emission and deposition fluxes, on a molar basis for (A) 10 major compounds, (B) 4 different mass ranges categorized as  $m/z$  31–69 ( $n = 61$ ),  $m/z$  69–136 ( $n = 141$ ),  $m/z$  136–237 ( $n = 141$ ), and  $m/z$  237–1278 ( $n = 141$ ), and on a carbon mass basis for (C) 10 major masses and (D) 4 classes. Staged bar plots of 10 masses and 4 classes with the largest fluxes are shown as diurnal cycles with  $m/z$  (or  $m/z$  range) indicated in the legend. The scale of the y axis in (C) is half that of (D). Reprinted with permission from ref 197. Copyright 2013 American Association for the Advancement of Science.

inconsistency between measured and predicted emissions.<sup>258</sup> Flux measurements in pine forests found that monoterpene emissions were significantly higher after a hailstorm.<sup>102,259</sup> Distinct from forest emissions, biogenic emissions from grasslands<sup>250</sup> and crops<sup>260</sup> are usually dominated by oxygenated VOCs, including methanol, acetaldehyde, and acetone. Large emissions of some unexpected biogenic compounds have been proposed from PTR-MS measurements, such as benzenoid species.<sup>261</sup>

Because TOF mass spectrometers measure all masses simultaneously, PTR-TOF allows flux measurements of many VOC species at the same time. In recent years, PTR-TOF has been deployed in various ecosystems to measure emissions and deposition of biogenic VOCs, including temperate forests,<sup>102,262</sup> grasslands,<sup>144,250,259</sup> and agricultural lands.<sup>197,235,255,263</sup> As shown in Figure 10, biogenic VOC (BVOC) flux measurements by PTR-TOF in an orange grove indicated that many product ion masses (494 ions) were associated with bidirectional fluxes, implying a strongly active atmosphere–ecosystem exchange of the vast majority of detected VOC species.<sup>197</sup> Many of these VOC species are not included in current BVOC-emission models, but they could

be important for regional photochemistry and SOA formation.<sup>197</sup>

In the recent years, PTR-MS instruments have been deployed on research aircraft to measure regional biogenic VOC emissions using airborne eddy-covariance techniques.<sup>264,265</sup> The measured isoprene fluxes were compared with current BVOC emission models.<sup>266,267</sup> The comparison showed agreement of >50% for more than half of the ecoregions between measured and modeled emissions.<sup>266</sup> In addition to emission estimates, flux-divergence information derived from airborne eddy-covariance measurements of BVOC fluxes can be used to infer concentrations of OH radicals,<sup>265,268</sup> the intensity of segregation in isoprene oxidation,<sup>269</sup> and the entrainment velocity into the free troposphere.<sup>265,268</sup>

PTR-MS measurements in BVOC-dominated regions have enabled advances in understanding the chemical mechanisms of BVOC oxidation, especially of isoprene. It was shown that isoprene is oxidized by hydroxyl radical (OH) to ISOPOOH under the pristine conditions.<sup>270</sup> Further oxidation of these ISOPOOH species leads to formation of either epoxydiols (IEPOX)<sup>270</sup> or other low-volatility organic compounds (LVOC, e.g.,  $C_5H_{10}O_5$ ).<sup>271</sup> In contrast, the oxidation of

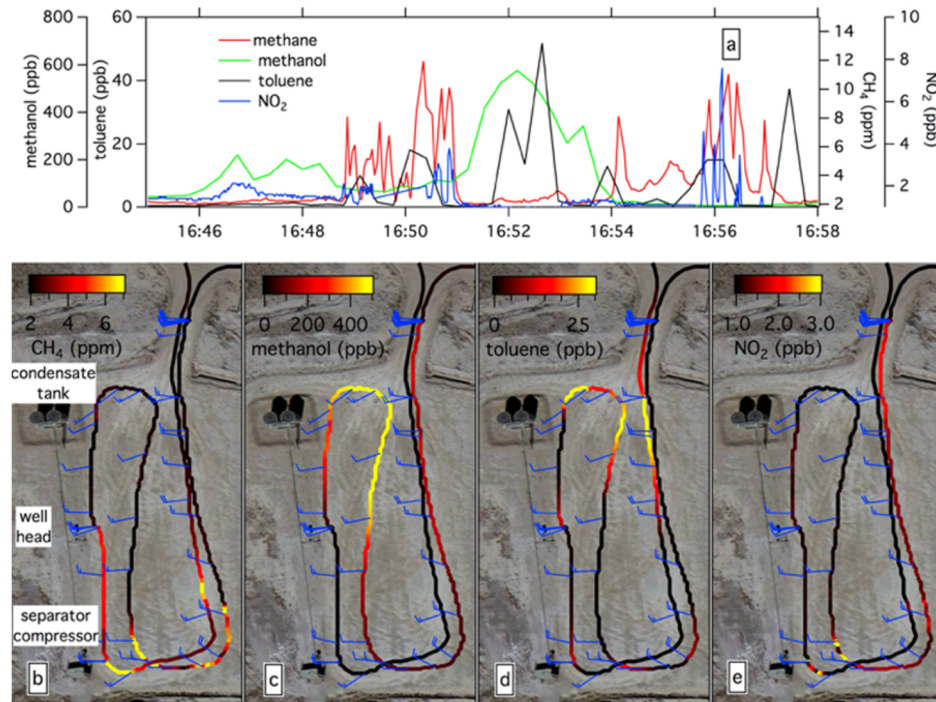


**Figure 11.** Drive track close to a gas well color coded by measured methane (b), methanol (c), toluene (d), and NO<sub>2</sub> (e). The wind barbs indicate the prevailing wind direction coming from left to right in the image. The time series for this period is shown in (a). Reprinted with permission from ref 159. Copyright 2014 Warneke and co-workers; CC Attribution 3.0 License.

isoprene in the presence of NO<sub>x</sub> mainly forms methyl vinyl ketone (MVK), methacrolein (MACR), and formaldehyde. As shown in section 3.2 (*m/z* 71), ISOPOOH isomers are detected as MVK or MACR (C<sub>4</sub>H<sub>6</sub>OH<sup>+</sup>) in PTR-MS (and GC-MS as well).<sup>127</sup> Subsequent laboratory experiments showed that ISOPOOH<sup>40</sup> and IEPOX<sup>272</sup> can be selectively detected at C<sub>3</sub>H<sub>9</sub>O<sup>+</sup> and C<sub>5</sub>H<sub>6</sub>O<sup>+</sup> using NO<sup>+</sup> chemistry, respectively. No selective measurement of ISOPOOH and IEPOX using NO<sup>+</sup> chemistry has yet been reported in the ambient atmosphere. Another approach to selective measurements of these species is removal of the less-volatile ISOPOOH using a cold trap (−40 °C) in the inlet.<sup>189,190</sup> Using this method, the yields of MVK (3.8%) and MACR (2.5%) in low-NO<sub>x</sub> conditions were found to be significantly lower than in previous measurements.<sup>190</sup> The deployment of the same instrumentation setup in the Amazon rainforest demonstrated that the ratio of the reaction rate of isoprene peroxy radicals (ISOPOO) with HO<sub>2</sub> relative to that with NO is ~1 for background conditions in the Amazon rainforest.<sup>189</sup>

#### 4.4. Oil and Gas Emissions

Extraction of crude oil and natural gas can have large impacts on regional air quality and can emit greenhouse gases. Recent applications of PTR-MS in oil- and gas-extraction regions have helped to quantify these environmental impacts. PTR-MS measurements showed that concentrations of cycloalkanes, aromatics, and some oxygenated VOCs (e.g., methanol) were extremely high (up to 500 ppbv for methanol) in oil- and gas-extraction regions.<sup>115,159,273</sup> Release of various hydrocarbons was observed by PTR-MS from fractured shale in a laboratory experiment.<sup>274</sup> High concentrations of toxic H<sub>2</sub>S (0.6 ± 0.3 ppbv) in a natural gas production region were also observed from PTR-MS deployments.<sup>73,115</sup> These VOC species and other air toxics can be emitted from a number of sources or operational activities. Mobile measurements using PTR-MS in

an oil and gas basin in Utah indicated that VOCs were mainly emitted from oil and condensate tanks, pneumatic devices, and pumps (Figure 11).<sup>159</sup> Photochemistry of VOCs in oil and gas regions can lead to severe ozone pollution in the wintertime.<sup>275</sup> The atmospheric oxidants in wintertime ozone formation were primarily produced from photolysis of carbonyls (e.g., formaldehyde and methylglyoxal), and this was confirmed by *in situ* VOC measurements using PTR-TOF and PTR-QMS.<sup>43,276</sup> High-time-resolution measurements of aromatics by PTR-MS in oil- and gas-extraction regions can be valuable, as the concentration ratios and their variability can be used to estimate VOC emission rates and ambient OH radical concentrations.<sup>196</sup> It was also shown that airborne measurements of aromatics by PTR-MS over oil and gas basins can provide constraints on VOC emission rates.<sup>277</sup>

In addition to routine operations in oil and gas extraction, PTR-MS was also used to study an unintentional oil spill. Highly time-resolved measurements of aromatics by PTR-MS over the Deepwater Horizon oil spill were used to estimate their emission rates, which were further extrapolated to total VOC emissions (i.e., the leak rate of the oil spill).<sup>278</sup> The spatial distributions of these aromatics underlying their emission extent in the oil spill were also used to determine the relative importance of organic compounds with different volatilities to the SOA formation observed downwind from the Deepwater Horizon oil spill.<sup>279</sup>

#### 4.5. Agricultural Emissions

Agricultural sources can emit many different air pollutants, affecting climate and regional air quality. In this section, we will highlight recent research into VOC emissions from livestock operations. PTR-MS was used to measure VOC emissions inside feeding facilities with different animals, including dairy cattle,<sup>280,281</sup> pigs,<sup>74</sup> and sheep.<sup>282</sup> These PTR-MS measurements showed strong temporal variations in VOC emissions.<sup>74</sup>

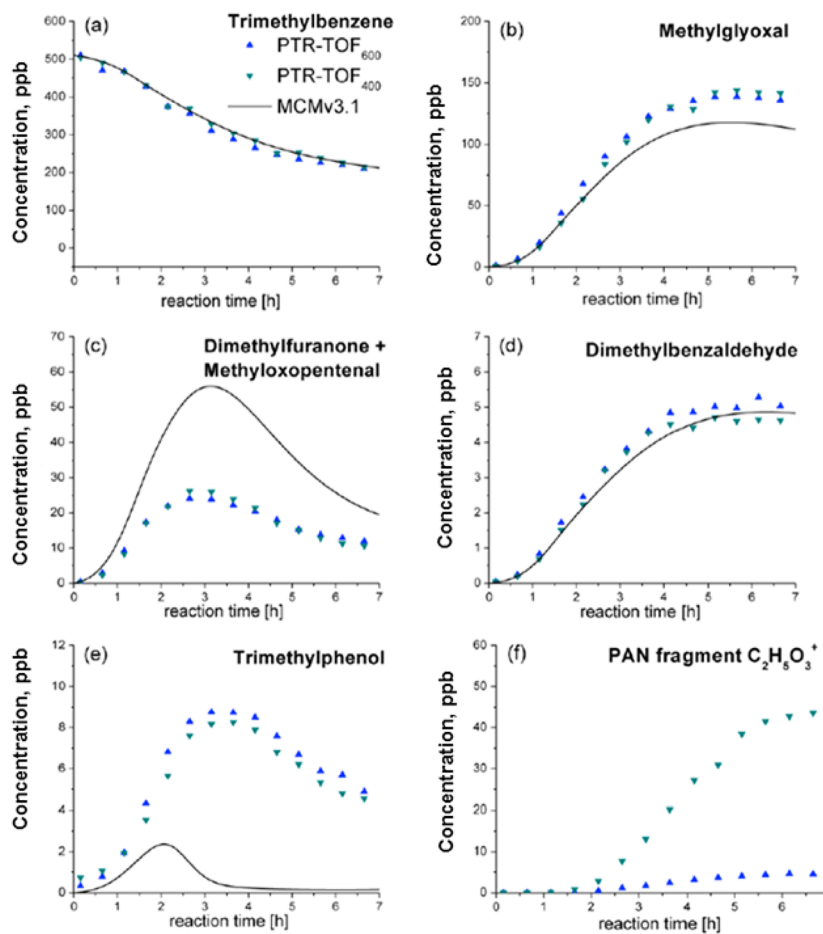


**Figure 12.** Time evolution of (a) 1,3,5-trimethylbenzene and (b–f) selected 1,3,5-trimethylbenzene degradation products as measured during two experiments, during which the PTR-TOF drift tube was operated at 600 V (PTR-TOF<sub>600</sub>) and 400 V (PTR-TOF<sub>400</sub>), respectively. The black lines illustrate corresponding MCM 3.1 predictions. Reprinted with permission from ref 213. Copyright 2012 Müller and co-workers; CC Attribution 3.0 License.

VOC emissions were shown to be associated with feeding activities, as VOC concentrations were significantly higher when animal waste was removed and feed was provided.<sup>281,282</sup> The VOC species emitted from livestock operations include carboxylic acids (acetic acid and butyric acid), alcohols (ethanol), phenols (phenol and cresol), and sulfur-containing ( $\text{H}_2\text{S}$ , methanethiol, and DMS) and nitrogen-containing (trimethylamine, formamide, and indole) compounds.<sup>74,280</sup> Many of these species are difficult to quantify by conventional analytical methods, such as offline samples followed by GC-MS analysis, but accurate measurements of these VOC compounds are more straightforward using PTR-MS.<sup>154</sup>

High-time-resolution measurements of VOCs from livestock operations by PTR-MS afford the opportunity to explore emission processes of various VOCs. Fast measurements of trimethylamine (TMA) and other VOCs (e.g., acetone) by PTR-MS were conducted in a dairy farm.<sup>151</sup> A recent comprehensive study pointed out that trimethylamine emissions were primarily from animal waste (i.e., feces and urine).<sup>151</sup> Recently, a PTR-TOF instrument was deployed on a mobile laboratory to measure VOC emissions from several concentrated animal-feeding operations.<sup>143</sup> The mobile measurements with high measurement frequency allowed the separation of VOC sources from different parts of the facilities.<sup>143</sup> The results indicate that ethanol emissions were predominantly from feed storage and handling, whereas

emissions of phenolic species and nitrogen-containing species were mainly emitted from animal waste.<sup>143</sup> PTR-MS was also shown to be a promising tool to evaluate the effectiveness of odor-mitigation measures in feeding facilities.<sup>283,284</sup>

#### 4.6. Marine Environments

The oceans play important roles in the global budget of many VOCs, including DMS, methanol, acetaldehyde, and acetone,<sup>285–288</sup> but both magnitudes and distribution of the oceanic sources and sinks are highly uncertain.<sup>289,290</sup> PTR-MS measurements of VOCs in marine environments helped to advance understanding of these issues. Long-term measurements (5 years) of methanol, acetaldehyde, and acetone by a PTR-MS were taken at a remote Atlantic site.<sup>291</sup> Comparison between measurements and a global chemical-transport model indicated that the tropical Atlantic was a net sink for acetone but a net source for methanol and acetaldehyde.<sup>291</sup> A ship-based measurement in the Arctic Ocean suggested that biologically active waters in the high Arctic acted as sinks for acetone and methanol.<sup>292</sup>

PTR-MS was deployed to directly measure VOC fluxes over oceans using surface-layer gradient,<sup>293</sup> disjunct-eddy covariance,<sup>294</sup> and eddy-covariance methods.<sup>295,296</sup> Flux measurements of acetone over the Atlantic Ocean suggested a net sink in high Northern latitudes, a net source in the subtropics, and a near-zero net flux in the South Atlantic.<sup>295,297</sup> Mixed flux results

for acetone were obtained by other researchers as well: a net sink of acetone was observed in the South Atlantic,<sup>294</sup> whereas an emission of acetone in the western Pacific Ocean was found.<sup>293</sup> In contrast to acetone, consistent fluxes of methanol from the atmosphere to the ocean were measured in the Atlantic ocean.<sup>296</sup>

Measurements of VOC concentrations in seawater along with atmospheric concentrations provide an additional means to estimate the air–sea exchange of VOCs. Measurements of DMS, methanol, acetone, and acetonitrile in seawater by PTR-MS were first demonstrated using a purge-trap method.<sup>298</sup> Later, Kameyama and co-workers deployed a bubbler-type equilibrator inlet coupled with PTR-MS (EI-PTR-MS) to measure seawater concentrations of DMS, methanol, acetone, acetonitrile, and isoprene in the western Pacific Ocean<sup>299,300</sup> and isoprene in the Southern Ocean.<sup>301</sup> Recently, a membrane inlet-PTR-MS (MI-PTR-MS) system was proposed for monitoring OVOC concentrations in seawater.<sup>302</sup> The MI-PTR-MS system was deployed during an Atlantic transect cruise<sup>303</sup> and an annual study at the English Channel in the United Kingdom<sup>304</sup> to measure seawater concentrations of methanol, acetone, and acetaldehyde.

#### 4.7. Laboratory Studies of Atmospheric Chemistry

PTR-MS has been applied in numerous laboratory studies in atmospheric sciences, including chamber experiments,<sup>181,305–307</sup> flow-tube experiments,<sup>308–311</sup> and other types of laboratory studies (e.g., aqueous reactions).<sup>312</sup> Many PTR-MS instruments have been used exclusively for laboratory purposes. In many laboratory studies, PTR-MS is commonly used to monitor concentrations of hydrocarbon precursors and/or their oxidation products, to support experiments investigating the kinetics and mechanism of VOC oxidation, and to explore the secondary formation of fine particles, e.g., refs 306 and 311. Specifically, PTR-MS measurements of 9-fold deuterated butanol (butanol-*d*<sub>9</sub>, *m/z* 66.126) have been used as an effective approach to estimate OH exposure in chamber studies.<sup>313</sup> We note that the application of PTR-MS in laboratory studies can be substantially different from those in ambient environments, because frequently only a limited number of hydrocarbon precursors are introduced into the experimental system, and thus attribution of various PTR-MS masses is considerably easier than in ambient air.

Recent applications of PTR-TOF in chamber studies demonstrated that PTR-TOF is a valuable tool to study chemical mechanisms in oxidations of organic compounds.<sup>55,213,314–316</sup> As an example, Figure 12 shows time evolution of 1,3,5-trimethylbenzene and its gas-phase oxidation products during a chamber experiment, measured by a high-resolution PTR-TOF.<sup>213</sup> When comparing PTR-TOF measurements with the model predictions from a state-of-the-art chemical mechanism (MCM 3.1), the agreement was excellent for some products, while others exhibited significant discrepancies, implying potential problems in current chemical mechanisms.<sup>213</sup>

#### 4.8. Indoor Air

PTR-MS has been applied to study VOC concentrations, sources, and their potential chemistry in indoor environments. Several VOCs, including acetone, isoprene, methanol, and acetic acid, are present in human breath, as they are produced during human metabolic processes.<sup>31</sup> These species have been reported to be among the most abundant VOCs in the indoor air of public spaces (e.g., university classrooms), suggesting that

human metabolic emissions are important VOC sources in indoor air.<sup>317,318</sup> The applications of PTR-TOF offer the opportunity to identify some novel VOC species in indoor environments, such as cyclic volatile methylsiloxanes.<sup>169</sup> Siloxanes emitted from personal care products can account for large fractions of VOC mass concentrations in indoor air.<sup>169,317</sup> An additional source of VOCs in indoor environments is human skin oil oxidized by ozone.<sup>317,318</sup> Related compounds include 4-oxopentanal (4-OHA) and 6-methyl-5-hepten-2-one (6-MHO), produced from ozonolysis of squalene as proposed by Wisthaler and Weschler.<sup>319</sup> Formation of these secondary VOC species, along with the decrease of ozone concentrations, was observed in indoor environments (see example in Figure 13)<sup>318,319</sup> and even in outdoor environments

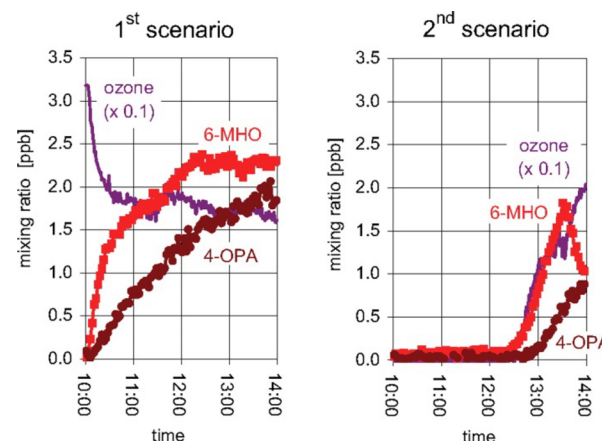


**Figure 13.** Mixing ratios of O<sub>3</sub> (values plotted are 1/10 measured values), 6-MHO, and 4-OHA in the simulated office. (Left) First scenario: two subjects entered at 10:00 and remained in the room until the end of the experiment. (Right) Second scenario: two subjects entered the simulated room at 09:00; at 12:00 the ozone generators were turned on; at 13:30 the subjects left the room, and the ozone generators remained on. Reprinted with permission from ref 319. Copyright 2010 Proceedings of the National Academy of Sciences.

with large crowds.<sup>320</sup> Other sources may also contribute to VOC emissions in indoor environments and/or outdoor environments with large crowds, such as acetonitrile, acetaldehyde, and diacetyl from cigarette smoking and ethanol from alcohol consumption.<sup>320</sup> Food preparation including cooking can emit large amounts of aldehydes<sup>321</sup> and monoterpenes,<sup>322</sup> which may also be significant VOC sources in household environments. In addition to indoor air quality, VOC measurements in indoor environments by PTR-MS may provide unexpected information on human behaviors. VOC compositions measured by PTR-MS in a movie theater were shown to change associated with specific scenes in the movie, which may be a result of human group response to related audiovisual stimuli.<sup>323</sup> In addition, the use of PTR-MS to study VOC emissions from building materials and drying processes of painting has been reported.<sup>324</sup>

## 5. OTHER INSTRUMENT DEVELOPMENTS

### 5.1. Switchable Reagent Ions

A number of researchers have modified PTR-MS instruments to utilize reagent ions other than H<sub>3</sub>O<sup>+</sup>. This allows measurements of trace gases that are not detectable with H<sub>3</sub>O<sup>+</sup> chemistry; the separation of isobars (for unit-mass-

resolution or UMR MS), isomers (UMR and high-resolution MS), or interferences due to fragmentation; and an improvement in sensitivity for VOCs that are detected at lower sensitivity by  $\text{H}_3\text{O}^+$  chemistry. This technique has been termed “switchable-reagent-ion” or “selective-reagent-ion” MS (SRI-MS).<sup>27,187</sup> Early work was conducted by Wyche et al.<sup>325</sup> and Blake et al.,<sup>326</sup> while a more recent commercial SRI-MS instrument has been used extensively.<sup>27</sup>

There are several advantages to modifying a PTR-MS instrument rather than using an alternative technique such as selected-ion flow-tube mass spectrometry (SIFT-MS), other than the obvious issue of cost. SRI-MS is relatively easy to implement; it requires only an additional reagent source gas and possibly a few valves and/or flow controllers.<sup>27,110,326,327</sup>

SRI-MS instruments can switch quickly between different reagent ion chemistries: switching times on the order of one second to a few minutes have been reported.<sup>27,325,327,328</sup> SRI-MS also avoids the large transmission losses of selecting reagent ions using an additional quadrupole mass filter in SIFT techniques, allowing high sensitivities.<sup>329</sup>

Several conceptually different alternative-reagent-ion techniques have been explored. The most common is to produce the alternate reagent ion directly by adding a different source gas to the ion source. This technique has been used successfully with both radioactive ion sources<sup>326,330</sup> and hollow-cathode ion sources.<sup>27,110,331</sup> The most frequently used alternate reagent ions are  $\text{NO}^+$  (created by adding either air or a mixture of NO in  $\text{N}_2$  to the ion source);  $\text{O}_2^+$  (created by adding pure  $\text{O}_2$  to the ion source); and  $\text{NH}_4^+$  (created by adding pure  $\text{NH}_3$  to the ion source). All three ions result in VOC sensitivities on the same order as  $\text{H}_3\text{O}^+$ .<sup>27,110,326</sup>

$\text{NO}^+$  is the most commonly applied. Its strengths are the detection of alkanes (Figure 14)<sup>110,332</sup> and organic nitrates<sup>113</sup>

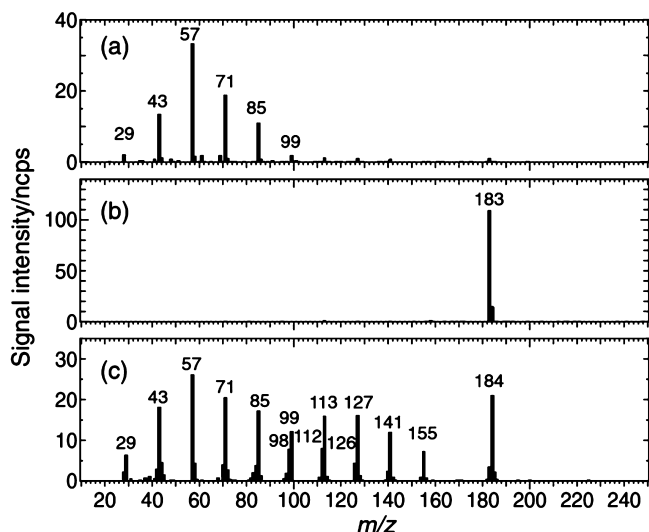


**Figure 14.** Chemical-ionization mass spectra of *n*-tridecane with (a)  $\text{H}_3\text{O}^+$ , (b)  $\text{NO}^+$ , and (c)  $\text{O}_2^+$  reagent ions. Reprinted with permission from ref 332. Copyright 2014 Chemical Society of Japan.

and the differentiation of isomers based on functional-group-dependent ionization mechanism.<sup>27,110,179,187,325</sup> There are three common reaction mechanisms for  $\text{NO}^+$ :<sup>110</sup> charge transfer (e.g., alkenes, aromatics,<sup>110</sup> and organosulfur<sup>333</sup>), hydride abstraction (e.g., aldehyde, alcohols, and large alkanes<sup>110</sup>), and cluster formation (e.g., ketones<sup>110</sup> and

carboxylic acids<sup>117</sup>).  $\text{NO}^+$  has been applied in measurements of alkanes emitted from petrochemical and vehicular sources<sup>331,334,335</sup> and biogenic VOCs.<sup>187,190,247</sup>

$\text{O}_2^+$  extensively fragments VOCs, resulting in complex mass spectra.<sup>179,326,332</sup> However, only a single ionization mechanism—charge transfer—occurs, and  $\text{O}_2^+$  can efficiently ionize some molecules that  $\text{H}_3\text{O}^+$  cannot.  $\text{O}_2^+$  has been successfully applied to fast and quantitative measurement of ammonia<sup>126,170,171</sup> and ethene.<sup>336</sup>

$\text{NH}_4^+$  ionizes by proton transfer and VOC- $\text{NH}_4^+$  adduct formation.<sup>326</sup> The higher proton affinity of  $\text{NH}_3$ , compared to  $\text{H}_2\text{O}$ , leads to higher VOC selectivity than conventional PTR-MS.<sup>326</sup> This higher selectivity has been long recognized as a way to distinguish isobaric compounds.<sup>14</sup> Although  $\text{NH}_4^+$  has not yet seen significant use in atmospheric chemistry, it has been used to detect and identify gas-phase explosives residues.<sup>337</sup> It is worth noting that an instrument using  $\text{NH}_4^+$  may not switch back to other reagent ions quickly, due to the slow degassing of surface-bound ammonia.

Recently, a few other reagent ions have been explored. Because of its very high ionization energy,  $\text{Kr}^+$  (created by adding pure Kr to the ion source) has been investigated by Sulzer et al.<sup>329</sup> and Edtbauer et al.<sup>338</sup> for the measurements of  $\text{CO}$ ,  $\text{CO}_2$ ,  $\text{CH}_4$ ,  $\text{NO}_2$ , and  $\text{SO}_2$ . This technique opens the possibility of universal trace gas analysis with a single instrument but has significant drawbacks, especially the necessity of diluting the sample air by a factor of 500 with He or  $\text{N}_2$  in order to avoid saturation by secondary  $\text{O}_2^+$ . Recent work by Blake et al.<sup>339</sup> using  $\text{CF}_4$  to produce  $\text{CF}_3^+$  and  $\text{CF}_2\text{H}^+$  ions has suggested a promising method for studying small *n*-alkanes (ethane and larger) with low fragmentation and detection limits around 10 ppbv. A negative reagent ion,  $\text{OH}^-$ , was also generated in the hollow-cathode ion source of PTR-MS using water vapor.<sup>340</sup> Switching between  $\text{H}_3\text{O}^+$  and  $\text{OH}^-$  has been successfully demonstrated for a PTR-MS.<sup>341</sup> The advantage of  $\text{OH}^-$  as the alternative reagent ion is no need to change the source gas into the ion source.<sup>341</sup>  $\text{OH}^-$  chemistry is able to detect both VOCs and some inorganic compounds, e.g.,  $\text{CO}_2$ .<sup>340</sup> However, switching between positive and negative reagent ions may not be possible for the hardware (e.g., power supply) of some PTR-MS instruments.

A second approach uses a two-stage reagent-ion-generation process, where  $\text{H}_3\text{O}^+$  ions are created and then reacted with a reagent source gas to transform  $\text{H}_3\text{O}^+$  into new reagent ions that react with the sampled air. This technique was pioneered by Inomata and Tanimoto<sup>342</sup> and Blake et al.<sup>327</sup> and has the advantage that a wide range of reagent ions can be created by adding a large quantity of any VOC with proton affinity higher than water either at the top of the drift tube or to the sample inlet. The two-stage technique has been demonstrated as a method of separating isomers that have proton affinities bracketing that of the VOC reagent.<sup>327</sup> The relative contributions of the isomers can be quantified by rapidly (~2 min) switching between the VOC reagent ion and  $\text{H}_3\text{O}^+$  and have been demonstrated for isomer pairs 1,4-dioxane and ethyl acetate, butanal and butanone, and methyl vinyl ketone and methacrolein.<sup>327,342</sup> The two-stage technique has also been used by Latappy et al.<sup>343</sup> to create  $\text{C}_6\text{H}_5\text{F}_2^+$  reagent ion from difluorobenzene, which resulted in greatly reduced fragmentation of alcohols compared to  $\text{H}_3\text{O}^+$  PTR-MS.

A third approach changes the ion source and drift-tube operating conditions to vary the relative quantities of reagent ions that are typically generated by conventional PTR-MS

( $\text{H}_3\text{O}^+$ ,  $\text{H}_3\text{O}^+(\text{H}_2\text{O})$ ,  $\text{O}_2^+$ , and  $\text{NO}^+$ ). Fortner and Knighton<sup>344</sup> changed drift-tube conditions to promote  $\text{H}_3\text{O}^+(\text{H}_2\text{O})$  and were able to demonstrate the separation of isobaric compounds acrolein and 1-butene, based on the relative proton affinities of acrolein, 1-butene, and water dimer. Amador-Muñoz et al.<sup>345</sup> created a mixture of  $\text{O}_2^+$ ,  $\text{H}_3\text{O}^+$ , and  $\text{NO}^+$  by modifying the hollow-cathode extraction voltages and drift-tube voltage, and they demonstrated the applicability of this technique to studying complex mixtures of aliphatic hydrocarbons.

There are several common challenges in the use of alternate reagent ions. Switching from  $\text{H}_3\text{O}^+$  to other reagent ions in PTR-MS often leads to contaminant  $\text{H}_2\text{O}$ -related ions from residual water in the instrument.<sup>27,326</sup> It has been reported that product-ion distributions of VOCs produced with the same reagent ion seem to vary considerably between adapted PTR-MS instruments and between adapted PTR-MS and SIFT-MS studies.<sup>110,326</sup> Finally, many alternate reagent ions result in complex mass spectra, and little work exists to assist in interpreting these measurements.<sup>110,325,326,332,345</sup>

## 5.2. Improvement of the Sensitivity

As discussed in section 2.1 (and shown in Figure 1), new ion-guiding interfaces for better ion transmission in PTR-TOF instruments have drastically enhanced VOC sensitivities in the past few years.<sup>24,36</sup> On the basis of the fundamental controls over the PTR-MS sensitivity (e.g., eq 10 in the paper by Taipale et al.<sup>80</sup> and eq 10 in section 2.4), the approaches to increase PTR-MS sensitivity (cps/ppbv) include (1) higher reagent ion ( $\text{H}_3\text{O}^+$ ) signals; (2) higher conversion efficiency of  $\text{H}_3\text{O}^+$  to product ions by using a higher pressure and/or longer drift tube; and (3) more-efficient extraction of ions from the drift tube to the mass analyzer. The first approach is primarily related to the ion source, while the second approach generally requires higher dc voltages applied to the two ends of the drift tube to maintain the same collision energies (i.e.,  $E/N$ ). A voltage of 500–1000 V has been applied to the drift tube for current instrumentation. Higher voltages can be supplied, but this enhances the likelihood of electric discharges in the instrument. An improved ion transmission has been achieved by the applications of the new ion interfaces, including multipole ion guides and ion funnel. To further boost the sensitivity of PTR-TOF instruments, ion funnel and multipole ion guides can be used in series in a PTR-TOF instrument, which has been demonstrated by the new PTR-TOF 6000 X2 introduced by Ionicon Analytik (<http://www.ionicon.com/product/ptr-ms/ptr-tofms-series/ptr-tof-6000-x2>).

The sensitivity of PTR-MS can also be improved using unconventional reaction-chamber designs. In the conventional drift-tube design, the ion kinetic energy is enhanced in the forward direction, which limits cluster ion formation but also the reaction time and therefore the sensitivity. More advanced drift-tube designs enhance the ion kinetic energy in the transverse direction, which greatly increases the reaction time and sensitivity while maintaining the same declustering conditions. Recently, a PTR-TOF instrument with an innovative reaction chamber (PTR3) was developed at the University of Innsbruck.<sup>37</sup> The reaction chamber of the new instrument consists of a tripole, which is operated with RF voltages to generate an electric field only in the radial direction. The axial movement of the ions is driven by the gas flow only. The sensitivities of organic gases are up to 18 000 cps/ppbv (e.g., ketones) with the ability to measure concentrations at ppqv ( $1 \times 10^{-15}$ ) range, as the result of 30-fold longer reaction

time and 40-fold increase in drift-tube pressure compared to standard PTR-TOF.<sup>37</sup> However, the sensitivities of many common VOCs are significantly lower than those of ketones (e.g., benzene is only 872 cps/ppbv in dry conditions), and the sensitivities exhibit much stronger humidity dependence (e.g., up to a factor of ~100 for methanol) than that with other PTR-MS instruments.<sup>37</sup> Combining with an inlet consisting of a critical orifice (rather than capillary used for most PTR-MS instruments), measurements of highly oxidized multifunctional organic molecules (HOMs) by the PTR3 instrument are demonstrated from a chamber experiment in studying ozone oxidation of  $\alpha$ -pinene.<sup>37</sup> The PTR3 instrument was recently deployed to perform flux measurements in ambient air (Armin Hansel, personal communication). More recently, Tofwerk AG introduced a new PTR-ToF instrument that combines a radio-frequency field in the drift tube to focus the ions, with a higher-resolution TOF-MS. Preliminary results indicate that limits of detection (sub-pptv for 1 min integration) and instrument sensitivities toward benzene, toluene, and xylenes ( $\sim 2 \times 10^4$  cps/ppbv), listed by the company, are competitive, and they await detailed evaluation and publication in the peer-reviewed literature (<http://www.tofwerk.com/ptr>).

## 5.3. Improved Separation of Isobars and Isomers

Modern PTR-TOF instruments are able to separate many isobaric masses but not all. A recent study showed that the peak density in the TOF mass spectra from ambient air can be substantially higher than can be resolved using the current TOF-MS ( $R \approx 4000$ –6000).<sup>83</sup> In other words, many compounds present in the atmosphere are not resolvable with these instruments.<sup>83</sup> It stresses that the separation of heavier isobaric masses in PTR-TOF mass spectra can be an issue for complicated atmospheric samples. Incorporation of TOF mass spectrometers with better mass resolution would help to alleviate this issue. A new TOF mass spectrometer with a longer time-of-flight chamber (LTOF) was recently introduced by Tofwerk AG. The mass resolution of the LTOF is up to 14 000, compared to 4000–6000 for the widely used HTOF mass spectrometer. LTOF was recently used in the newly developed PTR3 instrument<sup>37</sup> (section 5.2) but has not yet been used in commercial PTR-TOF. The improvement of peak separation by LTOF-MS over current instrument design remains to be demonstrated by ambient measurements.

Current PTR-TOF instruments cannot separate isomers. Mass spectrometric techniques using CID analysis were demonstrated as a possible approach to differentiate isomers in PTR-MS. The CID method has been mainly applied in PTR-MS using ion-trap mass spectrometers (PTR-IT-MS). It has been used to distinguish MVK from methacrolein<sup>26,49</sup> and acetone from propanal<sup>25,52</sup> in laboratory and ambient environments. Differentiation of various monoterpene isomers was also explored using CID in PTR-IT-MS, but it proved to be difficult to quantitatively separate for a mixture of several monoterpenes.<sup>346</sup> A PTR-MS using a triple-quadrupole tandem mass spectrometer (QqQ-MS) was recently used to perform similar CID studies by means of MS/MS.<sup>48</sup> The MS/MS study demonstrated successful distinction of MVK and methacrolein, but selective detection of monoterpenes and sesquiterpenes in complex mixtures was not possible.<sup>48</sup> On the basis of experience in our group, CID analysis of many isomers often produces the same fragment ions; hence, the CID analysis only provides quantitative separation for a limited number of isomers in PTR-MS. For many isomers, the CID spectra are

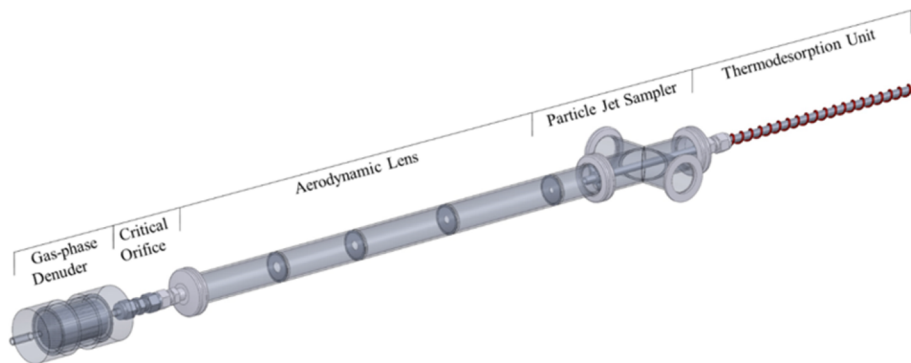


**Figure 15.** CHARON inlet with its main components including (1) a gas-phase denuder, (2) a critical orifice combined with an aerodynamic lens and an inertial sampler for the particle-enriched flow, and (3) a thermo-desorption unit. Reprinted with permission from ref 355. Copyright 2015 Eichler and co-workers; CC Attribution 3.0 License.

not sufficiently different from each other to allow an accurate determination of separate mixing ratios when both species are present.

Although CID analysis of specific ions is not possible for PTR-TOF instruments, varying voltages in the ion guides can provide fragmentation information. This may potentially assist in distinguishing different isomers, as shown in a study using a TOF-CIMS that is equipped with the same quadrupole ion guide from Tofwerk as the PTR-QiTof.<sup>114</sup> In addition to these “post-ionization” approaches, potential differentiation of monoterpene isomers was proposed by varying the electric field in the drift tube.<sup>347</sup> Similarly, rapidly switching on and off the RF voltages of the ion funnel in a PTR-TOF may be useful to separate isomers.<sup>348</sup>

Several studies sought to separate isomers based on their chemical or physical properties. This can be achieved by removing a certain class of compounds from the sample using various techniques. Baasandorj et al.<sup>76</sup> used an acid trap (KOH-treated CarboBlack B) to selectively remove formic acid and acetic acid from the sampled air of PTR-QMS. The contributions of formic acid and ethanol to  $m/z$  47, and acetic acid and glycolaldehyde to  $m/z$  61, were successfully determined in a biogenic environment. Knighton et al.<sup>150</sup> designed an aldehyde scrubber system to separate the signals of acrolein at  $m/z$  57 from other compounds that also contribute to  $m/z$  57. Liu et al.<sup>190</sup> utilized a cold trap ( $-40^{\circ}\text{C}$ ) to distinguish MVK and MACR from other low-volatility compounds produced from isoprene oxidation (mainly ISOPOOH). In addition, coupling of PTR-MS with GC techniques has been used extensively to separate different isomers in many PTR-MS studies (see detailed discussions in section 3.1).

#### 5.4. Aerosol Measurements

In addition to gas-phase measurement, PTR-MS has been used to measure chemical compositions in particles. The approach was first demonstrated by Hellen and colleagues, who designed a new heated inlet ( $120/150^{\circ}\text{C}$ ) for PTR-MS to vaporize particles.<sup>349</sup> Later, an aerosol collection/thermal desorption inlet was coupled with a PTR-IT-MS to measure organic compounds in aerosol.<sup>38</sup> In this system, aerosol was collected on a stainless-steel post through impaction, and the post was heated to  $150^{\circ}\text{C}$  after collection to desorb organic compounds from particles for analysis by PTR-IT-MS.<sup>38</sup> A similar collection/thermal desorption (CTD) inlet was built independently by Holzinger and co-workers at Utrecht University,

and the CTD inlet was used along with a PTR-QMS and later a PTR-TOF (referred to as TD-PTR-MS).<sup>350,351</sup> The TD-PTR-MS was employed intensively in recent years, including in a smog chamber for SOA formation from ozonolysis of biogenic VOCs,<sup>351</sup> at a rural site in The Netherlands,<sup>351</sup> at a remote mountain site in the Austrian Alps (Mt. Sonnblick observatory),<sup>350</sup> at an urban site in Los Angeles (Pasadena),<sup>352</sup> and at a forested site in the Southeastern United States.<sup>353</sup> The TD-PTR-MS was found to detect ~80% of the masses of SOA formed from ozone reaction with BVOCs,<sup>351</sup> whereas TD-PTR-MS may only detect ~50% of organic aerosol mass in an urban environment.<sup>352</sup> Reasonably quantitative agreements for individual organic compounds were observed between TD-PTR-MS and filter samples analyzed by GC  $\times$  GC-TOF-MS.<sup>354</sup> A recent systematic intercomparison between TD-PTR-MS and three other similar thermal-desorption techniques for measurements of gas-particle partitioning demonstrated that the campaign average partitioning fractions showed good agreement, but significant differences were present for detailed comparisons. This highlights the difficulty of this type of measurement and the need for further improvements and characterization of these techniques.<sup>353</sup>

The TD-PTR-MS systems commonly have a cycle time of tens of minutes to hours for aerosol collection and desorption. To overcome this issue, a novel inlet, the chemical analysis of aerosol online (CHARON), was designed for PTR-MS to measure aerosol chemical compositions in real time<sup>355</sup> (Figure 15). The CHARON inlet consists of a gas-phase denuder, an aerosol aerodynamic lens system for enriching particles, and a thermal-desorption unit for particle volatilization.<sup>355</sup> The initial proof-of-principle work demonstrated measurements of organic compounds in aerosol at a time resolution of several minutes.<sup>355</sup> Recently, the CHARON-PTR-TOF system was deployed to characterize organic aerosol from ship-engine exhaust.<sup>356</sup> Results showed that emissions of organic aerosol were dominated by C20–C39 polycycloalkanes, suggesting lubricating oil as the main source of organic aerosol.<sup>356</sup>

In addition to in situ aerosol measurements by PTR-MS, offline analysis by PTR-MS of organic vapors from desorption of filter samples has been developed in several research groups.<sup>354,357,358</sup> The analysis typically works by placing the filters in a temperature-controlled filter holder or oven and using a nitrogen flow to deliver desorbed volatiles to PTR-MS. Offline TD-PTR-MS systems were used to analyze filter samples of SOA from ozone reaction with isoprene,<sup>357</sup> filters from vehicular emissions,<sup>359</sup> and filters collected at urban<sup>358,360</sup>

and forest sites.<sup>360</sup> Comparison between offline and online TD-PTR-MS found positive sampling artifacts from adsorption of semivolatile organic compounds (SVOCs) and negative sampling artifacts from incomplete desorption of high-loading filters for the offline technique.<sup>354</sup>

As discussed by Eichler et al.,<sup>355</sup> aerosol measurements using PTR-MS have two main advantages compared with other mass spectrometric techniques: (1) PTR-MS can theoretically detect almost all of the organic molecules present in particles. (2) The sensitivity of PTR-MS usually varies only by 30–50% between species, and the sensitivity can be easily predicted (see discussion in section 2.4). There are also some drawbacks to PTR-MS analysis of aerosol:<sup>355</sup> (1) Even with PTR-TOF, isomeric species cannot be separated. (2) Fragmentation can still be important for some species, e.g., loss of H<sub>2</sub>O for species with –OH or of HNO<sub>3</sub> for –ONO<sub>2</sub> functional groups (see section 2.4.3), which leads to inability to measure these species and additional uncertainties in bulk parameters from the mass spectra (e.g., O/C ratio, nitrogen content). Furthermore, the drift-tube temperature of PTR-MS is usually set at <100 °C owing to the Teflon rings in the drift tube, which may result in a long response time for low-volatility species in aerosol measurements. A PTR-MS with a drift tube that can operate at considerably higher temperatures (up to 250 °C) was developed to alleviate this issue.<sup>39</sup>

### 5.5. OH Reactivity Measurements and Other Indirect Measurements

Measurements of the OH reactivity, i.e., the total loss frequency of OH radicals in the atmosphere, can provide quantitative constraints on the total abundance of reactive constituents in the atmosphere. A technique to quantitatively measure OH reactivity using PTR-MS, referred to as the comparative reactivity method (CRM), was recently developed at the Max Planck Institute for Chemistry.<sup>361</sup> In the CRM method, a reactive compound X (commonly pyrrole) is introduced into a glass reactor and its concentrations are monitored by PTR-MS.<sup>361</sup> OH radicals are then generated in the glass reactor to react with the compound X, in the presence of first zero air and then ambient air.<sup>361</sup> The OH reactivity can be determined by comparing the concentrations of X at the three different operational stages.<sup>361</sup> The CRM method was recently systematically characterized by a series of laboratory experiments and numerical simulations to investigate potential artifacts in OH reactivity measurements,<sup>362</sup> e.g., the formation of additional OH radicals when NO<sub>x</sub> concentrations are high. After taking into account the corrections discussed by Michoud et al.,<sup>362</sup> the CRM method was compared to independent measurement techniques (pump–probe or laser flash photolysis method) at an urban site, obtaining agreements within the measurement uncertainties of the two methods.<sup>363</sup> Later, an intercomparison between two CRM systems in a rural environment also found good agreement.<sup>364</sup>

The deployment of the CRM method involves relatively simple modifications to the PTR-MS inlet, and PTR-MS can still alternate between OH reactivity and VOC concentration measurements.<sup>365</sup> The CRM method has been applied by several research groups in many different environments, including forests,<sup>366–369</sup> urban,<sup>370–372</sup> and rural areas.<sup>373</sup> The CRM method was also applied in emission studies from plants<sup>374,375</sup> and gasoline evaporation<sup>376</sup> to study emission rates of OH reactivity from these sources. PTR-QMS has been mainly used for earlier CRM applications,<sup>361</sup> and PTR-TOF

began to be used recently.<sup>362,363</sup> Coupling of CRM with PTR-TOF may provide additional insights on the “missing” OH reactivity by comparing ambient and OH radical-exposed mass spectra of PTR-TOF.

Derivatization prior to PTR-MS sampling can be used to detect some additional compounds that cannot be measured by PTR-MS directly. A PTR-TOF instrument with a spin-trap system has been used to measure Criegee intermediates (CIs), a type of radicals formed from ozonolysis of alkenes in the atmosphere.<sup>377,378</sup> These CIs were first stabilized by spin traps (5,5-dimethylpyrrolidine N-oxide, DMPO), and then the CI-spin-trap adducts were detected using a PTR-TOF.<sup>377,378</sup> This system has been successfully used to detect CIs from a number of different biogenic and anthropogenic alkenes in the laboratory.<sup>377</sup> However, applications of this method in ambient measurements would not be possible, as ambient concentrations of the CIs are 4–5 orders of magnitude lower than the achieved detection limits.<sup>377</sup>

## 6. CONCLUSION AND FUTURE OUTLOOK

As an excellent technique to measure a broad spectrum of VOC compounds in the atmosphere, PTR-MS has been used extensively in many different fields of atmospheric sciences, ranging from laboratory experiments to field studies, from VOC emissions to VOC chemical evolution in the atmosphere, and from ambient air quality to indoor air studies. These PTR-MS applications have enabled important advances in understanding sources and fates of many VOCs, as well as their environmental effects in the atmosphere.

In the past few decades, many new mass spectrometric techniques were applied to PTR-MS instruments, and the performance of PTR-MS has improved significantly. Time-of-flight mass spectrometers became the preferred mass analyzers for PTR-MS instruments after PTR-TOF was commercialized in the last years of the 2000s. PTR-TOF increases the number of VOC species that can be quantified and provides high mass-resolution measurements that can distinguish many isobaric VOCs. Applications of the new ion interfaces in recent years have dramatically enhanced instrument sensitivities and achieved much better detection limits for VOC measurements. Utilizing reagent ions other than H<sub>3</sub>O<sup>+</sup> in PTR-MS (e.g., NO<sup>+</sup> chemistry) further expands the detection capability of PTR-MS instruments. As recognized in a previous review,<sup>31</sup> these fast developments of PTR-MS instruments would have not been possible without the contributions from the commercialized instrument companies (Ionicon Analytik and Kore Technology, and also Tofwerk AG now). These instrument companies played pivotal roles in the quick expansion of the use of new techniques in mass spectrometry in the PTR-MS community.

Along with the introduction of new versions of PTR-MS instruments, characterization of these new PTR-MS instruments is important to ensure data quality of VOC measurements. Some unexpected results related to VOC quantification have been observed for new types of PTR-MS instruments. However, detailed characterization of several recent PTR-MS instruments with novel techniques is still not available in the literature. Scientists in the PTR-MS community should make equal efforts to instrument development and instrument characterization.

The ability to measure many novel species by PTR-TOF also calls for innovative approaches to easily calibrate the large number of VOC species. Nevertheless, calibrations of all of the hundreds of different VOCs would seem to be impractical.

Thus, development of an effective method to predict the sensitivities for the uncalibrated VOC species is critical. Some recent attempts in this direction have been demonstrated in the literature, but more work is needed.

## ASSOCIATED CONTENT

### Supporting Information

The Supporting Information is available free of charge on the ACS Publications website at DOI: [10.1021/acs.chemrev.7b00325](https://doi.org/10.1021/acs.chemrev.7b00325).

Uncertainties in high-resolution peak fitting; intercomparison results for PTR-MS ([PDF](#))

## AUTHOR INFORMATION

### Corresponding Authors

\*E-mail: [yuanbin501@gmail.com](mailto:yuanbin501@gmail.com).

\*E-mail: [carsten.warneke@noaa.gov](mailto:carsten.warneke@noaa.gov).

\*E-mail: [jdeguw@gmail.com](mailto:jdeguw@gmail.com).

### ORCID

Bin Yuan: [0000-0003-3041-0329](https://orcid.org/0000-0003-3041-0329)

Joost A. de Gouw: [0000-0002-0385-1826](https://orcid.org/0000-0002-0385-1826)

### Notes

The authors declare the following competing financial interest(s): One of the Authors (J. de Gouw) worked as a part-time consultant for Aerodyne Inc. during the last stages of manuscript preparation.

### Biographies

Bin Yuan graduated from Peking University, China, with Bachelor's degrees in Environmental Sciences and Economics. He then received a Ph.D. in Environmental Sciences at Peking University with the honor of Excellent Doctoral Dissertation in 2012. Since then, he has continued his research at NOAA Earth System Research Laboratory (ESRL) in United States and at Paul Scherrer Institute (PSI) in Switzerland. He now works as a faculty member at the Institute for Environment and Climate Research (ECI) of Jinan University in Guangzhou, China. His research is focused on investigations of emissions and evolution of organic compounds as well as mass spectrometric techniques in detection of organic compounds in the atmosphere.

Abigail R. Koss received her B.S. in Chemistry from the Massachusetts Institute of Technology in 2012. She recently received a Ph.D. in Analytical Chemistry from the University of Colorado, Boulder, under the direction of Joost de Gouw. Her thesis research comprised applications of PTR-MS to tropospheric measurement of VOCs associated with fossil fuels, with a particular focus on air-quality impacts of oil and natural gas production. Her research interests include the development and application of mass spectrometry techniques to atmospheric chemistry.

Dr. Carsten Warneke studied physics at the University of Innsbruck, Austria, and later received his Ph.D. there in 1998 under the supervision of Prof. Werner Lindinger, where he worked on the early development and applications of PTR-MS. After a postdoc from 1999 to 2001 at the University of Utrecht in the Institute for Marine and Atmospheric Research, he moved to Boulder, Colorado, to work for the University of Colorado, Boulder, at the NOAA Chemical Sciences Division (CSD) on atmospheric measurements of volatile organic compounds using PTR-MS on ground and mobile platforms. At NOAA CSD he is currently the leader of the VOC group and mission scientist for the aircraft experiment studying western U.S. wildfires.

Matthew Coggon was educated as a chemical engineer at the University of Massachusetts, Amherst, and earned a Ph.D. from the California Institute of Technology in 2015. Currently, he is a postdoctoral researcher at the National Oceanic and Atmospheric Administration and Cooperative Institute for Research in Environmental Sciences at the University of Colorado, Boulder. Broadly, his research is focused on the measurement of VOC and aerosol composition by mass spectrometry; however, he is currently working on characterizing the emissions and chemical evolution of VOCs resulting from biomass burning. His research interests include evaluating field measurements to understand VOC emission mechanisms, VOC oxidation pathways, and SOA formation by gas-phase and heterogeneous processes.

Kanako Sekimoto is currently an assistant professor in Yokohama City University (YCU) in Japan. She received her Ph.D. from YCU in 2010. After postdoctoral training at National Institute for Environmental Studies in Japan, she joined the faculty in YCU. She is now working as a visiting researcher at NOAA ESRL, funded by JSPS Overseas Research Fellowships. Her research interests include fundamental ion chemistry and application of mass spectrometry to environmental analysis.

Joost de Gouw holds a Ph.D. in Physics from the University of Utrecht in The Netherlands. He is a Research Scientist and Fellow with the Cooperative Institute for Research in Environmental Sciences (CIRES) of the University of Colorado. He is also an Adjoint Professor in the Department of Chemistry and Biochemistry. He has worked on the development and use of PTR-MS since 1998. He has deployed PTR-MS and other instruments to measure VOCs during numerous field missions and served as Principal Investigator for several NOAA field missions. His research is focused on understanding the emissions, chemical transformations, and loss processes of organic carbon compounds in the atmosphere, as well as the role these processes play in air quality and climate change.

## ACKNOWLEDGMENTS

A.R.K. is supported by an NSF Graduate Research Fellowship. K.S. acknowledges the JSPS Overseas Research Fellowships. This work is supported by Guangdong Innovative and Entrepreneurial Research Team Program (2016ZT06N263). One of the authors (J.A.d.G.) worked as a part-time consultant for Aerodyne, Inc., during the last stages of manuscript preparation. We also thank Dr. Dylan Millet at the University of Minnesota, Dr. Armin Hansel, Dr. Martin Graus, and Dr. Thomas Karl at the University of Innsbruck, Dr. Rupert Holzinger at Utrecht University, Dr. Armin Wisthaler at the University of Oslo, and Dr. Paul Monks at the University of Leicester for helpful discussions and suggestions on the manuscript.

## REFERENCES

- (1) Koppmann, R. *Volatile Organic Compounds in the Atmosphere*; Blackwell Publishing Ltd.: Oxford, U.K., 2007.
- (2) Hallquist, M.; Wenger, J. C.; Baltensperger, U.; Rudich, Y.; Simpson, D.; Claeys, M.; Dommen, J.; Donahue, N. M.; George, C.; Goldstein, A. H.; et al. The formation, properties and impact of secondary organic aerosol: current and emerging issues. *Atmos. Chem. Phys.* **2009**, *9*, 5155–5236.
- (3) Monks, P. S.; Granier, C.; Fuzzi, S.; Stohl, A.; Williams, M. L.; Akimoto, H.; Amann, M.; Baklanov, A.; Baltensperger, U.; Bey, I.; et al. Atmospheric composition change – global and regional air quality. *Atmos. Environ.* **2009**, *43*, 5268–5350.
- (4) Monks, P. S.; Archibald, A. T.; Colette, A.; Cooper, O.; Coyle, M.; Derwent, R.; Fowler, D.; Granier, C.; Law, K. S.; Mills, G. E.; et al.

- Tropospheric ozone and its precursors from the urban to the global scale from air quality to short-lived climate forcer. *Atmos. Chem. Phys.* **2015**, *15*, 8889–8973.
- (5) Goldstein, A. H.; Galbally, I. E. Known and unexplored organic constituents in the Earth's atmosphere. *Environ. Sci. Technol.* **2007**, *41*, 1514–1521.
- (6) Atkinson, R.; Arey, J. Atmospheric degradation of volatile organic compounds. *Chem. Rev.* **2003**, *103*, 4605–4638.
- (7) de Gouw, J. A.; Middlebrook, A. M.; Warneke, C.; Goldan, P. D.; Kuster, W. C.; Roberts, J. M.; Fehsenfeld, F. C.; Worsnop, D. R.; Canagaratna, M. R.; Pszenny, A. A. P.; et al. Budget of organic carbon in a polluted atmosphere: Results from the New England Air Quality Study in 2002. *J. Geophys. Res.* **2005**, *110*, D16305.
- (8) Helmig, D.; Rossabi, S.; Hueber, J.; Tans, P.; Montzka, S. A.; Masarie, K.; Thoning, K.; Plass-Duelmer, C.; Claude, A.; Carpenter, L. J.; et al. Reversal of global atmospheric ethane and propane trends largely due to US oil and natural gas production. *Nat. Geosci.* **2016**, *9*, 490–495.
- (9) Laj, P.; Klausen, J.; Bilde, M.; Plaß-Duelmer, C.; Pappalardo, G.; Clerbaux, C.; Baltensperger, U.; Hjorth, J.; Simpson, D.; Reimann, S.; et al. Measuring atmospheric composition change. *Atmos. Environ.* **2009**, *43*, 5351–5414.
- (10) Nozière, B.; Kalberer, M.; Claeys, M.; Allan, J.; D'Anna, B.; Decesari, S.; Finassi, E.; Glasius, M.; Grgić, I.; Hamilton, J. F.; et al. The molecular identification of organic compounds in the atmosphere: state of the art and challenges. *Chem. Rev.* **2015**, *115*, 3919–3983.
- (11) Seeley, J. V.; Seeley, S. K. Multidimensional gas chromatography: fundamental advances and new applications. *Anal. Chem.* **2013**, *85*, 557–78.
- (12) Lewis, A. C.; Carslaw, N.; Marriott, P. J.; Kinghorn, R. M.; Morrison, P.; Lee, A. L.; Bartle, K. D.; Pilling, M. J. A larger pool of ozone-forming carbon compounds in urban atmospheres. *Nature* **2000**, *405*, 778–781.
- (13) Zhao, Y.; Hennigan, C. J.; May, A. A.; Tkacik, D. S.; de Gouw, J. A.; Gilman, J. B.; Kuster, W. C.; Borbon, A.; Robinson, A. L. Intermediate-volatility organic compounds: a large source of secondary organic aerosol. *Environ. Sci. Technol.* **2014**, *48*, 13743–13750.
- (14) Lindinger, W.; Hansel, A.; Jordan, A. On-line monitoring of volatile organic compounds at pptv levels by means of proton-transfer-reaction mass spectrometry (PTR-MS) - Medical applications, food control and environmental research. *Int. J. Mass Spectrom. Ion Processes* **1998**, *173*, 191–241.
- (15) Wert, B. P.; Trainer, M.; Fried, A.; Ryerson, T. B.; Henry, B.; Potter, W.; Angevine, W. M.; Atlas, E.; Donnelly, S. G.; Fehsenfeld, F. C.; et al., Signatures of terminal alkene oxidation in airborne formaldehyde measurements during TexAQS 2000. *J. Geophys. Res.* **2003**, *108*, DOI: [10.1029/2002JD002502](https://doi.org/10.1029/2002JD002502).
- (16) Yacovitch, T. I.; Herndon, S. C.; Roscioli, J. R.; Floerchinger, C.; McGovern, R. M.; Agnese, M.; Pétron, G.; Kofler, J.; Sweeney, C.; Karion, A.; et al. Demonstration of an ethane spectrometer for methane source identification. *Environ. Sci. Technol.* **2014**, *48*, 8028–8034.
- (17) Cazorla, M.; Wolfe, G. M.; Bailey, S. A.; Swanson, A. K.; Arkinson, H. L.; Hanisco, T. F. A new airborne laser-induced fluorescence instrument for in situ detection of formaldehyde throughout the troposphere and lower stratosphere. *Atmos. Meas. Tech.* **2015**, *8*, 541–552.
- (18) Harren, F. J.; Mandon, J.; Cristescu, S. M. Photoacoustic spectroscopy in trace gas monitoring. *Encyclopedia of Analytical Chemistry*; John Wiley and Sons: Chichester, U.K., 2012; DOI: [10.1002/9780470027318.a0718.pub2](https://doi.org/10.1002/9780470027318.a0718.pub2).
- (19) Hansel, A.; Jordan, A.; Holzinger, R.; Prazeller, P.; Vogel, W.; Lindinger, W. Proton-transfer reaction mass-spectrometry - online trace gas-analysis at the ppb level. *Int. J. Mass Spectrom. Ion Processes* **1995**, *149-150*, 609–619.
- (20) de Gouw, J. A.; Goldan, P. D.; Warneke, C.; Kuster, W. C.; Roberts, J. M.; Marchewka, M.; Bertman, S. B.; Pszenny, A. A. P.; Keene, W. C. Validation of proton transfer reaction-mass spectrometry (PTR-MS) measurements of gas-phase organic compounds in the atmosphere during the New England Air Quality Study (NEAQS) in 2002. *J. Geophys. Res.* **2003**, *108*, DOI: [10.1029/2003JD003863](https://doi.org/10.1029/2003JD003863).
- (21) de Gouw, J.; Warneke, C. Measurements of volatile organic compounds in the earth's atmosphere using proton-transfer-reaction mass spectrometry. *Mass Spectrom. Rev.* **2007**, *26*, 223–257.
- (22) Graus, M.; Muller, M.; Hansel, A. High resolution PTR-TOF: quantification and formula confirmation of VOC in real time. *J. Am. Soc. Mass Spectrom.* **2010**, *21*, 1037–1044.
- (23) Jordan, A.; Haidacher, S.; Hanel, G.; Hartungen, E.; Mark, L.; Seehauser, H.; Schottkowsky, R.; Sulzer, P.; Mark, T. D. A high resolution and high sensitivity proton-transfer-reaction time-of-flight mass spectrometer (PTR-TOF-MS). *Int. J. Mass Spectrom.* **2009**, *286*, 122–128.
- (24) Sulzer, P.; Hartungen, E.; Hanel, G.; Feil, S.; Winkler, K.; Mutschlechner, P.; Haidacher, S.; Schottkowsky, R.; Gunsch, D.; Seehauser, H.; et al. A Proton Transfer Reaction-Quadrupole interface Time-Of-Flight Mass Spectrometer (PTR-QiTof): High speed due to extreme sensitivity. *Int. J. Mass Spectrom.* **2014**, *368*, 1–5.
- (25) Warneke, C.; de Gouw, J. A.; Lovejoy, E. R.; Murphy, P. C.; Kuster, W. C.; Fall, R. Development of proton-transfer ion trap-mass spectrometry: On-line detection and identification of volatile organic compounds in air. *J. Am. Soc. Mass Spectrom.* **2005**, *16*, 1316–1324.
- (26) Mielke, L. H.; Erickson, D. E.; McLuckey, S. A.; Muller, M.; Wisthaler, A.; Hansel, A.; Shepson, P. B. Development of a proton-transfer reaction-linear ion trap mass spectrometer for quantitative determination of volatile organic compounds. *Anal. Chem.* **2008**, *80*, 8171–8177.
- (27) Jordan, A.; Haidacher, S.; Hanel, G.; Hartungen, E.; Herbig, J.; Mark, L.; Schottkowsky, R.; Seehauser, H.; Sulzer, P.; Mark, T. D. An online ultra-high sensitivity Proton-transfer-reaction mass-spectrometer combined with switchable reagent ion capability (PTR+SRI-MS). *Int. J. Mass Spectrom.* **2009**, *286*, 32–38.
- (28) Lindinger, W.; Jordan, A. Proton-transfer-reaction mass spectrometry (PTR-MS): on-line monitoring of volatile organic compounds at pptv levels. *Chem. Soc. Rev.* **1998**, *27*, 347–375.
- (29) Lindinger, W.; Fall, R.; Karl, T. G. Environmental, food and medical applications of proton-transfer-reaction mass spectrometry (PTR-MS). In *Advances in Gas Phase Ion Chemistry*; Adams, N. G., Babcock, L. M., Eds.; Elsevier: Amsterdam, The Netherlands, 2001; Vol. 4, pp 1–48.
- (30) Hewitt, C. N.; Hayward, S.; Tani, A. The application of proton transfer reaction-mass spectrometry (PTR-MS) to the monitoring and analysis of volatile organic compounds in the atmosphere. *J. Environ. Monit.* **2003**, *5*, 1–7.
- (31) Blake, R. S.; Monks, P. S.; Ellis, A. M. Proton-transfer reaction mass spectrometry. *Chem. Rev.* **2009**, *109*, 861–896.
- (32) Biasioli, F.; Yeretzian, C.; Märk, T. D.; Dewulf, J.; Van Langenhove, H. Direct-injection mass spectrometry adds the time dimension to (B)VOC analysis. *TrAC, Trends Anal. Chem.* **2011**, *30*, 1003–1017.
- (33) Hartungen, E.; Jürschik, S.; Jordan, A.; Edtbauer, A.; Feil, S.; Hanel, G.; Seehauser, H.; Haidacher, S.; Schottkowsky, R.; Märk, L. Proton transfer reaction-mass spectrometry: fundamentals, recent advances and applications. *Eur. Phys. J.: Appl. Phys.* **2013**, *61*, 24303.
- (34) Ellis, A. M.; Mayhew, C. A. *Proton transfer reaction mass spectrometry: Principles and applications*; John Wiley & Sons: West Sussex, U.K., 2014.
- (35) Barber, S.; Blake, R. S.; White, I. R.; Monks, P. S.; Reich, F.; Mullock, S.; Ellis, A. M. Increased sensitivity in proton transfer reaction mass spectrometry by incorporation of a radio frequency ion funnel. *Anal. Chem.* **2012**, *84*, 5387–91.
- (36) Brown, P. A.; Cristescu, S. M.; Mullock, S. J.; Reich, D. F.; Lamont-Smith, C. S.; Harren, F. J. M. Implementation and characterization of an RF ion funnel ion guide as a proton transfer reaction chamber. *Int. J. Mass Spectrom.* **2017**, *414*, 31–38.
- (37) Breitenlechner, M.; Fischer, L.; Hainer, M.; Heinritz, M.; Curtius, J.; Hansel, A. PTR3: an instrument for studying the lifecycle of reactive organic carbon in the atmosphere. *Anal. Chem.* **2017**, *89*, 5824–5831.

- (38) Thornberry, T.; Murphy, D. M.; Thomson, D. S.; de Gouw, J.; Warneke, C.; Bates, T. S.; Quinn, P. K.; Coffman, D. Measurement of aerosol organic compounds Using a novel collection/thermal-desorption PTR-ITMS instrument. *Aerosol Sci. Technol.* **2009**, *43*, 486–501.
- (39) Mikoviny, T.; Kaser, L.; Wisthaler, A. Development and characterization of a High-Temperature Proton-Transfer-Reaction Mass Spectrometer (HT-PTR-MS). *Atmos. Meas. Tech.* **2010**, *3*, 537–544.
- (40) Bernhammer, A. K.; Breitenlechner, M.; Keutsch, F. N.; Hansel, A. Technical note: conversion of isoprene hydroxy hydroperoxides (ISOPPOOH) on metal environmental simulation chamber walls. *Atmos. Chem. Phys.* **2017**, *17*, 4053–4062.
- (41) Inomata, S.; Tanimoto, H.; Kato, S.; Suthawaree, J.; Kanaya, Y.; Pochanart, P.; Liu, Y.; Wang, Z. PTR-MS measurements of non-methane volatile organic compounds during an intensive field campaign at the summit of Mount Tai, China, in June 2006. *Atmos. Chem. Phys.* **2010**, *10*, 7085–7099.
- (42) Vlasenko, A.; Slowik, J. G.; Bottenheim, J. W.; Brickell, P. C.; Chang, R. Y. W.; Macdonald, A. M.; Shantz, N. C.; Sjostedt, S. J.; Wiebe, H. A.; Leaitch, W. R., et al. Measurements of VOCs by proton transfer reaction mass spectrometry at a rural Ontario site: Sources and correlation to aerosol composition. *J. Geophys. Res.* **2009**, *114*, DOI: [10.1029/2009JD012025](https://doi.org/10.1029/2009JD012025).
- (43) Warneke, C.; Veres, P. R.; Murphy, S. M.; Soltis, J.; Field, R. A.; Graus, M. G.; Koss, A.; Li, S. M.; Li, R.; Yuan, B.; et al. PTR-QMS versus PTR-TOF comparison in a region with oil and natural gas extraction industry in the Uintah Basin in 2013. *Atmos. Meas. Tech.* **2015**, *8*, 411–420.
- (44) Müller, M.; Anderson, B. E.; Beyersdorf, A. J.; Crawford, J. H.; Diskin, G. S.; Eichler, P.; Fried, A.; Keutsch, F. N.; Mikoviny, T.; Thornhill, K. L.; et al. In situ measurements and modeling of reactive trace gases in a small biomass burning plume. *Atmos. Chem. Phys.* **2016**, *16*, 3813–3824.
- (45) Karl, T. G.; Spirig, C.; Rinne, J.; Stroud, C.; Prevost, P.; Greenberg, J.; Fall, R.; Guenther, A. Virtual disjunct eddy covariance measurements of organic compound fluxes from a subalpine forest using proton transfer reaction mass spectrometry. *Atmos. Chem. Phys.* **2002**, *2*, 279–291.
- (46) Kim, S.; Karl, T.; Guenther, A.; Tyndall, G.; Orlando, J.; Harley, P.; Rasmussen, R.; Apel, E. Emissions and ambient distributions of Biogenic Volatile Organic Compounds (BVOC) in a ponderosa pine ecosystem: interpretation of PTR-MS mass spectra. *Atmos. Chem. Phys.* **2010**, *10*, 1759–1771.
- (47) Steinbacher, M.; Dommen, J.; Ammann, C.; Spirig, C.; Neftel, A.; Prevot, A. S. H. Performance characteristics of a proton-transfer-reaction mass spectrometer (PTR-MS) derived from laboratory and field measurements. *Int. J. Mass Spectrom.* **2004**, *239*, 117–128.
- (48) Müller, M.; Mielke, L. H.; Breitenlechner, M.; McLuckey, S. A.; Shepson, P. B.; Wisthaler, A.; Hansel, A. MS/MS studies for the selective detection of isomeric biogenic VOCs using a Townsend Discharge Triple Quadrupole Tandem MS and a PTR-Linear Ion Trap MS. *Atmos. Meas. Tech.* **2009**, *2*, 703–712.
- (49) Prazeller, P.; Palmer, P. T.; Boscaini, E.; Jobson, T.; Alexander, M. Proton transfer reaction ion trap mass spectrometer. *Rapid Commun. Mass Spectrom.* **2003**, *17*, 1593–1599.
- (50) Steeghs, M. M. L.; Sikkens, C.; Crespo, E.; Cristescu, S. M.; Harren, F. J. M. Development of a proton-transfer reaction ion trap mass spectrometer: Online detection and analysis of volatile organic compounds. *Int. J. Mass Spectrom.* **2007**, *262*, 16–24.
- (51) Warneke, C.; Rosen, S.; Lovejoy, E. R.; de Gouw, J. A.; Fall, R. Two additional advantages of proton-transfer ion trap mass spectrometry. *Rapid Commun. Mass Spectrom.* **2004**, *18*, 133–134.
- (52) Warneke, C.; Kato, S.; De Gouw, J. A.; Goldan, P. D.; Kuster, W. C.; Shao, M.; Lovejoy, E. R.; Fall, R.; Fehsenfeld, F. C. Online volatile organic compound measurements using a newly developed proton-transfer ion-trap mass spectrometry instrument during New England Air Quality Study - Intercontinental Transport and Chemical Transformation 2004: Performance, intercomparison, and compound identification. *Environ. Sci. Technol.* **2005**, *39*, 5390–5397.
- (53) Bon, D. M.; Ulbrich, I. M.; de Gouw, J. A.; Warneke, C.; Kuster, W. C.; Alexander, M. L.; Baker, A.; Beyersdorf, A. J.; Blake, D.; Fall, R.; et al. Measurements of volatile organic compounds at a suburban ground site (T1) in Mexico City during the MILAGRO 2006 campaign: measurement comparison, emission ratios, and source attribution. *Atmos. Chem. Phys.* **2011**, *11*, 2399–2421.
- (54) Warneke, C.; Roberts, J. M.; Veres, P.; Gilman, J.; Kuster, W. C.; Burling, I.; Yokelson, R.; de Gouw, J. A. VOC identification and inter-comparison from laboratory biomass burning using PTR-MS and PIT-MS. *Int. J. Mass Spectrom.* **2011**, *303*, 6–14.
- (55) Wyche, K. P.; Blake, R. S.; Ellis, A. M.; Monks, P. S.; Brauers, T.; Koppmann, R.; Apel, E. C. Performance of Chemical Ionization Reaction Time-of-Flight Mass Spectrometry (CIR-TOF-MS) for the measurement of atmospherically significant oxygenated volatile organic compounds. *Atmos. Chem. Phys.* **2007**, *7*, 609–620.
- (56) Blake, R. S.; Whyte, C.; Hughes, C. O.; Ellis, A. M.; Monks, P. S. Demonstration of proton-transfer reaction time-of-flight mass spectrometry for real-time analysis of trace volatile organic compounds. *Anal. Chem.* **2004**, *76*, 3841–3845.
- (57) Ennis, C. J.; Reynolds, J. C.; Keely, B. J.; Carpenter, L. J. A hollow cathode proton transfer reaction time of flight mass spectrometer. *Int. J. Mass Spectrom.* **2005**, *247*, 72–80.
- (58) Inomata, S.; Tanimoto, H.; Aoki, N.; Hirokawa, J.; Sadanaga, Y. A novel discharge source of hydronium ions for proton transfer reaction ionization: design, characterization, and performance. *Rapid Commun. Mass Spectrom.* **2006**, *20*, 1025–1029.
- (59) Tanimoto, H.; Aoki, N.; Inomata, S.; Hirokawa, J.; Sadanaga, Y. Development of a PTR-TOFMS instrument for real-time measurements of volatile organic compounds in air. *Int. J. Mass Spectrom.* **2007**, *263*, 1–11.
- (60) Müller, M.; Mikoviny, T.; Feil, S.; Haidacher, S.; Hanel, G.; Hartungen, E.; Jordan, A.; Märk, L.; Mutschlechner, P.; Schottkowsky, R.; et al. A compact PTR-ToF-MS instrument for airborne measurements of volatile organic compounds at high spatiotemporal resolution. *Atmos. Meas. Tech.* **2014**, *7*, 3763–3772.
- (61) Yuan, B.; Koss, A.; Warneke, C.; Gilman, J. B.; Lerner, B. M.; Stark, H.; de Gouw, J. A. A high-resolution time-of-flight chemical ionization mass spectrometer utilizing hydronium ions ( $\text{H}_3\text{O}^+$  ToF-CIMS) for measurements of volatile organic compounds in the atmosphere. *Atmos. Meas. Tech.* **2016**, *9*, 2735–2752.
- (62) Hu, Q.; Noll, R. J.; Li, H.; Makarov, A.; Hardman, M.; Graham Cooks, R. The Orbitrap: a new mass spectrometer. *J. Mass Spectrom.* **2005**, *40*, 430–443.
- (63) Dehon, C.; Gaüzère, E.; Vaissier, J.; Heninger, M.; Tchapla, A.; Bleton, J.; Mestdagh, H. Quantitative analysis of a complex mixture using proton transfer reaction in an FTICR mass spectrometer. *Int. J. Mass Spectrom.* **2008**, *272*, 29–37.
- (64) Sarrabi, S.; Colin, X.; Tcharkhtchi, A.; Heninger, M.; Leprovost, J.; Mestdagh, H. Real time analysis of volatile organic compounds from polypropylene thermal Oxidation using chemical ionization fourier transform ion cyclotron resonance mass spectrometry. *Anal. Chem.* **2009**, *81*, 6013–6020.
- (65) Chernushevich, I. V.; Loboda, A. V.; Thomson, B. A. An introduction to quadrupole–time-of-flight mass spectrometry. *J. Mass Spectrom.* **2001**, *36*, 849–865.
- (66) Kelly, R. T.; Tolmachev, A. V.; Page, J. S.; Tang, K.; Smith, R. D. The ion funnel: Theory, implementations, and applications. *Mass Spectrom. Rev.* **2010**, *29*, 294–312.
- (67) Jordan, A.; Feil, S.; Mutschlechner, P.; Hanel, G.; Hartungen, E.; Herbig, J.; Mark, L.; Sulzer, P.; Jurschik, S.; Jaksch, S. In *Improving the sensitivity of proton transfer reaction–time-of-flight–mass spectrometry (PTR-TOFMS)*; 7th International Conference on Proton Transfer Reaction Mass Spectrometry and Its Applications, Obergurgl, Austria, 2016; Hansel, A., Dunkl, J., Eds.; Innsbruck University Press: Obergurgl, Austria, 2016; pp 147–150.
- (68) Inomata, S.; Tanimoto, H.; Kamayama, S.; Tsunogai, U.; Irie, H.; Kanaya, Y.; Wang, Z. Determination of formaldehyde mixing ratios

- in air with PTR-MS: laboratory experiments and field measurements. *Atmos. Chem. Phys.* **2008**, *8*, 273–284.
- (69) Vlasenko, A.; Macdonald, A. M.; Sjostedt, S. J.; Abbatt, J. P. D. Formaldehyde measurements by Proton transfer reaction – Mass Spectrometry (PTR-MS): correction for humidity effects. *Atmos. Meas. Tech.* **2010**, *3*, 1055–1062.
- (70) Warneke, C.; Veres, P.; Holloway, J. S.; Stutz, J.; Tsai, C.; Alvarez, S.; Rappenglueck, B.; Fehsenfeld, F. C.; Graus, M.; Gilman, J. B.; et al. Airborne formaldehyde measurements using PTR-MS: calibration, humidity dependence, inter-comparison and initial results. *Atmos. Meas. Tech.* **2011**, *4*, 2345–2358.
- (71) Knighton, W. B.; Fortner, E. C.; Midey, A. J.; Viggiano, A. A.; Herndon, S. C.; Wood, E. C.; Kolb, C. E. HCN detection with a proton transfer reaction mass spectrometer. *Int. J. Mass Spectrom.* **2009**, *283*, 112–121.
- (72) Moussa, S. G.; Leithead, A.; Li, S.-M.; Chan, T. W.; Wentzell, J. J. B.; Stroud, C.; Zhang, J.; Lee, P.; Lu, G.; Brook, J. R.; et al. Emissions of hydrogen cyanide from on-road gasoline and diesel vehicles. *Atmos. Environ.* **2016**, *131*, 185–195.
- (73) Li, R.; Warneke, C.; Graus, M.; Field, R.; Geiger, F.; Veres, P. R.; Soltis, J.; Li, S. M.; Murphy, S. M.; Sweeney, C.; et al. Measurements of hydrogen sulfide (H<sub>2</sub>S) using PTR-MS: calibration, humidity dependence, inter-comparison and results from field studies in an oil and gas production region. *Atmos. Meas. Tech.* **2014**, *7*, 3597–3610.
- (74) Feilberg, A.; Liu, D.; Adamsen, A. P. S.; Hansen, M. J.; Jonassen, K. E. N. Odorant emissions from intensive pig production measured by online proton-transfer-reaction mass spectrometry. *Environ. Sci. Technol.* **2010**, *44*, 5894–5900.
- (75) Spanel, P.; Smith, D. SIFT studies of the reactions of H<sub>3</sub>O<sup>+</sup>, NO<sup>+</sup> and O<sub>2</sub>(+) with a series of alcohols. *Int. J. Mass Spectrom. Ion Processes* **1997**, *167*–168, 375–388.
- (76) Baasandorj, M.; Millet, D. B.; Hu, L.; Mitroo, D.; Williams, B. J. Measuring acetic and formic acid by proton-transfer-reaction mass spectrometry: sensitivity, humidity dependence, and quantifying interferences. *Atmos. Meas. Tech.* **2015**, *8*, 1303–1321.
- (77) Tani, A.; Hayward, S.; Hewitt, C. N. Measurement of monoterpenes and related compounds by proton transfer reaction-mass spectrometry (PTR-MS). *Int. J. Mass Spectrom.* **2003**, *223*–224, 561–578.
- (78) Tani, A.; Hayward, S.; Hansel, A.; Hewitt, C. N. Effect of water vapour pressure on monoterpene measurements using proton transfer reaction-mass spectrometry (PTR-MS). *Int. J. Mass Spectrom.* **2004**, *239*, 161–169.
- (79) Kim, S.; Karl, T.; Helmgig, D.; Daly, R.; Rasmussen, R.; Guenther, A. Measurement of atmospheric sesquiterpenes by proton transfer reaction-mass spectrometry (PTR-MS). *Atmos. Meas. Tech.* **2009**, *2*, 99–112.
- (80) Taipale, R.; Ruuskanen, T. M.; Rinne, J.; Kajos, M. K.; Hakola, H.; Pohja, T.; Kulmala, M. Technical Note: Quantitative long-term measurements of VOC concentrations by PTR-MS; measurement, calibration, and volume mixing ratio calculation methods. *Atmos. Chem. Phys.* **2008**, *8*, 6681–6698.
- (81) Müller, M.; George, C.; D'Anna, B. Enhanced spectral analysis of C-TOF Aerosol Mass Spectrometer data: Iterative residual analysis and cumulative peak fitting. *Int. J. Mass Spectrom.* **2011**, *306*, 1–8.
- (82) DeCarlo, P. F.; Kimmel, J. R.; Trimborn, A.; Northway, M. J.; Jayne, J. T.; Aiken, A. C.; Gonin, M.; Fuhrer, K.; Horvath, T.; Docherty, K. S.; et al. Field-deployable, high-resolution, time-of-flight Aerosol Mass Spectrometer. *Anal. Chem.* **2006**, *78*, 8281–8289.
- (83) Stark, H.; Yatavelli, R. L. N.; Thompson, S. L.; Kimmel, J. R.; Cubison, M. J.; Chhabra, P. S.; Canagaratna, M. R.; Jayne, J. T.; Worsnop, D. R.; Jimenez, J. L. Methods to extract molecular and bulk chemical information from series of complex mass spectra with limited mass resolution. *Int. J. Mass Spectrom.* **2015**, *389*, 26–38.
- (84) Titzmann, T.; Graus, M.; Müller, M.; Hansel, A.; Ostermann, A. Improved peak analysis of signals based on counting systems: Illustrated for proton-transfer-reaction time-of-flight mass spectrometry. *Int. J. Mass Spectrom.* **2010**, *295*, 72–77.
- (85) Müller, M.; Mikoviny, T.; Jud, W.; D'Anna, B.; Wisthaler, A. A new software tool for the analysis of high resolution PTR-TOF mass spectra. *Chemom. Intell. Lab. Syst.* **2013**, *127*, 158–165.
- (86) Cappellin, L.; Biasioli, F.; Schuhfried, E.; Soukoulis, C.; Mark, T. D.; Gasperi, F. Extending the dynamic range of proton transfer reaction time-of-flight mass spectrometers by a novel dead time correction. *Rapid Commun. Mass Spectrom.* **2011**, *25*, 179–83.
- (87) Cappellin, L.; Biasioli, F.; Granitto, P. M.; Schuhfried, E.; Soukoulis, C.; Costa, F.; Märk, T. D.; Gasperi, F. On data analysis in PTR-TOF-MS: From raw spectra to data mining. *Sens. Actuators, B* **2011**, *155*, 183–190.
- (88) Timonen, H.; Cubison, M.; Aurela, M.; Brus, D.; Lihavainen, H.; Hillamo, R.; Canagaratna, M.; Nekat, B.; Weller, R.; Worsnop, D.; et al. Applications and limitations of constrained high-resolution peak fitting on low resolving power mass spectra from the ToF-ACSM. *Atmos. Meas. Tech.* **2016**, *9*, 3263–3281.
- (89) Cappellin, L.; Biasioli, F.; Fabris, A.; Schuhfried, E.; Soukoulis, C.; Märk, T. D.; Gasperi, F. Improved mass accuracy in PTR-TOF-MS: Another step towards better compound identification in PTR-MS. *Int. J. Mass Spectrom.* **2010**, *290*, 60–63.
- (90) Stockwell, C. E.; Veres, P. R.; Williams, J.; Yokelson, R. J. Characterization of biomass burning emissions from cooking fires, peat, crop residue, and other fuels with high-resolution proton-transfer-reaction time-of-flight mass spectrometry. *Atmos. Chem. Phys.* **2015**, *15*, 845–865.
- (91) Cappellin, L.; Karl, T.; Probst, M.; Ismailova, O.; Winkler, P. M.; Soukoulis, C.; Aprea, E.; Mark, T. D.; Gasperi, F.; Biasioli, F. On quantitative determination of volatile organic compound concentrations using proton transfer reaction time-of-flight mass spectrometry. *Environ. Sci. Technol.* **2012**, *46*, 2283–90.
- (92) Müller, M.; Mikoviny, T.; Wisthaler, A. Detector aging induced mass discrimination and non-linearity effects in PTR-ToF-MS. *Int. J. Mass Spectrom.* **2014**, *365*–366, 93–97.
- (93) Holzinger, R. PTRwid: A new widget tool for processing PTR-TOF-MS data. *Atmos. Meas. Tech.* **2015**, *8*, 3903–3922.
- (94) Junninen, H.; Ehn, M.; Petäjä, T.; Luosujärvi, L.; Kotiaho, T.; Kostainen, R.; Rohner, U.; Gonin, M.; Fuhrer, K.; Kulmala, M.; et al. A high-resolution mass spectrometer to measure atmospheric ion composition. *Atmos. Meas. Tech.* **2010**, *3*, 1039–1053.
- (95) Corbin, J. C.; Othman, A.; Allan, J. D.; Worsnop, D. R.; Haskins, J. D.; Sierau, B.; Lohmann, U.; Mensah, A. A. Peak-fitting and integration imprecision in the Aerodyne aerosol mass spectrometer: effects of mass accuracy on location-constrained fits. *Atmos. Meas. Tech.* **2015**, *8*, 4615–4636.
- (96) Cubison, M. J.; Jimenez, J. L. Statistical precision of the intensities retrieved from constrained fitting of overlapping peaks in high-resolution mass spectra. *Atmos. Meas. Tech.* **2015**, *8*, 2333–2345.
- (97) Yuan, B.; Liggio, J.; Wentzell, J.; Li, S. M.; Stark, H.; Roberts, J. M.; Gilman, J.; Lerner, B.; Warneke, C.; Li, R.; et al. Secondary formation of nitrated phenols: insights from observations during the Uintah Basin Winter Ozone Study (UBWOS) 2014. *Atmos. Chem. Phys.* **2016**, *16*, 2139–2153.
- (98) Mitchell, G. D. A review of permeation tubes and permeators. *Sep. Purif. Methods* **2000**, *29*, 119–128.
- (99) Altshuller, A. P.; Cohen, I. R. Application of diffusion cells to production of known concentration of gaseous hydrocarbons. *Anal. Chem.* **1960**, *32*, 802–810.
- (100) Veres, P.; Gilman, J. B.; Roberts, J. M.; Kuster, W. C.; Warneke, C.; Burling, I. R.; de Gouw, J. Development and validation of a portable gas phase standard generation and calibration system for volatile organic compounds. *Atmos. Meas. Tech.* **2010**, *3*, 683–691.
- (101) Jardine, K. J.; Henderson, W. M.; Huxman, T. E.; Abrell, L. Dynamic Solution Injection: a new method for preparing pptv-ppbv standard atmospheres of volatile organic compounds. *Atmos. Meas. Tech.* **2010**, *3*, 1569–1576.
- (102) Kaser, L.; Karl, T.; Guenther, A.; Graus, M.; Schnitzhofer, R.; Turnipseed, A.; Fischer, L.; Harley, P.; Madronich, M.; Gochis, D.; et al. Undisturbed and disturbed above canopy ponderosa pine

- emissions: PTR-TOF-MS measurements and MEGAN 2.1 model results. *Atmos. Chem. Phys.* **2013**, *13*, 11935–11947.
- (103) Gilman, J. B.; Lerner, B. M.; Kuster, W. C.; Goldan, P. D.; Warneke, C.; Veres, P. R.; Roberts, J. M.; de Gouw, J. A.; Burling, I. R.; Yokelson, R. J. Biomass burning emissions and potential air quality impacts of volatile organic compounds and other trace gases from fuels common in the US. *Atmos. Chem. Phys.* **2015**, *15*, 13915–13938.
- (104) Smith, D.; Pysanenko, A.; Španěl, P. Ionic diffusion and mass discrimination effects in the new generation of short flow tube SIFT-MS instruments. *Int. J. Mass Spectrom.* **2009**, *281*, 15–23.
- (105) Ammann, C.; Spirig, C.; Neftel, A.; Steinbacher, M.; Komenda, M.; Schaub, A. Application of PTR-MS for measurements of biogenic VOC in a deciduous forest. *Int. J. Mass Spectrom.* **2004**, *239*, 87–101.
- (106) Gueneron, M.; Erickson, M. H.; VanderSchelden, G. S.; Jobson, B. T. PTR-MS fragmentation patterns of gasoline hydrocarbons. *Int. J. Mass Spectrom.* **2015**, *379*, 97–109.
- (107) Kalogridis, C.; Gros, V.; Sarda-Esteve, R.; Langford, B.; Loubet, B.; Bonsang, B.; Bonnaire, N.; Nemitz, E.; Genard, A. C.; Boissard, C.; et al. Concentrations and fluxes of isoprene and oxygenated VOCs at a French Mediterranean oak forest. *Atmos. Chem. Phys.* **2014**, *14*, 10085–10102.
- (108) Inomata, S.; Tanimoto, H. A deuterium-labeling study on the reproduction of hydronium ions in the PTR-MS detection of ethanol. *Int. J. Mass Spectrom.* **2009**, *285*, 95–99.
- (109) Warneke, C.; De Gouw, J. A.; Kuster, W. C.; Goldan, P. D.; Fall, R. Validation of atmospheric VOC measurements by proton-transfer-reaction mass spectrometry using a gas-chromatographic preseparation method. *Environ. Sci. Technol.* **2003**, *37*, 2494–2501.
- (110) Koss, A. R.; Warneke, C.; Yuan, B.; Coggon, M. M.; Veres, P. R.; de Gouw, J. A. Evaluation of NO<sup>+</sup> reagent ion chemistry for online measurements of atmospheric volatile organic compounds. *Atmos. Meas. Tech.* **2016**, *9*, 2909–2925.
- (111) von Hartungen, E.; Wisthaler, A.; Mikoviny, T.; Jaksch, D.; Boscaini, E.; Dunphy, P. J.; Mark, T. D. Proton-transfer-reaction mass spectrometry (PTR-MS) of carboxylic acids - Determination of Henry's law constants and axillary odour investigations. *Int. J. Mass Spectrom.* **2004**, *239*, 243–248.
- (112) Aoki, N.; Inomata, S.; Tanimoto, H. Detection of C-1-C-5 alkyl nitrates by proton transfer reaction time-of-flight mass spectrometry. *Int. J. Mass Spectrom.* **2007**, *263*, 12–21.
- (113) Duncianu, M.; David, M.; Kartigueyane, S.; Cirtog, M.; Doussin, J. F.; Picquet-Varraud, B. Measurement of alkyl and multifunctional organic nitrates by proton-transfer-reaction mass spectrometry. *Atmos. Meas. Tech.* **2017**, *10*, 1445–1463.
- (114) Lopez-Hilfiker, F. D.; Iyer, S.; Mohr, C.; Lee, B. H.; D'Ambro, E. L.; Kurtén, T.; Thornton, J. A. Constraining the sensitivity of iodide adduct chemical ionization mass spectrometry to multifunctional organic molecules using the collision limit and thermodynamic stability of iodide ion adducts. *Atmos. Meas. Tech.* **2016**, *9*, 1505–1512.
- (115) Koss, A.; Yuan, B.; Warneke, C.; Gilman, J. B.; Lerner, B. M.; Veres, P. R.; Peischl, J.; Eilerman, S.; Wild, R.; Brown, S. S.; et al. Observations of VOC emissions and photochemical products over US oil- and gas-producing regions using high-resolution H<sub>3</sub>O<sup>+</sup> CIMS (PTR-ToF-MS). *Atmos. Meas. Tech.* **2017**, *10*, 2941–2968.
- (116) Spanel, P.; Ji, Y. F.; Smith, D. SIFT studies of the reactions of H<sub>3</sub>O<sup>+</sup>, NO<sup>+</sup> and O<sub>2</sub>(+)<sup>·</sup> with a series of aldehydes and ketones. *Int. J. Mass Spectrom. Ion Processes* **1997**, *165*–166, 25–37.
- (117) Spanel, P.; Smith, D. SIFT studies of the reactions of H<sub>3</sub>O<sup>+</sup>, NO<sup>+</sup> and O<sub>2</sub>(+)<sup>·</sup> with a series of volatile carboxylic acids and esters. *Int. J. Mass Spectrom. Ion Processes* **1998**, *172*, 137–147.
- (118) Spanel, P.; Smith, D. Selected ion flow tube studies of the reactions of H<sub>3</sub>O<sup>+</sup>, NO<sup>+</sup> and O<sub>2</sub>(+)<sup>·</sup> with several amines and some other nitrogen-containing molecules. *Int. J. Mass Spectrom.* **1998**, *176*, 203–211.
- (119) Su, T.; Bowers, M. T. Theory of ion-polar molecule collisions. Comparison with experimental charge transfer reactions of rare gas ions to geometric isomers of difluorobenzene and dichloroethylene. *J. Chem. Phys.* **1973**, *58*, 3027–3037.
- (120) Su, T.; Bowers, M. T. Ion-Polar molecule collisions: the effect of ion size on ion-polar molecule rate constants; the parameterization of the average-dipole-orientation theory. *Int. J. Mass Spectrom. Ion Phys.* **1973**, *12*, 347–356.
- (121) Su, T. Parametrization of kinetic energy dependences of ion-polar molecule collision rate constants by trajectory calculations. *J. Chem. Phys.* **1994**, *100*, 4703–4703.
- (122) Zhao, J.; Zhang, R. Y. Proton transfer reaction rate constants between hydronium ion (H<sub>3</sub>O<sup>+</sup>(+)) and volatile organic compounds. *Atmos. Environ.* **2004**, *38*, 2177–2185.
- (123) Cappellin, L.; Probst, M.; Limtrakul, J.; Biasioli, F.; Schuhfried, E.; Soukoulis, C.; Märk, T. D.; Gasperi, F. Proton transfer reaction rate coefficients between H<sub>3</sub>O<sup>+</sup> and some sulphur compounds. *Int. J. Mass Spectrom.* **2010**, *295*, 43–48.
- (124) Sekimoto, K.; Li, S.-M.; Yuan, B.; Koss, A.; Coggon, M.; Warneke, C.; de Gouw, J. Calculation of the sensitivity of proton-transfer-reaction mass spectrometry (PTR-MS) for organic trace gases using molecular properties. *Int. J. Mass Spectrom.* **2017**, DOI: [10.1016/j.ijms.2017.04.006](https://doi.org/10.1016/j.ijms.2017.04.006).
- (125) Bertram, T. H.; Kimmel, J. R.; Crisp, T. A.; Ryder, O. S.; Yatavelli, R. L. N.; Thornton, J. A.; Cubison, M. J.; Gonin, M.; Worsnop, D. R. A field-deployable, chemical ionization time-of-flight mass spectrometer. *Atmos. Meas. Tech.* **2011**, *4*, 1471–1479.
- (126) Sintermann, J.; Spirig, C.; Jordan, A.; Kuhn, U.; Ammann, C.; Neftel, A. Eddy covariance flux measurements of ammonia by high temperature chemical ionisation mass spectrometry. *Atmos. Meas. Tech.* **2011**, *4*, 599–616.
- (127) Rivera-Rios, J. C.; Nguyen, T. B.; Crounse, J. D.; Jud, W.; St. Clair, J. M.; Mikoviny, T.; Gilman, J. B.; Lerner, B. M.; Kaiser, J. B.; de Gouw, J.; et al. Conversion of hydroperoxides to carbonyls in field and laboratory instrumentation: Observational bias in diagnosing pristine versus anthropogenically controlled atmospheric chemistry. *Geophys. Res. Lett.* **2014**, *41*, 8645–8651.
- (128) Lindinger, C.; Pollien, P.; Ali, S.; Yeretzian, C.; Blank, I.; Mark, T. Unambiguous identification of volatile organic compounds by proton-transfer reaction mass spectrometry coupled with GC/MS. *Anal. Chem.* **2005**, *77*, 4117–4124.
- (129) Karl, T.; Fall, R.; Crutzen, P. J.; Jordan, A.; Lindinger, W. High concentrations of reactive biogenic VOCs at a high altitude site in late autumn. *Geophys. Res. Lett.* **2001**, *28*, 507–510.
- (130) Yuan, B.; Warneke, C.; Shao, M.; de Gouw, J. A. Interpretation of volatile organic compound measurements by proton-transfer-reaction mass spectrometry over the deepwater horizon oil spill. *Int. J. Mass Spectrom.* **2014**, *358*, 43–48.
- (131) Karl, T. G.; Christian, T. J.; Yokelson, R. J.; Artaxo, P.; Hao, W. M.; Guenther, A. The Tropical Forest and Fire Emissions Experiment: method evaluation of volatile organic compound emissions measured by PTR-MS, FTIR, and GC from tropical biomass burning. *Atmos. Chem. Phys.* **2007**, *7*, 5883–5897.
- (132) Romano, A.; Fischer, L.; Herbig, J.; Campbell-Sills, H.; Coulon, J.; Lucas, P.; Cappellin, L.; Biasioli, F. Wine analysis by FastGC proton-transfer reaction-time-of-flight-mass spectrometry. *Int. J. Mass Spectrom.* **2014**, *369*, 81–86.
- (133) Materic, D.; Lanza, M.; Sulzer, P.; Herbig, J.; Bruhn, D.; Turner, C.; Mason, N.; Gauci, V. Monoterpene separation by coupling proton transfer reaction time-of-flight mass spectrometry with fastGC. *Anal. Bioanal. Chem.* **2015**, *407*, 7757–63.
- (134) Pallozzi, E.; Guidolotti, G.; Ciccioli, P.; Brilli, F.; Feil, S.; Calfapietra, C. Does the novel fast-GC coupled with PTR-TOF-MS allow a significant advancement in detecting VOC emissions from plants? *Agricultural and Forest Meteorology* **2016**, *216*, 232–240.
- (135) Wood, E. C.; Knighton, W. B.; Fortner, E. C.; Herndon, S. C.; Onasch, T. B.; Franklin, J. P.; Worsnop, D. R.; Dallmann, T. R.; Gentner, D. R.; Goldstein, A. H.; et al. Ethylene glycol emissions from on-road vehicles. *Environ. Sci. Technol.* **2015**, *49*, 3322–9.
- (136) Kaser, L.; Karl, T.; Schnitzhofer, R.; Graus, M.; Herdlinger-Blatt, I. S.; DiGangi, J. P.; Sive, B.; Turnipseed, A.; Hornbrook, R. S.; Zheng, W.; et al. Comparison of different real time VOC measurement

- techniques in a ponderosa pine forest. *Atmos. Chem. Phys.* **2013**, *13*, 2893–2906.
- (137) Apel, E. C.; Brauers, T.; Koppmann, R.; Bandowe, B.; Bossmeyer, J.; Holzke, C.; Tillmann, R.; Wahner, A.; Wegener, R.; Brunner, A.; et al. Intercomparison of oxygenated volatile organic compound measurements at the SAPHIR atmosphere simulation chamber. *J. Geophys. Res.* **2008**, *113*, D20307.
- (138) Christian, T. J.; Kleiss, B.; Yokelson, R. J.; Holzinger, R.; Crutzen, P. J.; Hao, W. M.; Shirai, T.; Blake, D. R. Comprehensive laboratory measurements of biomass-burning emissions: 2. First intercomparison of open-path FTIR, PTR-MS, and GC-MS/FID/ECD. *J. Geophys. Res.* **2004**, *109*, D02311.
- (139) Hatch, L. E.; Yokelson, R. J.; Stockwell, C. E.; Veres, P. R.; Simpson, I. J.; Blake, D. R.; Orlando, J. J.; Barsanti, K. C. Multi-instrument comparison and compilation of non-methane organic gas emissions from biomass burning and implications for smoke-derived secondary organic aerosol precursors. *Atmos. Chem. Phys.* **2017**, *17*, 1471–1489.
- (140) Hornbrook, R. S.; Blake, D. R.; Diskin, G. S.; Fried, A.; Fuelberg, H. E.; Meinardi, S.; Mikoviny, T.; Richter, D.; Sachse, G. W.; Vay, S. A.; et al. Observations of nonmethane organic compounds during ARCTAS; Part 1: Biomass burning emissions and plume enhancements. *Atmos. Chem. Phys.* **2011**, *11*, 11103–11130.
- (141) Hughey, C. A.; Hendrickson, C. L.; Rodgers, R. P.; Marshall, A. G.; Qian, K. Kendrick mass defect spectrum: a compact visual analysis for ultrahigh-resolution broadband mass spectra. *Anal. Chem.* **2001**, *73*, 4676–4681.
- (142) Yassine, M. M.; Harir, M.; Dabek-Zlotorzynska, E.; Schmitt-Kopplin, P. Structural characterization of organic aerosol using Fourier transform ion cyclotron resonance mass spectrometry: Aromaticity equivalent approach. *Rapid Commun. Mass Spectrom.* **2014**, *28*, 2445–2454.
- (143) Yuan, B.; Coggon, M. M.; Koss, A. R.; Warneke, C.; Eilerman, S.; Peischl, J.; Aikin, K. C.; Ryerson, T. B.; de Gouw, J. A. Emissions of volatile organic compounds (VOCs) from concentrated animal feeding operations (CAFOs): chemical compositions and separation of sources. *Atmos. Chem. Phys.* **2017**, *17*, 4945–4956.
- (144) Müller, M.; Graus, M.; Ruuskanen, T. M.; Schnitzhofer, R.; Bamberger, I.; Kaser, L.; Titzmann, T.; Hörtnagl, L.; Wohlfahrt, G.; Karl, T.; et al. First eddy covariance flux measurements by PTR-TOF. *Atmos. Meas. Tech.* **2010**, *3*, 387–395.
- (145) Sarkar, C.; Sinha, V.; Kumar, V.; Rupakheti, M.; Panday, A.; Mahata, K. S.; Rupakheti, D.; Kathayat, B.; Lawrence, M. G. Overview of VOC emissions and chemistry from PTR-TOF-MS measurements during the SusKat-ABC campaign: high acetaldehyde, isoprene and isocyanic acid in wintertime air of the Kathmandu Valley. *Atmos. Chem. Phys.* **2016**, *16*, 3979–4003.
- (146) Jankowski, M. J.; Olsen, R.; Nielsen, C. J.; Thomassen, Y.; Molander, P. The applicability of proton transfer reaction-mass spectrometry (PTR-MS) for determination of isocyanic acid (ICA) in work room atmospheres. *Environmental science. Processes & impacts* **2014**, *16*, 2423–31.
- (147) Brilli, F.; Gioli, B.; Ciccioli, P.; Zona, D.; Loreto, F.; Janssens, I. A.; Ceulemans, R. Proton transfer reaction time-of-flight mass spectrometric (PTR-TOF-MS) determination of volatile organic compounds (VOCs) emitted from a biomass fire developed under stable nocturnal conditions. *Atmos. Environ.* **2014**, *97*, 54–67.
- (148) Gylestam, D.; Karlsson, D.; Dalene, M.; Skarping, G. Determination of gas phase isocyanates using proton transfer reaction mass spectrometry. *Anal. Chem. Lett.* **2011**, *1*, 261–271.
- (149) Gustavsson, M.; Meiby, E.; Gylestam, D.; Dahlin, J.; Spanne, M.; Karlsson, D.; Dalene, M.; Skarping, G.; Tveteras, B. O.; Pedersen, Å. E. Adsorption efficiency of respirator filter cartridges for isocyanates. *Ann. Occup. Hyg.* **2010**, *54*, 377–390.
- (150) Knighton, W. B.; Herndon, S. C.; Shorter, J. H.; Miake-Lye, R. C.; Zahniser, M. S.; Akiyama, K.; Shimono, A.; Kitasaka, K.; Shimajiri, H.; Sugihara, K. Laboratory evaluation of an aldehyde scrubber system specifically for the detection of acrolein. *J. Air Waste Manage. Assoc.* **2007**, *57*, 1370–1378.
- (151) Sintermann, J.; Schallhart, S.; Kajos, M.; Jocher, M.; Bracher, A.; Münger, A.; Johnson, D.; Neftel, A.; Ruuskanen, T. Trimethylamine emissions in animal husbandry. *Biogeosciences* **2014**, *11*, 5073–5085.
- (152) Haase, K. B.; Keene, W. C.; Pszenny, A. A. P.; Mayne, H. R.; Talbot, R. W.; Sive, B. C. Calibration and intercomparison of acetic acid measurements using proton-transfer-reaction mass spectrometry (PTR-MS). *Atmos. Meas. Tech.* **2012**, *5*, 2739–2750.
- (153) Yuan, B.; Hu, W. W.; Shao, M.; Wang, M.; Chen, W. T.; Lu, S. H.; Zeng, L. M.; Hu, M. VOC emissions, evolutions and contributions to SOA formation at a receptor site in eastern China. *Atmos. Chem. Phys.* **2013**, *13*, 8815–8832.
- (154) Perraud, V.; Meinardi, S.; Blake, D. R.; Finlayson-Pitts, B. J. Challenges associated with the sampling and analysis of organosulfur compounds in air using real-time PTR-ToF-MS and offline GC-FID. *Atmos. Meas. Tech.* **2016**, *9*, 1325–1340.
- (155) Sinha, V.; Custer, T. G.; Kluepfel, T.; Williams, J. The effect of relative humidity on the detection of pyrrole by PTR-MS for OH reactivity measurements. *Int. J. Mass Spectrom.* **2009**, *282*, 108–111.
- (156) Karl, T.; Guenther, A.; Turnipseed, A.; Tyndall, G.; Artaxo, P.; Martin, S. Rapid formation of isoprene photo-oxidation products observed in Amazonia. *Atmos. Chem. Phys.* **2009**, *9*, 7753–7767.
- (157) Hansel, A.; Wisthaler, A. A method for real-time detection of PAN, PPN and MPAN in ambient air. *Geophys. Res. Lett.* **2000**, *27*, 895–898.
- (158) Bruns, E. A.; Slowik, J. G.; El Haddad, I.; Kilic, D.; Klein, F.; Dommen, J.; Temime-Roussel, B.; Marchand, N.; Baltensperger, U.; Prévôt, A. S. H. Characterization of gas-phase organics using proton transfer reaction time-of-flight mass spectrometry: fresh and aged residential wood combustion emissions. *Atmos. Chem. Phys.* **2017**, *17*, 705–720.
- (159) Warneke, C.; Geiger, F.; Edwards, P. M.; Dube, W.; Pétron, G.; Kofler, J.; Zahn, A.; Brown, S. S.; Graus, M.; Gilman, J.; et al. Volatile organic compound emissions from the oil and natural gas industry in the Uinta Basin, Utah: point sources compared to ambient air composition. *Atmos. Chem. Phys.* **2014**, *14*, 10977–10988.
- (160) Jobson, B. T.; Volkamer, R. A.; Velasco, E.; Allwine, G.; Westberg, H.; Lamb, B. K.; Alexander, M. L.; Berkowitz, C. M.; Molina, L. T. Comparison of aromatic hydrocarbon measurements made by PTR-MS, DOAS and GC-FID during the MCMA 2003 Field Experiment. *Atmos. Chem. Phys.* **2010**, *10*, 1989–2005.
- (161) Coggon, M. M.; Veres, P. R.; Yuan, B.; Koss, A.; Warneke, C.; Gilman, J. B.; Lerner, B. M.; Peischl, J.; Aikin, K. C.; Stockwell, C. E.; et al. Emissions of nitrogen-containing organic compounds from the burning of herbaceous and arborescent biomass: Fuel composition dependence and the variability of commonly used nitrile tracers. *Geophys. Res. Lett.* **2016**, *43*, 9903–9912.
- (162) Karl, T.; Harren, F.; Warneke, C.; de Gouw, J.; Grayless, C.; Fall, R. Senescing grass crops as regional sources of reactive volatile organic compounds. *J. Geophys. Res.* **2005**, *110*, D15302.
- (163) Brilli, F.; Ruuskanen, T. M.; Schnitzhofer, R.; Muller, M.; Breitenlechner, M.; Bittner, V.; Wohlfahrt, G.; Loreto, F.; Hansel, A. Detection of plant volatiles after leaf wounding and darkening by proton transfer reaction "time-of-flight" mass spectrometry (PTR-TOF). *PLoS One* **2011**, *6*, e20419.
- (164) Brilli, F.; Hörtnagl, L.; Bamberger, I.; Schnitzhofer, R.; Ruuskanen, T. M.; Hansel, A.; Loreto, F.; Wohlfahrt, G. Qualitative and quantitative characterization of volatile organic compound emissions from cut grass. *Environ. Sci. Technol.* **2012**, *46*, 3859–65.
- (165) Inomata, S.; Tanimoto, H.; Fujitani, Y.; Sekimoto, K.; Sato, K.; Fushimi, A.; Yamada, H.; Hori, S.; Kumazawa, Y.; Shimono, A.; et al. On-line measurements of gaseous nitro-organic compounds in diesel vehicle exhaust by proton-transfer-reaction mass spectrometry. *Atmos. Environ.* **2013**, *73*, 195–203.
- (166) Inomata, S.; Fushimi, A.; Sato, K.; Fujitani, Y.; Yamada, H. 4-Nitrophenol, 1-nitropyrene, and 9-nitroanthracene emissions in exhaust particles from diesel vehicles with different exhaust gas treatments. *Atmos. Environ.* **2015**, *110*, 93–102.

- (167) Demarcke, M.; Amelynck, C.; Schoon, N.; Dhooghe, F.; Van Langenhove, H.; Dewulf, J. Laboratory studies in support of the detection of sesquiterpenes by proton-transfer-reaction-mass-spectrometry. *Int. J. Mass Spectrom.* **2009**, *279*, 156–162.
- (168) Dhooghe, F.; Amelynck, C.; Schoon, N.; Debie, E.; Bultinck, P.; Vanhaecke, F. A selected ion flow tube study of the reactions of  $\text{H}_3\text{O}^+$ ,  $\text{NO}^+$  and  $\text{O}_2^+$  with a series of sesquiterpenes. *Int. J. Mass Spectrom.* **2008**, *272*, 137–148.
- (169) Tang, X.; Misztal, P. K.; Nazaroff, W. W.; Goldstein, A. H. Siloxanes are the most abundant volatile organic compound emitted from engineering students in a classroom. *Environ. Sci. Technol. Lett.* **2015**, *2*, 303–307.
- (170) Norman, M.; Hansel, A.; Wisthaler, A.  $\text{O}_2(+)$  as reagent ion in the PTR-MS instrument: Detection of gas-phase ammonia. *Int. J. Mass Spectrom.* **2007**, *265*, 382–387.
- (171) Norman, M.; Spirig, C.; Wolff, V.; Trebs, I.; Flechard, C.; Wisthaler, A.; Schnitzhofer, R.; Hansel, A.; Neftel, A. Intercomparison of ammonia measurement techniques at an intensively managed grassland site (Oensingen, Switzerland). *Atmos. Chem. Phys.* **2009**, *9*, 2635–2645.
- (172) Cui, L.; Zhang, Z.; Huang, Y.; Lee, S. C.; Blake, D. R.; Ho, K. F.; Wang, B.; Gao, Y.; Wang, X. M.; Louie, P. K. K. Measuring OVOCs and VOCs by PTR-MS in an urban roadside microenvironment of Hong Kong: relative humidity and temperature dependence, and field intercomparisons. *Atmos. Meas. Tech.* **2016**, *9*, 5763–5779.
- (173) Jobson, B. T.; McCoskey, J. K. Sample drying to improve HCHO measurements by PTR-MS instruments: laboratory and field measurements. *Atmos. Chem. Phys.* **2010**, *10*, 1821–1835.
- (174) Wisthaler, A.; Apel, E. C.; Bossmeyer, J.; Hansel, A.; Junkermann, W.; Koppmann, R.; Meier, R.; Muller, K.; Solomon, S. J.; Steinbrecher, R.; et al. Technical Note: Intercomparison of formaldehyde measurements at the atmosphere simulation chamber SAPHIR. *Atmos. Chem. Phys.* **2008**, *8*, 2189–2200.
- (175) Schripp, T.; Fauck, C.; Salthammer, T. Interferences in the determination of formaldehyde via PTR-MS: What do we learn from  $m/z$  31? *Int. J. Mass Spectrom.* **2010**, *289*, 170–172.
- (176) Stonner, C.; Derstroff, B.; Klupfel, T.; Crowley, J. N.; Williams, J. Glyoxal measurement with a proton transfer reaction time of flight mass spectrometer (PTR-TOF-MS): characterization and calibration. *J. Mass Spectrom.* **2017**, *52*, 30–35.
- (177) de Gouw, J.; Warneke, C.; Karl, T.; Eerdekens, G.; van der Veen, C.; Fall, R. Sensitivity and specificity of atmospheric trace gas detection by proton-transfer-reaction mass spectrometry. *Int. J. Mass Spectrom.* **2003**, *223*–224, 365–382.
- (178) de Gouw, J. A.; Warneke, C.; Parrish, D. D.; Holloway, J. S.; Trainer, M.; Fehsenfeld, F. C. Emission sources and ocean uptake of acetonitrile ( $\text{CH}_3\text{CN}$ ) in the atmosphere. *J. Geophys. Res.* **2003**, *108*, DOI: [10.1029/2002JD002897](https://doi.org/10.1029/2002JD002897).
- (179) Dunne, E.; Galbally, I. E.; Lawson, S.; Patti, A. Interference in the PTR-MS measurement of acetonitrile at  $m/z$  42 in polluted urban air—A study using switchable reagent ion PTR-MS. *Int. J. Mass Spectrom.* **2012**, *319*–320, 40–47.
- (180) Roberts, J. M.; Veres, P. R.; Cochran, A. K.; Warneke, C.; Burling, I. R.; Yokelson, R. J.; Lerner, B.; Gilman, J. B.; Kuster, W. C.; Fall, R.; et al. Isocyanic acid in the atmosphere and its possible link to smoke-related health effects. *Proc. Natl. Acad. Sci. U. S. A.* **2011**, *108*, 8966–71.
- (181) Bunkan, A. J.; Mikoviny, T.; Nielsen, C. J.; Wisthaler, A.; Zhu, L. Experimental and theoretical study of the OH-initiated photo-oxidation of formamide. *J. Phys. Chem. A* **2016**, *120*, 1222–30.
- (182) Hunter, E. P. L.; Lias, S. G. Evaluated gas phase basicities and proton affinities of molecules: an update. *J. Phys. Chem. Ref. Data* **1998**, *27*, 413–656.
- (183) Kajos, M. K.; Rantala, P.; Hill, M.; Hellén, H.; Aalto, J.; Patokoski, J.; Taipale, R.; Hoerger, C. C.; Reimann, S.; Ruuskanen, T. M.; et al. Ambient measurements of aromatic and oxidized VOCs by PTR-MS and GC-MS: intercomparison between four instruments in a boreal forest in Finland. *Atmos. Meas. Tech.* **2015**, *8*, 4453–4473.
- (184) Dunne, E.; Galbally, I. E.; Cheng, M.; Selleck, P.; Molloy, S. B.; Lawson, S. J. Comparison of VOC measurements made by PTR-MS, Adsorbent Tube/GC-FID-MS and DNPH-derivatization/HPLC during the Sydney Particle Study, 2012: a contribution to the assessment of uncertainty in current atmospheric VOC measurements. *Atmos. Meas. Technol. Discuss.* **2017**, *2017*, 1–24.
- (185) Veres, P.; Roberts, J. M.; Burling, I. R.; Warneke, C.; de Gouw, J.; Yokelson, R. J. Measurements of gas-phase inorganic and organic acids from biomass fires by negative-ion proton-transfer chemical-ionization mass spectrometry. *J. Geophys. Res.* **2010**, *115*, DOI: [10.1029/2010JD014033](https://doi.org/10.1029/2010JD014033).
- (186) Perraud, V.; Horne, J. R.; Martinez, A. S.; Kalinowski, J.; Meinardi, S.; Dawson, M. L.; Wingen, L. M.; Dabdub, D.; Blake, D. R.; Gerber, R. B.; et al. The future of airborne sulfur-containing particles in the absence of fossil fuel sulfur dioxide emissions. *Proc. Natl. Acad. Sci. U. S. A.* **2015**, *112*, 13514–13519.
- (187) Karl, T.; Hansel, A.; Cappellin, L.; Kaser, L.; Herdlinger-Blatt, I.; Jud, W. Selective measurements of isoprene and 2-methyl-3-butene-2-ol based on  $\text{NO}^+$  ionization mass spectrometry. *Atmos. Chem. Phys.* **2012**, *12*, 11877–11884.
- (188) Kefsel, S.; Cabrera-Perez, D.; Horowitz, A.; Veres, P. R.; Sander, R.; Taraborrelli, D.; Tucceri, M.; Crowley, J. N.; Pozzer, A.; Stonner, C.; et al. Atmospheric chemistry, sources and sinks of carbon suboxide,  $\text{C}_3\text{O}_2$ . *Atmos. Chem. Phys.* **2017**, *17*, 8789–8804.
- (189) Liu, Y.; Brito, J.; Dorris, M. R.; Rivera-Rios, J. C.; Seco, R.; Bates, K. H.; Artaxo, P.; Duvoisin, S., Jr.; Keutsch, F. N.; Kim, S.; et al. Isoprene photochemistry over the Amazon rainforest. *Proc. Natl. Acad. Sci. U. S. A.* **2016**, *113*, 6125–30.
- (190) Liu, Y. J.; Herdlinger-Blatt, I.; McKinney, K. A.; Martin, S. T. Production of methyl vinyl ketone and methacrolein via the hydroperoxy pathway of isoprene oxidation. *Atmos. Chem. Phys.* **2013**, *13*, 5715–5730.
- (191) Yáñez-Serrano, A. M.; Nölscher, A. C.; Bourtsoukidis, E.; Derstroff, B.; Zannoni, N.; Gros, V.; Lanza, M.; Brito, J.; Noe, S. M.; House, E.; et al. Atmospheric mixing ratios of methyl ethyl ketone (2-butanone) in tropical, boreal, temperate and marine environments. *Atmos. Chem. Phys.* **2016**, *16*, 10965–10984.
- (192) Holzinger, R.; Millet, D. B.; Williams, B.; Lee, A.; Kreisberg, N.; Hering, S. V.; Jimenez, J.; Allan, J. D.; Worsnop, D. R.; Goldstein, A. H. Emission, oxidation, and secondary organic aerosol formation of volatile organic compounds as observed at Chebogue Point, Nova Scotia. *J. Geophys. Res.* **2007**, *112*, D10S24.
- (193) Hellén, H.; Schallhart, S.; Praplan, A. P.; Petäjä, T.; Hakola, H. Using in situ GC-MS for analysis of C<sub>2</sub>–C<sub>7</sub> volatile organic acids in ambient air of a boreal forest site. *Atmos. Meas. Tech.* **2017**, *10*, 281–289.
- (194) Ambrose, J. L.; Haase, K.; Russo, R. S.; Zhou, Y.; White, M. L.; Frinak, E. K.; Jordan, C.; Mayne, H. R.; Talbot, R.; Sive, B. C. A comparison of GC-FID and PTR-MS toluene measurements in ambient air under conditions of enhanced monoterpene loading. *Atmos. Meas. Tech.* **2010**, *3*, 959–980.
- (195) Midey, A. J.; Williams, S.; Miller, T. M.; Viggiano, A. A. Reactions of  $\text{O}_2^+$ ,  $\text{NO}^+$  and  $\text{H}_3\text{O}^+$  with methylcyclohexane (C<sub>7</sub>H<sub>14</sub>) and cyclooctane (C<sub>8</sub>H<sub>16</sub>) from 298 to 700 K. *Int. J. Mass Spectrom.* **2003**, *222*, 413–430.
- (196) Koss, A. R.; de Gouw, J.; Warneke, C.; Gilman, J. B.; Lerner, B. M.; Graus, M.; Yuan, B.; Edwards, P.; Brown, S. S.; Wild, R.; et al. Photochemical aging of volatile organic compounds associated with oil and natural gas extraction in the Uintah Basin, UT, during a wintertime ozone formation event. *Atmos. Chem. Phys.* **2015**, *15*, 5727–5741.
- (197) Park, J.-H.; Goldstein, A. H.; Timkovsky, J.; Fares, S.; Weber, R.; Karlik, J.; Holzinger, R. Active atmosphere-ecosystem exchange of the vast majority of detected volatile organic compounds. *Science* **2013**, *341*, 643–647.
- (198) Rücker, C.; Kümmeler, K. Environmental chemistry of organosiloxanes. *Chem. Rev.* **2015**, *115*, 466–524.
- (199) Genualdi, S.; Harner, T.; Cheng, Y.; MacLeod, M.; Hansen, K. M.; van Egmond, R.; Shoeib, M.; Lee, S. C. Global distribution of

- linear and cyclic volatile methyl siloxanes in air. *Environ. Sci. Technol.* **2011**, *45*, 3349–3354.
- (200) Mackay, D.; Cowan-Ellsberry, C. E.; Powell, D. E.; Woodburn, K. B.; Xu, S.; Kozerski, G. E.; Kim, J. Decamethylcyclopentasiloxane (D5) environmental sources, fate, transport, and routes of exposure. *Environ. Toxicol. Chem.* **2015**, *34*, 2689–2702.
- (201) Buser, A. M.; Kierkegaard, A.; Bogdal, C.; MacLeod, M.; Scheringer, M.; Hungerbühler, K. Concentrations in ambient air and emissions of cyclic volatile methylsiloxanes in Zurich, Switzerland. *Environ. Sci. Technol.* **2013**, *47*, 7045–7051.
- (202) Yucuis, R. A.; Stanier, C. O.; Hornbuckle, K. C. Cyclic siloxanes in air, including identification of high levels in Chicago and distinct diurnal variation. *Chemosphere* **2013**, *92*, 905–910.
- (203) Song, Y.; Dai, W.; Shao, M.; Liu, Y.; Lu, S. H.; Kuster, W.; Goldan, P. Comparison of receptor models for source apportionment of volatile organic compounds in Beijing, China. *Environ. Pollut.* **2008**, *156*, 174–183.
- (204) Wyche, K. P.; Monks, P. S.; Smallbone, K. L.; Hamilton, J. F.; Alfara, M. R.; Rickard, A. R.; McFiggans, G. B.; Jenkin, M. E.; Blos, W. J.; Ryan, A. C.; et al. Mapping gas-phase organic reactivity and concomitant secondary organic aerosol formation: chemometric dimension reduction techniques for the deconvolution of complex atmospheric data sets. *Atmos. Chem. Phys.* **2015**, *15*, 8077–8100.
- (205) Yuan, B.; Shao, M.; de Gouw, J.; Parrish, D. D.; Lu, S.; Wang, M.; Zeng, L.; Zhang, Q.; Song, Y.; Zhang, J.; et al. Volatile organic compounds (VOCs) in urban air: How chemistry affects the interpretation of positive matrix factorization (PMF) analysis. *J. Geophys. Res.* **2012**, *117*, D24302.
- (206) Chen, W. T.; Shao, M.; Lu, S. H.; Wang, M.; Zeng, L. M.; Yuan, B.; Liu, Y. Understanding primary and secondary sources of ambient carbonyl compounds in Beijing using the PMF model. *Atmos. Chem. Phys.* **2014**, *14*, 3047–3062.
- (207) Crippa, M.; Canonaco, F.; Slowik, J. G.; El Haddad, I.; DeCarlo, P. F.; Mohr, C.; Heringa, M. F.; Chirico, R.; Marchand, N.; Temime-Roussel, B.; et al. Primary and secondary organic aerosols origin by combined gas-particle phase source apportionment. *Atmos. Chem. Phys.* **2013**, *13*, 8411–8426.
- (208) Slowik, J. G.; Vlasenko, A.; McGuire, M.; Evans, G. J.; Abbott, J. P. D. Simultaneous factor analysis of organic particle and gas mass spectra: AMS and PTR-MS measurements at an urban site. *Atmos. Chem. Phys.* **2010**, *10*, 1969–1988.
- (209) Canonaco, F.; Crippa, M.; Slowik, J. G.; Baltensperger, U.; Prévôt, A. S. H. SoFi, an IGOR-based interface for the efficient use of the generalized multilinear engine (ME-2) for the source apportionment: ME-2 application to aerosol mass spectrometer data. *Atmos. Meas. Tech.* **2013**, *6*, 3649–3661.
- (210) Zhao, W. X.; Hopke, P. K.; Karl, T. Source identification of volatile organic compounds in Houston, Texas. *Environ. Sci. Technol.* **2004**, *38*, 1338–1347.
- (211) Heald, C. L.; Kroll, J. H.; Jimenez, J. L.; Docherty, K. S.; DeCarlo, P. F.; Aiken, A. C.; Chen, Q.; Martin, S. T.; Farmer, D. K.; Artaxo, P. A simplified description of the evolution of organic aerosol composition in the atmosphere. *Geophys. Res. Lett.* **2010**, *37*, DOI: [10.1029/2010GL042737](https://doi.org/10.1029/2010GL042737).
- (212) Kroll, J. H.; Donahue, N. M.; Jimenez, J. L.; Kessler, S. H.; Canagaratna, M. R.; Wilson, K. R.; Altieri, K. E.; Mazzoleni, L. R.; Wozniak, A. S.; Bluhm, H.; et al. Carbon oxidation state as a metric for describing the chemistry of atmospheric organic aerosol. *Nat. Chem.* **2011**, *3*, 133–9.
- (213) Müller, M.; Graus, M.; Wisthaler, A.; Hansel, A.; Metzger, A.; Dommen, J.; Baltensperger, U. Analysis of high mass resolution PTR-TOF mass spectra from 1,3,5-trimethylbenzene (TMB) environmental chamber experiments. *Atmos. Chem. Phys.* **2012**, *12*, 829–843.
- (214) Zavala, M.; Herndon, S. C.; Slott, R. S.; Dunlea, E. J.; Marr, L. C.; Shorter, J. H.; Zahniser, M.; Knighton, W. B.; Rogers, T. M.; Kolb, C. E.; et al. Characterization of on-road vehicle emissions in the Mexico City Metropolitan Area using a mobile laboratory in chase and fleet average measurement modes during the MCMA-2003 field campaign. *Atmos. Chem. Phys.* **2006**, *6*, 5129–5142.
- (215) Zavala, M.; Herndon, S. C.; Wood, E. C.; Jayne, J. T.; Nelson, D. D.; Trimborn, A. M.; Dunlea, E.; Knighton, W. B.; Mendoza, A.; Allen, D. T.; et al. Comparison of emissions from on-road sources using a mobile laboratory under various driving and operational sampling modes. *Atmos. Chem. Phys.* **2009**, *9*, 1–14.
- (216) Herndon, S. C.; Jayne, J. T.; Zahniser, M. S.; Worsnop, D. R.; Knighton, B.; Alwine, E.; Lamb, B. K.; Zavala, M.; Nelson, D. D.; McManus, J. B.; et al. Characterization of urban pollutant emission fluxes and ambient concentration distributions using a mobile laboratory with rapid response instrumentation. *Faraday Discuss.* **2005**, *130*, 327–339.
- (217) Inomata, S.; Fujitani, Y.; Fushimi, A.; Tanimoto, H.; Sekimoto, K.; Yamada, H. Field measurement of nitromethane from automotive emissions at a busy intersection using proton-transfer-reaction mass spectrometry. *Atmos. Environ.* **2014**, *96*, 301–309.
- (218) Sekimoto, K.; Inomata, S.; Tanimoto, H.; Fushimi, A.; Fujitani, Y.; Sato, K.; Yamada, H. Characterization of nitromethane emission from automotive exhaust. *Atmos. Environ.* **2013**, *81*, 523–531.
- (219) Erickson, M. H.; Gueneron, M.; Jobson, B. T. Measuring long chain alkanes in diesel engine exhaust by thermal desorption PTR-MS. *Atmos. Meas. Tech.* **2014**, *7*, 225–239.
- (220) Drozd, G. T.; Zhao, Y.; Saliba, G.; Frodin, B.; Maddox, C.; Weber, R. J.; Chang, M. O.; Maldonado, H.; Sardar, S.; Robinson, A. L.; et al. Time resolved measurements of speciated tailpipe Eemissions from motor vehicles: trends with emission control technology, cold start effects, and speciation. *Environ. Sci. Technol.* **2016**, *50*, 13592–13599.
- (221) Kilic, D.; Brem, B. T.; Klein, F.; El-Haddad, I.; Durdina, L.; Rindlisbacher, T.; Setyan, A.; Huang, R.; Wang, J.; Slowik, J. G.; et al. Characterization of gas-phase organics using proton transfer reaction time-of-flight mass spectrometry: aircraft turbine engines. *Environ. Sci. Technol.* **2017**, *51*, 3621–3629.
- (222) de Gouw, J. A.; Welsh-Bon, D.; Warneke, C.; Kuster, W. C.; Alexander, L.; Baker, A. K.; Beyersdorf, A. J.; Blake, D. R.; Canagaratna, M.; Celada, A. T.; et al. Emission and chemistry of organic carbon in the gas and aerosol phase at a sub-urban site near Mexico City in March 2006 during the MILAGRO study. *Atmos. Chem. Phys.* **2009**, *9*, 3425–3442.
- (223) Sonderfeld, H.; White, I. R.; Goodall, I. C. A.; Hopkins, J. R.; Lewis, A. C.; Koppmann, R.; Monks, P. S. What effect does VOC sampling time have on derived OH reactivity? *Atmos. Chem. Phys.* **2016**, *16*, 6303–6318.
- (224) Yang, Y. D.; Shao, M.; Wang, X. M.; Nolscher, A. C.; Kessel, S.; Guenther, A.; Williams, J. Towards a quantitative understanding of total OH reactivity: A review. *Atmos. Environ.* **2016**, *134*, 147–161.
- (225) Sahu, L. K.; Saxena, P. High time and mass resolved PTR-TOF-MS measurements of VOCs at an urban site of India during winter: Role of anthropogenic, biomass burning, biogenic and photochemical sources. *Atmos. Res.* **2015**, *164–165*, 84–94.
- (226) Sahu, L. K.; Yadav, R.; Pal, D. Source identification of VOCs at an urban site of western India: Effect of marathon events and anthropogenic emissions. *Journal of Geophysical Research: Atmospheres* **2016**, *121*, 2416–2433.
- (227) Velasco, E.; Lamb, B.; Pressley, S.; Allwine, E.; Westberg, H.; Jobson, B. T.; Alexander, M.; Prazeller, P.; Molina, L.; Molina, M. Flux measurements of volatile organic compounds from an urban landscape. *Geophys. Res. Lett.* **2005**, *32*, L20802.
- (228) Velasco, E.; Pressley, S.; Grivice, R.; Allwine, E.; Coons, T.; Foster, W.; Jobson, B. T.; Westberg, H.; Ramos, R.; Hernandez, F.; et al. Eddy covariance flux measurements of pollutant gases in urban Mexico City. *Atmos. Chem. Phys.* **2009**, *9*, 7325–7342.
- (229) Langford, B.; Davison, B.; Nemitz, E.; Hewitt, C. N. Mixing ratios and eddy covariance flux measurements of volatile organic compounds from an urban canopy (Manchester, UK). *Atmos. Chem. Phys.* **2009**, *9*, 1971–1987.
- (230) Langford, B.; Nemitz, E.; House, E.; Phillips, G. J.; Famulari, D.; Davison, B.; Hopkins, J. R.; Lewis, A. C.; Hewitt, C. N. Fluxes and concentrations of volatile organic compounds above central London, UK. *Atmos. Chem. Phys.* **2010**, *10*, 627–645.

- (231) Valach, A. C.; Langford, B.; Nemitz, E.; MacKenzie, A. R.; Hewitt, C. N. Seasonal and diurnal trends in concentrations and fluxes of volatile organic compounds in central London. *Atmos. Chem. Phys.* **2015**, *15*, 7777–7796.
- (232) Rantala, P.; Järvi, L.; Taipale, R.; Laurila, T. K.; Patokoski, J.; Kajos, M. K.; Kurppa, M.; Haapanala, S.; Siivola, E.; Petäjä, T.; et al. Anthropogenic and biogenic influence on VOC fluxes at an urban background site in Helsinki, Finland. *Atmos. Chem. Phys.* **2016**, *16*, 7981–8007.
- (233) Karl, T.; Apel, E.; Hodzic, A.; Riemer, D. D.; Blake, D. R.; Wiedinmyer, C. Emissions of volatile organic compounds inferred from airborne flux measurements over a megacity. *Atmos. Chem. Phys.* **2009**, *9*, 271–285.
- (234) Vaughan, A. R.; Lee, J. D.; Shaw, M. D.; Misztal, P. K.; Metzger, S.; Vieno, M.; Davison, B.; Karl, T. G.; Carpenter, L. J.; Lewis, A. C.; et al. VOC emission rates over London and South East England obtained by airborne eddy covariance. *Faraday Discuss.* **2017**, *200*, 599–620.
- (235) Park, J. H.; Goldstein, A. H.; Timkovsky, J.; Fares, S.; Weber, R.; Karlik, J.; Holzinger, R. Eddy covariance emission and deposition flux measurements using proton transfer reaction-time of flight-mass spectrometry (PTR-TOF-MS): comparison with PTR-MS measured vertical gradients and fluxes. *Atmos. Chem. Phys.* **2013**, *13*, 1439–1456.
- (236) Naehler, L. P.; Brauer, M.; Lipsett, M.; Zelikoff, J. T.; Simpson, C. D.; Koenig, J. Q.; Smith, K. R. Woodsmoke health effects: a review. *Inhalation Toxicol.* **2007**, *19*, 67–106.
- (237) Szidat, S.; Prévôt, A. S. H.; Sandradewi, J.; Alfara, M. R.; Synal, H.-A.; Wacker, L.; Baltensperger, U. Dominant impact of residential wood burning on particulate matter in Alpine valleys during winter. *Geophys. Res. Lett.* **2007**, *34*, DOI: [10.1029/2006GL028325](https://doi.org/10.1029/2006GL028325).
- (238) Florou, K.; Papanastasiou, D. K.; Pikridas, M.; Kaltonoudis, C.; Louvaris, E.; Gkatzelis, E.; Patoulas, D.; Mihalopoulos, N.; Pandis, S. N. The contribution of wood burning and other pollution sources to wintertime organic aerosol levels in two Greek cities. *Atmos. Chem. Phys.* **2017**, *17*, 3145–3163.
- (239) Holzinger, R.; Warneke, C.; Hansel, A.; Jordan, A.; Lindinger, W.; Scharffe, D. H.; Schade, G.; Crutzen, P. J. Biomass burning as a source of formaldehyde, acetaldehyde, methanol, acetone, acetonitrile, and hydrogen cyanide. *Geophys. Res. Lett.* **1999**, *26*, 1161–1164.
- (240) Holzinger, R.; Williams, J.; Salisbury, G.; Klupfel, T.; de Reus, M.; Traub, M.; Crutzen, P. J.; Lelieveld, J. Oxygenated compounds in aged biomass burning plumes over the Eastern Mediterranean: evidence for strong secondary production of methanol and acetone. *Atmos. Chem. Phys.* **2005**, *5*, 39–46.
- (241) Yuan, B.; Liu, Y.; Shao, M.; Lu, S.; Streets, D. G. Biomass burning contributions to ambient VOCs species at a receptor site in the Pearl River Delta (PRD), China. *Environ. Sci. Technol.* **2010**, *44*, 4577–4582.
- (242) Liu, X.; Zhang, Y.; Huey, L. G.; Yokelson, R. J.; Wang, Y.; Jimenez, J. L.; Campuzano-Jost, P.; Beyersdorf, A. J.; Blake, D. R.; Choi, Y.; et al. Agricultural fires in the southeastern U.S. during SEAC4RS: Emissions of trace gases and particles and evolution of ozone, reactive nitrogen, and organic aerosol. *Journal of Geophysical Research: Atmospheres* **2016**, *121*, 7383–7414.
- (243) Bruns, E. A.; El Haddad, I.; Slowik, J. G.; Kilic, D.; Klein, F.; Baltensperger, U.; Prevot, A. S. Identification of significant precursor gases of secondary organic aerosols from residential wood combustion. *Sci. Rep.* **2016**, *6*, 27881.
- (244) Yáñez-Serrano, A. M.; Nölscher, A. C.; Williams, J.; Wolff, S.; Alves, E.; Martins, G. A.; Bourtsoukidis, E.; Brito, J.; Jardine, K.; Artaxo, P.; et al. Diel and seasonal changes of biogenic volatile organic compounds within and above an Amazonian rainforest. *Atmos. Chem. Phys.* **2015**, *15*, 3359–3378.
- (245) Langford, B.; Misztal, P. K.; Nemitz, E.; Davison, B.; Helfter, C.; Pugh, T. A. M.; MacKenzie, A. R.; Lim, S. F.; Hewitt, C. N. Fluxes and concentrations of volatile organic compounds from a South-East Asian tropical rainforest. *Atmos. Chem. Phys.* **2010**, *10*, 8391–8412.
- (246) Patokoski, J.; Ruuskanen, T. M.; Kajos, M. K.; Taipale, R.; Rantala, P.; Aalto, J.; Ryypä, T.; Nieminen, T.; Hakola, H.; Rinne, J. Sources of long-lived atmospheric VOCs at the rural boreal forest site, SMEAR II. *Atmos. Chem. Phys.* **2015**, *15*, 13413–13432.
- (247) Karl, T.; Kaser, L.; Turnipseed, A. Eddy covariance measurements of isoprene and 232-MBO based on NO<sub>x</sub> time-of-flight mass spectrometry. *Int. J. Mass Spectrom.* **2014**, *365–366*, 15–19.
- (248) Karl, T.; Guenther, A.; Turnipseed, A.; Patton, E. G.; Jardine, K. Chemical sensing of plant stress at the ecosystem scale. *Biogeosciences* **2008**, *5*, 1287–1294.
- (249) Bouvier-Brown, N. C.; Goldstein, A. H.; Worton, D. R.; Matross, D. M.; Gilman, J. B.; Kuster, W. C.; Welsh-Bon, D.; Warneke, C.; de Gouw, J. A.; Cahill, T. M.; et al. Methyl chavicol: characterization of its biogenic emission rate, abundance, and oxidation products in the atmosphere. *Atmos. Chem. Phys.* **2009**, *9*, 2061–2074.
- (250) Ruuskanen, T. M.; Müller, M.; Schnitzhofer, R.; Karl, T.; Graus, M.; Bamberger, I.; Hörtoggl, L.; Brill, F.; Wohlfahrt, G.; Hansel, A. Eddy covariance VOC emission and deposition fluxes above grassland using PTR-TOF. *Atmos. Chem. Phys.* **2011**, *11*, 611–625.
- (251) Kim, S.; Guenther, A.; Apel, E. Quantitative and qualitative sensing techniques for biogenic volatile organic compounds and their oxidation products. *Environmental science. Processes & impacts* **2013**, *15*, 1301–14.
- (252) Karl, T.; Guenther, A.; Jordan, A.; Fall, R.; Lindinger, W. Eddy covariance measurement of biogenic oxygenated VOC emissions from hay harvesting. *Atmos. Environ.* **2001**, *35*, 491–495.
- (253) Park, J. H.; Fares, S.; Weber, R.; Goldstein, A. H. Biogenic volatile organic compound emissions during BEARPEX 2009 measured by eddy covariance and flux-gradient similarity methods. *Atmos. Chem. Phys.* **2014**, *14*, 231–244.
- (254) Graus, M.; Hansel, A.; Wisthaler, A.; Lindinger, C.; Forkel, R.; Hauff, K.; Klauer, M.; Pfichner, A.; Rappenglück, B.; Steigner, D.; et al. A relaxed-eddy-accumulation method for the measurement of isoprenoid canopy-fluxes using an online gas-chromatographic technique and PTR-MS simultaneously. *Atmos. Environ.* **2006**, *40*, 43–54.
- (255) Karl, T.; Guenther, A.; Yokelson, R. J.; Greenberg, J.; Potosnak, M.; Blake, D. R.; Artaxo, P. The tropical forest and fire emissions experiment: Emission, chemistry, and transport of biogenic volatile organic compounds in the lower atmosphere over Amazonia. *J. Geophys. Res.* **2007**, *112*, DOI: [10.1029/2007JD008539](https://doi.org/10.1029/2007JD008539).
- (256) Warneke, C.; de Gouw, J. A.; Del Negro, L.; Brioude, J.; McKeen, S.; Stark, H.; Kuster, W. C.; Goldan, P. D.; Trainer, M.; Fehsenfeld, F. C., et al. Biogenic emission measurement and inventories determination of biogenic emissions in the eastern United States and Texas and comparison with biogenic emission inventories. *J. Geophys. Res.* **2010**, *115*, DOI: [10.1029/2009JD012445](https://doi.org/10.1029/2009JD012445).
- (257) Karl, T.; Harley, P.; Emmons, L.; Thornton, B.; Guenther, A.; Basu, C.; Turnipseed, A.; Jardine, K. Efficient atmospheric cleansing of oxidized organic trace gases by vegetation. *Science* **2010**, *330*, 816–819.
- (258) Hewitt, C. N.; Ashworth, K.; Boynard, A.; Guenther, A.; Langford, B.; MacKenzie, A. R.; Misztal, P. K.; Nemitz, E.; Owen, S. M.; Possell, M.; et al. Ground-level ozone influenced by circadian control of isoprene emissions. *Nat. Geosci.* **2011**, *4*, 671–674.
- (259) Bamberger, I.; Hörtoggl, L.; Ruuskanen, T. M.; Schnitzhofer, R.; Müller, M.; Graus, M.; Karl, T.; Wohlfahrt, G.; Hansel, A. Deposition fluxes of terpenes over grassland. *J. Geophys. Res.* **2011**, *116*, D14305.
- (260) Graus, M.; Eller, A. S. D.; Fall, R.; Yuan, B.; Qian, Y.; Westra, P.; de Gouw, J.; Warneke, C. Biosphere-atmosphere exchange of volatile organic compounds over C4 biofuel crops. *Atmos. Environ.* **2013**, *66*, 161–168.
- (261) Misztal, P. K.; Hewitt, C. N.; Wildt, J.; Blande, J. D.; Eller, A. S.; Fares, S.; Gentner, D. R.; Gilman, J. B.; Graus, M.; Greenberg, J.; et al. Atmospheric benzenoid emissions from plants rival those from fossil fuels. *Sci. Rep.* **2015**, *5*, 12064.
- (262) Fares, S.; Schnitzhofer, R.; Jiang, X.; Guenther, A.; Hansel, A.; Loreto, F. Observations of diurnal to weekly variations of monoterpane-dominated fluxes of volatile organic compounds from

- mediterranean forests: implications for regional modeling. *Environ. Sci. Technol.* **2013**, *47*, 11073–82.
- (263) Brilli, F.; Gioli, B.; Zona, D.; Pallozzi, E.; Zenone, T.; Fratini, G.; Calfapietra, C.; Loreto, F.; Janssens, I. A.; Ceulemans, R. Simultaneous leaf- and ecosystem-level fluxes of volatile organic compounds from a poplar-based SRC plantation. *Agricultural and Forest Meteorology* **2014**, *187*, 22–35.
- (264) Misztal, P. K.; Karl, T.; Weber, R.; Jonsson, H. H.; Guenther, A. B.; Goldstein, A. H. Airborne flux measurements of biogenic isoprene over California. *Atmos. Chem. Phys.* **2014**, *14*, 10631–10647.
- (265) Karl, T.; Misztal, P. K.; Jonsson, H. H.; Shertz, S.; Goldstein, A. H.; Guenther, A. B. Airborne flux measurements of BVOCs above californian oak forests: experimental investigation of surface and entrainment fluxes, OH densities, and damköhler numbers. *J. Atmos. Sci.* **2013**, *70*, 3277–3287.
- (266) Misztal, P. K.; Avise, J. C.; Karl, T.; Scott, K.; Jonsson, H. H.; Guenther, A. B.; Goldstein, A. H. Evaluation of regional isoprene emission factors and modeled fluxes in California. *Atmos. Chem. Phys.* **2016**, *16*, 9611–9628.
- (267) Yu, H.; Guenther, A.; Gu, D.; Warneke, C.; Geron, C.; Goldstein, A.; Graus, M.; Karl, T.; Kaser, L.; Misztal, P.; et al. Airborne measurements of isoprene and monoterpene emissions from southeastern U.S. forests. *Sci. Total Environ.* **2017**, *595*, 149–158.
- (268) Wolfe, G. M.; Hanisco, T. F.; Arkinson, H. L.; Bui, T. P.; Crounse, J. D.; Dean-Day, J.; Goldstein, A.; Guenther, A.; Hall, S. R.; Huey, G.; et al. Quantifying sources and sinks of reactive gases in the lower atmosphere using airborne flux observations. *Geophys. Res. Lett.* **2015**, *42*, 8231–8240.
- (269) Kaser, L.; Karl, T.; Yuan, B.; Mauldin, R. L.; Cantrell, C. A.; Guenther, A. B.; Patton, E. G.; Weinheimer, A. J.; Knote, C.; Orlando, J.; et al. Chemistry-turbulence interactions and mesoscale variability influence the cleansing efficiency of the atmosphere. *Geophys. Res. Lett.* **2015**, *42*, 10894–10903.
- (270) Paulot, F.; Crounse, J. D.; Kjaergaard, H. G.; Kroll, J. H.; Seinfeld, J. H.; Wennberg, P. O. Isoprene photooxidation: new insights into the production of acids and organic nitrates. *Atmos. Chem. Phys.* **2009**, *9*, 1479–1501.
- (271) Krechmer, J. E.; Coggon, M. M.; Massoli, P.; Nguyen, T. B.; Crounse, J. D.; Hu, W.; Day, D. A.; Tyndall, G. S.; Henze, D. K.; Rivera-Rios, J. C.; et al. Formation of low volatility organic compounds and secondary organic aerosol from isoprene hydroxyhydroperoxide low-NO oxidation. *Environ. Sci. Technol.* **2015**, *49*, 10330–9.
- (272) Liu, Y.; Kuwata, M.; Strick, B. F.; Geiger, F. M.; Thomson, R. J.; McKinney, K. A.; Martin, S. T. Uptake of epoxydiol isomers accounts for half of the particle-phase material produced from isoprene photooxidation via the HO<sub>2</sub> pathway. *Environ. Sci. Technol.* **2015**, *49*, 250–8.
- (273) Halliday, H. S.; Thompson, A. M.; Wisthaler, A.; Blake, D. R.; Hornbrook, R. S.; Mikoviny, T.; Müller, M.; Eichler, P.; Apel, E. C.; Hills, A. J. Atmospheric benzene observations from oil and gas production in the Denver-Julesburg Basin in July and August 2014. *Journal of Geophysical Research: Atmospheres* **2016**, *121*, 11055–11074.
- (274) Sommariva, R.; Blake, R. S.; Cuss, R. J.; Cordell, R. L.; Harrington, J. F.; White, I. R.; Monks, P. S. Observations of the release of non-methane hydrocarbons from fractured shale. *Environ. Sci. Technol.* **2014**, *48*, 8891–6.
- (275) Schnell, R. C.; Oltmans, S. J.; Neely, R. R.; Endres, M. S.; Molnar, J. V.; White, A. B. Rapid photochemical production of ozone at high concentrations in a rural site during winter. *Nat. Geosci.* **2009**, *2*, 120–122.
- (276) Edwards, P. M.; Brown, S. S.; Roberts, J. M.; Ahmadov, R.; Banta, R. M.; deGouw, J. A.; Dube, W. P.; Field, R. A.; Flynn, J. H.; Gilman, J. B.; et al. High winter ozone pollution from carbonyl photolysis in an oil and gas basin. *Nature* **2014**, *514*, 351–354.
- (277) Yuan, B.; Kaser, L.; Karl, T.; Graus, M.; Peischl, J.; Campos, T. L.; Shertz, S.; Apel, E. C.; Hornbrook, R. S.; Hills, A.; et al. Airborne flux measurements of methane and volatile organic compounds over the Haynesville and Marcellus shale gas production regions. *Journal of Geophysical Research: Atmospheres* **2015**, *120*, 6271–6289.
- (278) Ryerson, T. B.; Aikin, K. C.; Angevine, W. M.; Atlas, E. L.; Blake, D. R.; Brock, C. A.; Fehsenfeld, F. C.; Gao, R. S.; de Gouw, J. A.; Fahey, D. W.; et al. Atmospheric emissions from the Deepwater Horizon spill constrain air-water partitioning, hydrocarbon fate, and leak rate. *Geophys. Res. Lett.* **2011**, *38*, L07803.
- (279) de Gouw, J. A.; Middlebrook, A. M.; Warneke, C.; Ahmadov, R.; Atlas, E. L.; Bahreini, R.; Blake, D. R.; Brock, C. A.; Brioude, J.; Fahey, D. W.; et al. Organic aerosol formation downwind from the Deepwater Horizon Oil Spill. *Science* **2011**, *331*, 1295–1299.
- (280) Shaw, S. L.; Mitloehner, F. M.; Jackson, W.; DePeters, E. J.; Fadel, J. G.; Robinson, P. H.; Holzinger, R.; Goldstein, A. H. Volatile organic compound emissions from dairy cows and their waste as measured by proton-transfer-reaction mass spectrometry. *Environ. Sci. Technol.* **2007**, *41*, 1310–1316.
- (281) Ngwabie, N. M.; Schade, G. W.; Custer, T. G.; Linke, S.; Hinz, T. Abundances and flux estimates of volatile organic compounds from a dairy cowshed in Germany. *J. Environ. Qual.* **2008**, *37*, 565–573.
- (282) Ngwabie, N. M.; Schade, G. W.; Custer, T. G.; Linke, S.; Hinz, T. Volatile organic compound emission and other trace gases from selected animal buildings. *Landbauforsch Volk* **2007**, *57*, 273–284.
- (283) Hansen, M. J.; Liu, D.; Guldberg, L. B.; Feilberg, A. Application of proton-transfer-reaction mass spectrometry to the assessment of odorant removal in a biological air cleaner for pig production. *J. Agric. Food Chem.* **2012**, *60*, 2599–2606.
- (284) Liu, D.; Feilberg, A.; Adamsen, A. P. S.; Jonassen, K. E. N. The effect of slurry treatment including ozonation on odorant reduction measured by in-situ PTR-MS. *Atmos. Environ.* **2011**, *45*, 3786–3793.
- (285) Jacob, D. J.; Field, B. D.; Li, Q.; Blake, D. R.; de Gouw, J.; Warneke, C.; Hansel, A.; Wisthaler, A.; Singh, H. B.; Guenther, A. Global budget of methanol: Constraints from atmospheric observations. *J. Geophys. Res.* **2005**, *110*, DOI: [10.1029/2004JD005172](https://doi.org/10.1029/2004JD005172).
- (286) Millet, D. B.; Jacob, D. J.; Custer, T. G.; de Gouw, J. A.; Goldstein, A. H.; Karl, T.; Singh, H. B.; Sive, B. C.; Talbot, R. W.; Warneke, C.; et al. New constraints on terrestrial and oceanic sources of atmospheric methanol. *Atmos. Chem. Phys.* **2008**, *8*, 6887–6905.
- (287) Millet, D. B.; Guenther, A.; Siegel, D. A.; Nelson, N. B.; Singh, H. B.; de Gouw, J. A.; Warneke, C.; Williams, J.; Eerdeken, G.; Sinha, V.; et al. Global atmospheric budget of acetaldehyde: 3-D model analysis and constraints from in-situ and satellite observations. *Atmos. Chem. Phys.* **2010**, *10*, 3405–3425.
- (288) Fischer, E. V.; Jacob, D. J.; Millet, D. B.; Yantosca, R. M.; Mao, J. The role of the ocean in the global atmospheric budget of acetone. *Geophys. Res. Lett.* **2012**, *39*, L01807.
- (289) Carpenter, L. J.; Archer, S. D.; Beale, R. Ocean-atmosphere trace gas exchange. *Chem. Soc. Rev.* **2012**, *41*, 6473–6506.
- (290) Carpenter, L. J.; Nightingale, P. D. Chemistry and release of gases from the surface ocean. *Chem. Rev.* **2015**, *115*, 4015–34.
- (291) Read, K. A.; Carpenter, L. J.; Arnold, S. R.; Beale, R.; Nightingale, P. D.; Hopkins, J. R.; Lewis, A. C.; Lee, J. D.; Mendes, L.; Pickering, S. J. Multiannual observations of acetone, methanol, and acetaldehyde in remote tropical Atlantic air: implications for atmospheric OVOC budgets and oxidative capacity. *Environ. Sci. Technol.* **2012**, *46*, 11028–11039.
- (292) Sjostedt, S. J.; Leaitch, W. R.; Levasseur, M.; Scarratt, M.; Michaud, S.; Motard-Côté, J.; Burkhardt, J. H.; Abbatt, J. P. D. Evidence for the uptake of atmospheric acetone and methanol by the Arctic Ocean during late summer DMS-Emission plumes. *J. Geophys. Res.* **2012**, *117*, D12303.
- (293) Tanimoto, H.; Kameyama, S.; Iwata, T.; Inomata, S.; Omori, Y. Measurement of air-sea exchange of dimethyl sulfide and acetone by PTR-MS coupled with gradient flux technique. *Environ. Sci. Technol.* **2014**, *48*, 526–533.
- (294) Taddei, S.; Toscano, P.; Gioli, B.; Matese, A.; Miglietta, F.; Vaccari, F. P.; Zaldei, A.; Custer, T.; Williams, J. Carbon dioxide and acetone air–sea fluxes over the Southern Atlantic. *Environ. Sci. Technol.* **2009**, *43*, 5218–5222.
- (295) Yang, M.; Beale, R.; Liss, P.; Johnson, M.; Blomquist, B.; Nightingale, P. Air–sea fluxes of oxygenated volatile organic

- compounds across the Atlantic Ocean. *Atmos. Chem. Phys.* **2014**, *14*, 7499–7517.
- (296) Yang, M.; Nightingale, P. D.; Beale, R.; Liss, P. S.; Blomquist, B.; Fairall, C. Atmospheric deposition of methanol over the Atlantic Ocean. *Proc. Natl. Acad. Sci. U. S. A.* **2013**, *110*, 20034–9.
- (297) Yang, M.; Blomquist, B. W.; Nightingale, P. D. Air-sea exchange of methanol and acetone during HiWinGS: Estimation of air phase, water phase gas transfer velocities. *Journal of Geophysical Research: Oceans* **2014**, *119*, 7308–7323.
- (298) Williams, J.; Holzinger, R.; Gros, V.; Xu, X.; Atlas, E.; Wallace, D. W. R. Measurements of organic species in air and seawater from the tropical Atlantic. *Geophys. Res. Lett.* **2004**, *31*, L23S06.
- (299) Kameyama, S.; Tanimoto, H.; Inomata, S.; Tsunogai, U.; Ooki, A.; Takeda, S.; Obata, H.; Tsuda, A.; Uematsu, M. High-resolution measurement of multiple volatile organic compounds dissolved in seawater using equilibrator inlet–proton transfer reaction-mass spectrometry (EI–PTR-MS). *Mar. Chem.* **2010**, *122*, 59–73.
- (300) Kameyama, S.; Tanimoto, H.; Inomata, S.; Tsunogai, U.; Ooki, A.; Yokouchi, Y.; Takeda, S.; Obata, H.; Uematsu, M. Equilibrator inlet-proton transfer reaction-mass spectrometry (EI-PTR-MS) for sensitive, high-resolution measurement of dimethyl sulfide dissolved in seawater. *Anal. Chem.* **2009**, *81*, 9021–9026.
- (301) Kameyama, S.; Yoshida, S.; Tanimoto, H.; Inomata, S.; Suzuki, K.; Yoshikawa-Inoue, H. High-resolution observations of dissolved isoprene in surface seawater in the Southern Ocean during austral summer 2010–2011. *J. Oceanogr.* **2014**, *70*, 225–239.
- (302) Beale, R.; Liss, P. S.; Dixon, J. L.; Nightingale, P. D. Quantification of oxygenated volatile organic compounds in seawater by membrane inlet-proton transfer reaction/mass spectrometry. *Anal. Chim. Acta* **2011**, *706*, 128–134.
- (303) Beale, R.; Dixon, J. L.; Arnold, S. R.; Liss, P. S.; Nightingale, P. D. Methanol, acetaldehyde, and acetone in the surface waters of the Atlantic Ocean. *Journal of Geophysical Research: Oceans* **2013**, *118*, S412–S425.
- (304) Beale, R.; Dixon, J. L.; Smyth, T. J.; Nightingale, P. D. Annual study of oxygenated volatile organic compounds in UK shelf waters. *Mar. Chem.* **2015**, *171*, 96–106.
- (305) Fuchs, H.; Hofzumahaus, A.; Rohrer, F.; Bohn, B.; Brauers, T.; Dorn, H. P.; Haseler, R.; Holland, F.; Kaminski, M.; Li, X.; et al. Experimental evidence for efficient hydroxyl radical regeneration in isoprene oxidation. *Nat. Geosci.* **2013**, *6*, 1023–1026.
- (306) Hohaus, T.; Gensch, I.; Kimmel, J.; Worsnop, D. R.; Kiendler-Scharr, A. Experimental determination of the partitioning coefficient of beta-pinene oxidation products in SOAs. *Phys. Chem. Chem. Phys.* **2015**, *17*, 14796–804.
- (307) Borduas, N.; Abbott, J. P.; Murphy, J. G. Gas phase oxidation of monoethanolamine (MEA) with OH radical and ozone: kinetics, products, and particles. *Environ. Sci. Technol.* **2013**, *47*, 6377–6383.
- (308) Zhou, S.; Gonzalez, L.; Leithead, A.; Finewax, Z.; Thalman, R.; Vlasenko, A.; Vagle, S.; Miller, L. A.; Li, S. M.; Bureekul, S.; et al. Formation of gas-phase carbonyls from heterogeneous oxidation of polyunsaturated fatty acids at the air–water interface and of the sea surface microlayer. *Atmos. Chem. Phys.* **2014**, *14*, 1371–1384.
- (309) Kidd, C.; Perraud, V.; Finlayson-Pitts, B. J. New insights into secondary organic aerosol from the ozonolysis of alpha-pinene from combined infrared spectroscopy and mass spectrometry measurements. *Phys. Chem. Chem. Phys.* **2014**, *16*, 22706–16.
- (310) Vlasenko, A.; George, I. J.; Abbott, J. P. D. Formation of Volatile Organic Compounds in the Heterogeneous Oxidation of Condensed-Phase Organic Films by Gas-Phase OH. *J. Phys. Chem. A* **2008**, *112*, 1552–1560.
- (311) Palm, B. B.; Campuzano-Jost, P.; Ortega, A. M.; Day, D. A.; Kaser, L.; Jud, W.; Karl, T.; Hansel, A.; Hunter, J. F.; Cross, E. S.; et al. In situ secondary organic aerosol formation from ambient pine forest air using an oxidation flow reactor. *Atmos. Chem. Phys.* **2016**, *16*, 2943–2970.
- (312) Rossignol, S.; Tiné, L.; Bianco, A.; Passananti, M.; Brigante, M.; Donaldson, D. J.; George, C. Atmospheric photochemistry at a fatty acid-coated air-water interface. *Science* **2016**, *353*, 699–702.
- (313) Barmet, P.; Dommen, J.; DeCarlo, P. F.; Tritscher, T.; Praplan, A. P.; Platt, S. M.; Prévôt, A. S. H.; Donahue, N. M.; Baltensperger, U. OH clock determination by proton transfer reaction mass spectrometry at an environmental chamber. *Atmos. Meas. Tech.* **2012**, *5*, 647–656.
- (314) Brégonzio-Rozier, L.; Siekmann, F.; Giorio, C.; Pangui, E.; Morales, S. B.; Temime-Roussel, B.; Gratien, A.; Michoud, V.; Ravier, S.; Cazaunau, M.; et al. Gaseous products and secondary organic aerosol formation during long term oxidation of isoprene and methacrolein. *Atmos. Chem. Phys.* **2015**, *15*, 2953–2968.
- (315) Wyche, K. P.; Monks, P. S.; Ellis, A. M.; Cordell, R. L.; Parker, A. E.; Whyte, C.; Metzger, A.; Dommen, J.; Duplissy, J.; Prevot, A. S. H.; et al. Gas phase precursors to anthropogenic secondary organic aerosol: detailed observations of 1,3,5-trimethylbenzene photo-oxidation. *Atmos. Chem. Phys.* **2009**, *9*, 635–665.
- (316) Jenkin, M. E.; Wyche, K. P.; Evans, C. J.; Carr, T.; Monks, P. S.; Alfara, M. R.; Barley, M. H.; McFiggans, G. B.; Young, J. C.; Rickard, A. R. Development and chamber evaluation of the MCM v3.2 degradation scheme for  $\beta$ -caryophyllene. *Atmos. Chem. Phys.* **2012**, *12*, 5275–5308.
- (317) Tang, X.; Misztal, P. K.; Nazaroff, W. W.; Goldstein, A. H. Volatile organic compound emissions from humans indoors. *Environ. Sci. Technol.* **2016**, *50*, 12686–12694.
- (318) Liu, S.; Li, R.; Wild, R. J.; Warneke, C.; de Gouw, J. A.; Brown, S. S.; Miller, S. L.; Luongo, J. C.; Jimenez, J. L.; Ziemann, P. J. Contribution of human-related sources to indoor volatile organic compounds in a university classroom. *Indoor Air* **2016**, *26*, 925–938.
- (319) Wisthaler, A.; Weschler, C. J. Reactions of ozone with human skin lipids: sources of carbonyls, dicarbonyls, and hydroxycarbonyls in indoor air. *Proc. Natl. Acad. Sci. U. S. A.* **2010**, *107*, 6568–75.
- (320) Veres, P. R.; Faber, P.; Drewnick, F.; Lelieveld, J.; Williams, J. Anthropogenic sources of VOC in a football stadium: Assessing human emissions in the atmosphere. *Atmos. Environ.* **2013**, *77*, 1052–1059.
- (321) Klein, F.; Platt, S. M.; Farren, N. J.; Detournay, A.; Bruns, E. A.; Bozzetti, C.; Daellenbach, K. R.; Kilic, D.; Kumar, N. K.; Pieber, S. M.; et al. Characterization of gas-phase organics using proton transfer reaction time-of-flight mass spectrometry: cooking emissions. *Environ. Sci. Technol.* **2016**, *50*, 1243–50.
- (322) Klein, F.; Farren, N. J.; Bozzetti, C.; Daellenbach, K. R.; Kilic, D.; Kumar, N. K.; Pieber, S. M.; Slowik, J. G.; Tuthill, R. N.; Hamilton, J. F.; et al. Indoor terpene emissions from cooking with herbs and pepper and their secondary organic aerosol production potential. *Sci. Rep.* **2016**, *6*, 36623.
- (323) Williams, J.; Stonner, C.; Wicker, J.; Krauter, N.; Derstroff, B.; Bourtsoukidis, E.; Klupfel, T.; Kramer, S. Cinema audiences reproducibly vary the chemical composition of air during films, by broadcasting scene specific emissions on breath. *Sci. Rep.* **2016**, *6*, 25464.
- (324) Schripp, T.; Etienne, S.; Fauck, C.; Fuhrmann, F.; Mark, L.; Salthammer, T. Application of proton-transfer-reaction-mass-spectrometry for Indoor Air Quality research. *Indoor Air* **2014**, *24*, 178–89.
- (325) Wyche, K. P.; Blake, R. S.; Willis, K. A.; Monks, P. S.; Ellis, A. M. Differentiation of isobaric compounds using chemical ionization reaction mass spectrometry. *Rapid Commun. Mass Spectrom.* **2005**, *19*, 3356–3362.
- (326) Blake, R. S.; Wyche, K. P.; Ellis, A. M.; Monks, P. S. Chemical ionization reaction time-of-flight mass spectrometry: Multi-reagent analysis for determination of trace gas composition. *Int. J. Mass Spectrom.* **2006**, *254*, 85–93.
- (327) Blake, R. S.; Patel, M.; Monks, P. S.; Ellis, A. M.; Inomata, S.; Tanimoto, H. Aldehyde and ketone discrimination and quantification using two-stage proton transfer reaction mass spectrometry. *Int. J. Mass Spectrom.* **2008**, *278*, 15–19.
- (328) Sulzer, P.; Agarwal, B.; Jürschik, S.; Lanza, M.; Jordan, A.; Hartungen, E.; Hanel, G.; Märk, L.; Märk, T. D.; González-Méndez, R.; et al. Applications of switching reagent ions in proton transfer reaction mass spectrometric instruments for the improved selectivity

- of explosive compounds. *Int. J. Mass Spectrom.* **2013**, *354–355*, 123–128.
- (329) Sulzer, P.; Edtbauer, A.; Hartungen, E.; Jürschik, S.; Jordan, A.; Hanel, G.; Feil, S.; Jaksch, S.; Märk, L.; Märk, T. D. From conventional proton-transfer-reaction mass spectrometry (PTR-MS) to universal trace gas analysis. *Int. J. Mass Spectrom.* **2012**, *321–322*, 66–70.
- (330) Cordell, R. L.; Willis, K. A.; Wyche, K. P.; Blake, R. S.; Ellis, A. M.; Monks, P. S. Detection of chemical weapon agents and simulants using chemical ionization reaction time-of-flight mass spectrometry. *Anal. Chem.* **2007**, *79*, 8359–8366.
- (331) Knighton, W. B.; Fortner, E. C.; Herndon, S. C.; Wood, E. C.; Miake-Lye, R. C. Adaptation of a proton transfer reaction mass spectrometer instrument to employ NO<sup>+</sup> as reagent ion for the detection of 1,3-butadiene in the ambient atmosphere. *Rapid Commun. Mass Spectrom.* **2009**, *23*, 3301–3308.
- (332) Inomata, S.; Tanimoto, H.; Yamada, H. Mass spectrometric detection of alkanes using NO<sup>+</sup> chemical ionization in proton-transfer-reaction + switchable reagent ion Mmass spectrometry. *Chem. Lett.* **2014**, *43*, 538–540.
- (333) Mochalski, P.; Unterkofler, K.; Španěl, P.; Smith, D.; Amann, A. Product ion distributions for the reactions of NO<sup>+</sup> with some physiologically significant volatile organosulfur and organoselenium compounds obtained using a selective reagent ionization time-of-flight mass spectrometer. *Rapid Commun. Mass Spectrom.* **2014**, *28*, 1683–1690.
- (334) Knighton, W. B.; Herndon, S. C.; Wood, E. C.; Fortner, E. C.; Onasch, T. B.; Wormhoudt, J.; Kolb, C. E.; Lee, B. H.; Zavala, M.; Molina, L.; et al. Detecting fugitive emissions of 1,3-butadiene and styrene from a petrochemical facility: an application of a mobile laboratory and a modified proton transfer reaction mass spectrometer. *Ind. Eng. Chem. Res.* **2012**, *51*, 12706–12711.
- (335) Yamada, H.; Inomata, S.; Tanimoto, H. Evaporative emissions in three-day diurnal breathing loss tests on passenger cars for the Japanese market. *Atmos. Environ.* **2015**, *107*, 166–173.
- (336) Cappellin, L.; Makhoul, S.; Schuhfried, E.; Romano, A.; Sanchez del Pulgar, J.; Aprea, E.; Farneti, B.; Costa, F.; Gasperi, F.; Biasioli, F. Ethylene: Absolute real-time high-sensitivity detection with PTR/SRI-MS. The example of fruits, leaves and bacteria. *Int. J. Mass Spectrom.* **2014**, *365–366*, 33–41.
- (337) Shen, C.; Li, J.; Han, H.; Wang, H.; Jiang, H.; Chu, Y. Triacetone triperoxide detection using low reduced-field proton transfer reaction mass spectrometer. *Int. J. Mass Spectrom.* **2009**, *285*, 100–103.
- (338) Edtbauer, A.; Hartungen, E.; Jordan, A.; Hanel, G.; Herbig, J.; Jürschik, S.; Lanza, M.; Breiev, K.; Märk, L.; Sulzer, P. Theory and practical examples of the quantification of CH<sub>4</sub>, CO, O<sub>2</sub>, and CO<sub>2</sub> with an advanced proton-transfer-reaction/selective-reagent-ionization instrument (PTR/SRI-MS). *Int. J. Mass Spectrom.* **2014**, *365–366*, 10–14.
- (339) Blake, R. S.; Ouheda, S. A.; Evans, C. J.; Monks, P. S. CF<sub>3</sub><sup>+</sup> and CF<sub>2</sub>H<sup>+</sup>: new reagents for n-alkane determination in chemical ionisation reaction mass spectrometry. *Analyst* **2016**, *141*, 6564–6570.
- (340) Shen, C.; Niu, W.; Huang, C.; Xia, L.; Lu, Y.; Wang, S.; Wang, H.; Jiang, H.; Chu, Y. Proton-extraction-reaction mass spectrometry (PER-MS) for monitoring organic and inorganic compounds. *Int. J. Mass Spectrom.* **2014**, *371*, 36–41.
- (341) Pan, Y.; Zhang, Q.; Zhou, W.; Zou, X.; Wang, H.; Huang, C.; Shen, C.; Chu, Y. Detection of ketones by a novel technology: dipolar proton transfer reaction mass spectrometry (DP-PTR-MS). *J. Am. Soc. Mass Spectrom.* **2017**, *28*, 873–879.
- (342) Inomata, S.; Tanimoto, H. Differentiation of isomeric compounds by two-stage proton transfer reaction time-of-flight mass spectrometry. *J. Am. Soc. Mass Spectrom.* **2008**, *19*, 325–331.
- (343) Latappy, H.; Lemaire, J.; Heninger, M.; Louarn, E.; Bauchard, E.; Mestdagh, H. Protonated 1,4-difluorobenzene C<sub>6</sub>H<sub>5</sub>F<sub>2</sub><sup>+</sup>: A promising precursor for proton-transfer chemical ionization. *Int. J. Mass Spectrom.* **2016**, *405*, 13–23.
- (344) Fortner, E. C.; Knighton, W. B. Quantitatively resolving mixtures of isobaric compounds using chemical ionization mass spectrometry by modulating the reactant ion composition. *Rapid Commun. Mass Spectrom.* **2008**, *22*, 2597–2601.
- (345) Amador-Muñoz, O.; Misztal, P. K.; Weber, R.; Worton, D. R.; Zhang, H.; Drozd, G.; Goldstein, A. H. Sensitive detection of n-alkanes using a mixed ionization mode proton-transfer-reaction mass spectrometer. *Atmos. Meas. Tech.* **2016**, *9*, 5315–5329.
- (346) Steeghs, M. M. L.; Crespo, E.; Harren, F. J. M. Collision induced dissociation study of 10 monoterpenes for identification in trace gas measurements using the newly developed proton-transfer reaction ion trap mass spectrometer. *Int. J. Mass Spectrom.* **2007**, *263*, 204–212.
- (347) Misztal, P. K.; Heal, M. R.; Nemitz, E.; Cape, J. N. Development of PTR-MS selectivity for structural isomers: Monoterpenes as a case study. *Int. J. Mass Spectrom.* **2012**, *310*, 10–19.
- (348) Gonzalez-Mendez, R.; Watts, P.; Olivenza-Leon, D.; Reich, D. F.; Mullock, S. J.; Corlett, C. A.; Cairns, S.; Hickey, P.; Brookes, M.; Mayhew, C. A. Enhancement of compound selectivity using a radio frequency ion-funnel proton transfer reaction mass spectrometer: improved specificity for explosive compounds. *Anal. Chem.* **2016**, *88*, 10624–10630.
- (349) Hellen, H.; Dommen, J.; Metzger, A.; Gascho, A.; Duplissy, J.; Tritscher, T.; Prevot, A. S. H.; Baltensperger, U. Using proton transfer reaction mass spectrometry for online analysis of secondary organic aerosols. *Environ. Sci. Technol.* **2008**, *42*, 7347–7353.
- (350) Holzinger, R.; Kasper-Giebl, A.; Staudinger, M.; Schauer, G.; Röckmann, T. Analysis of the chemical composition of organic aerosol at the Mt. Sonnbliek observatory using a novel high mass resolution thermal-desorption proton-transfer-reaction mass-spectrometer (hr-TD-PTR-MS). *Atmos. Chem. Phys.* **2010**, *10*, 10111–10128.
- (351) Holzinger, R.; Williams, J.; Herrmann, F.; Lelieveld, J.; Donahue, N. M.; Röckmann, T. Aerosol analysis using a Thermal-Desorption Proton-Transfer-Reaction Mass Spectrometer (TD-PTR-MS): a new approach to study processing of organic aerosols. *Atmos. Chem. Phys.* **2010**, *10*, 2257–2267.
- (352) Holzinger, R.; Goldstein, A. H.; Hayes, P. L.; Jimenez, J. L.; Timkovsky, J. Chemical evolution of organic aerosol in Los Angeles during the CalNex 2010 study. *Atmos. Chem. Phys.* **2013**, *13*, 10125–10141.
- (353) Thompson, S. L.; Yatavelli, R. L. N.; Stark, H.; Kimmel, J. R.; Krechmer, J. E.; Day, D. A.; Hu, W.; Isaacman-VanWertz, G.; Yee, L.; Goldstein, A. H.; et al. Field intercomparison of the gas/particle partitioning of oxygenated organics during the Southern Oxidant and Aerosol Study (SOAS) in 2013. *Aerosol Sci. Technol.* **2017**, *51*, 30–56.
- (354) Timkovsky, J.; Chan, A. W. H.; Dorst, T.; Goldstein, A. H.; Oyama, B.; Holzinger, R. Comparison of advanced offline and in situ techniques of organic aerosol composition measurement during the CalNex campaign. *Atmos. Meas. Tech.* **2015**, *8*, 5177–5187.
- (355) Eichler, P.; Müller, M.; D'Anna, B.; Wisthaler, A. A novel inlet system for online chemical analysis of semi-volatile submicron particulate matter. *Atmos. Meas. Tech.* **2015**, *8*, 1353–1360.
- (356) Eichler, P.; Müller, M.; Rohmann, C.; Stengel, B.; Orasche, J.; Zimmermann, R.; Wisthaler, A. Lubricating oil as a major constituent of ship exhaust particles. *Environ. Sci. Technol. Lett.* **2017**, *4*, 54–58.
- (357) Inomata, S.; Sato, K.; Hirokawa, J.; Sakamoto, Y.; Tanimoto, H.; Okumura, M.; Tohno, S.; Imamura, T. Analysis of secondary organic aerosols from ozonolysis of isoprene by proton transfer reaction mass spectrometry. *Atmos. Environ.* **2014**, *97*, 397–405.
- (358) Salvador, C. M.; Ho, T. T.; Chou, C. C. K.; Chen, M. J.; Huang, W. R.; Huang, S. H. Characterization of the organic matter in submicron urban aerosols using a Thermo-Desorption Proton-Transfer-Reaction Time-of-Flight Mass Spectrometer (TD-PTR-TOF-MS). *Atmos. Environ.* **2016**, *140*, 565–575.
- (359) Oyama, B. S.; Andrade, M. D. F.; Herckes, P.; Dusek, U.; Röckmann, T.; Holzinger, R. Chemical characterization of organic particulate matter from on-road traffic in São Paulo, Brazil. *Atmos. Chem. Phys.* **2016**, *16*, 14397–14408.
- (360) Masalaite, A.; Holzinger, R.; Remeikis, V.; Röckmann, T.; Dusek, U. Characteristics, sources and evolution of fine aerosol (PM1)

- at urban, coastal and forest background sites in Lithuania. *Atmos. Environ.* **2017**, *148*, 62–76.
- (361) Sinha, V.; Williams, J.; Crowley, J. N.; Lelieveld, J. The Comparative Reactivity Method: a new tool to measure total OH Reactivity in ambient air. *Atmos. Chem. Phys.* **2008**, *8*, 2213–2227.
- (362) Michoud, V.; Hansen, R. F.; Locoge, N.; Stevens, P. S.; Dusander, S. Detailed characterizations of the new Mines Douai comparative reactivity method instrument via laboratory experiments and modeling. *Atmos. Meas. Tech.* **2015**, *8*, 3537–3553.
- (363) Hansen, R. F.; Blocquet, M.; Schoemaecker, C.; Léonardis, T.; Locoge, N.; Fittschen, C.; Hanoune, B.; Stevens, P. S.; Sinha, V.; Dusander, S. Intercomparison of the comparative reactivity method (CRM) and pump–probe technique for measuring total OH reactivity in an urban environment. *Atmos. Meas. Tech.* **2015**, *8*, 4243–4264.
- (364) Zannoni, N.; Dusander, S.; Gros, V.; Sarda Esteve, R.; Michoud, V.; Sinha, V.; Locoge, N.; Bonsang, B. Intercomparison of two comparative reactivity method instruments in the Mediterranean basin during summer 2013. *Atmos. Meas. Tech.* **2015**, *8*, 3851–3865.
- (365) Kumar, V.; Sinha, V. VOC–OHM: A new technique for rapid measurements of ambient total OH reactivity and volatile organic compounds using a single proton transfer reaction mass spectrometer. *Int. J. Mass Spectrom.* **2014**, *374*, 55–63.
- (366) Sinha, V.; Williams, J.; Lelieveld, J.; Ruuskanen, T. M.; Kajos, M. K.; Patokoski, J.; Hellen, H.; Hakola, H.; Mogensen, D.; Boy, M.; et al. OH reactivity measurements within a boreal forest: evidence for unknown reactive emissions. *Environ. Sci. Technol.* **2010**, *44*, 6614–6620.
- (367) Nölscher, A. C.; Williams, J.; Sinha, V.; Custer, T.; Song, W.; Johnson, A. M.; Axinte, R.; Bozem, H.; Fischer, H.; Pouvesle, N.; et al. Summertime total OH reactivity measurements from boreal forest during HUMPPA-COPEC 2010. *Atmos. Chem. Phys.* **2012**, *12*, 8257–8270.
- (368) Nölscher, A. C.; Yañez-Serrano, A. M.; Wolff, S.; de Araujo, A. C.; Lavrič, J. V.; Kesselmeier, J.; Williams, J. Unexpected seasonality in quantity and composition of Amazon rainforest air reactivity. *Nat. Commun.* **2016**, *7*, 10383.
- (369) Zannoni, N.; Gros, V.; Lanza, M.; Sarda, R.; Bonsang, B.; Kalogridis, C.; Preunkert, S.; Legrand, M.; Jambert, C.; Boissard, C.; et al. OH reactivity and concentrations of biogenic volatile organic compounds in a Mediterranean forest of downy oak trees. *Atmos. Chem. Phys.* **2016**, *16*, 1619–1636.
- (370) Dolgorouky, C.; Gros, V.; Sarda-Esteve, R.; Sinha, V.; Williams, J.; Marchand, N.; Sauvage, S.; Poulain, L.; Sciare, J.; Bonsang, B. Total OH reactivity measurements in Paris during the 2010 MEGAPOLI winter campaign. *Atmos. Chem. Phys.* **2012**, *12*, 9593–9612.
- (371) Williams, J.; Keßel, S. U.; Nölscher, A. C.; Yang, Y.; Lee, Y.; Yáñez-Serrano, A. M.; Wolff, S.; Kesselmeier, J.; Klüpfel, T.; Lelieveld, J.; et al. Opposite OH reactivity and ozone cycles in the Amazon rainforest and megacity Beijing: Subversion of biospheric oxidant control by anthropogenic emissions. *Atmos. Environ.* **2016**, *125*, 112–118.
- (372) Yang, Y.; Shao, M.; Keßel, S.; Li, Y.; Lu, K.; Lu, S.; Williams, J.; Zhang, Y.; Zeng, L.; Nölscher, A. C.; et al. How does the OH reactivity affect the ozone production efficiency: case studies in Beijing and Heshan. *Atmos. Chem. Phys.* **2017**, *17*, 7127–7142.
- (373) Sinha, V.; Williams, J.; Diesch, J. M.; Drewnick, F.; Martinez, M.; Harder, H.; Regelin, E.; Kubistin, D.; Bozem, H.; Hosaynali-Beygi, Z.; et al. Constraints on instantaneous ozone production rates and regimes during DOMINO derived using in-situ OH reactivity measurements. *Atmos. Chem. Phys.* **2012**, *12*, 7269–7283.
- (374) Kim, S.; Guenther, A.; Karl, T.; Greenberg, J. Contributions of primary and secondary biogenic VOC total OH reactivity during the CABINEX (Community Atmosphere-Biosphere INteractions Experiments)-09 field campaign. *Atmos. Chem. Phys.* **2011**, *11*, 8613–8623.
- (375) Nölscher, A. C.; Bourtsoukidis, E.; Bonn, B.; Kesselmeier, J.; Lelieveld, J.; Williams, J. Seasonal measurements of total OH reactivity emission rates from Norway spruce in 2011. *Biogeosciences* **2013**, *10*, 4241–4257.
- (376) Wu, Y.; Yang, Y.-D.; Shao, M.; Lu, S.-H. Missing in total OH reactivity of VOCs from gasoline evaporation. *Chin. Chem. Lett.* **2015**, *26*, 1246–1248.
- (377) Giorio, C.; Campbell, S. J.; Bruschi, M.; Archibald, A. T.; Kalberer, M. Detection and identification of Criegee intermediates from the ozonolysis of biogenic and anthropogenic VOCs: comparison between experimental measurements and theoretical calculations. *Faraday Discuss.* **2017**, *200*, 559–578.
- (378) Giorio, C.; Campbell, S. J.; Bruschi, M.; Tampieri, F.; Barbon, A.; Toffoletti, A.; Tapparo, A.; Paijens, C.; Wedlake, A. J.; Grice, P.; et al. Online quantification of Criegee intermediates of alpha-pinene ozonolysis by stabilization with spin traps and proton-transfer reaction mass spectrometry detection. *J. Am. Chem. Soc.* **2017**, *139*, 3999–4008.